



Durham E-Theses

Investigation into sterol signalling in Arabidopsis

Cope-Selby, Naomi L.

How to cite:

Cope-Selby, Naomi L. (2009) *Investigation into sterol signalling in Arabidopsis*, Durham theses, Durham University. Available at Durham E-Theses Online: <http://etheses.dur.ac.uk/2076/>

Use policy

The full-text may be used and/or reproduced, and given to third parties in any format or medium, without prior permission or charge, for personal research or study, educational, or not-for-profit purposes provided that:

- a full bibliographic reference is made to the original source
- a [link](#) is made to the metadata record in Durham E-Theses
- the full-text is not changed in any way

The full-text must not be sold in any format or medium without the formal permission of the copyright holders.

Please consult the [full Durham E-Theses policy](#) for further details.

Investigation into sterol signalling in *Arabidopsis*

MSc Thesis

2009

Supervisor: Prof. Keith Lindsey

The copyright of this thesis rests with the author or the university to which it was submitted. No quotation from it, or information derived from it may be published without the prior written consent of the author or university, and any information derived from it should be acknowledged.

Naomi L. Cope-Selby
School of Biological and Biomedical Sciences,
Durham University

12 AUG 2009

Abstract

The hydra sterol mutants (*hydra1* and *fk^{hyd2}*) phenotypes are characterised by short thickened roots and a shoot consisting of a mass of indistinct leaves. At the cellular level, cell patterning is disorganised and cell shape irregular. *hydra* sterol mutants are not phenotypically rescued by application of exogenous sterols (Lindsey *et al.*, 2003) and have auxin and ethylene signalling defects but no defects in biosynthesis (Souter *et al.*, 2002).

It is not known at the mechanistic level how the *hydra* phenotype is generated. The disruption in sterol biosynthesis and subsequent altered sterol profile may lead to a loss of sterol-based signals required for development (Schrack *et al.*, 2000), or disruption of other hormone signalling pathways (Souter *et al.*, 2002, 2004); or some other mechanism.

To determine whether sterol biosynthesis is required in specific cell types, we expressed the wild type *HYDRA1* and *HYDRA2* genes respectively under tissue specific promoters in the relevant *hydra* backgrounds and looked for evidence of phenotypic rescue. The analysis included examination of GFP expression in UAS enhancer trap lines, quantification of root length, examining the root tip cellular structure and characterization of cellular defects in mature plants using microscopy and tissue staining.

Phenotypic rescue occurred in all lines analysed, however there were differences in the extent of phenotypic rescue under different promoters and in different independent transgenic lines. Where the same promoters were used, there was a difference in the degree of rescue in *hydra1* to *fk^{hyd2}*. *fk^{hyd2}* displayed partial rescue whereas *hydra1* displayed almost complete restoration to wild type phenotype. *fk^{hyd2}* is known to have the more severe phenotype of the two mutants, this result may indicate the product of C-14 reductase has a critical role in plant development.

The major conclusion is correct sterol biosynthesis is not required in all root tissues for correct plant development.

Contents:

Abstract	i
Contents	ii
Abbreviations	vii
Acknowledgments	viii

1.0 Introduction

1.1	<i>Arabidopsis thaliana</i> -a model system for plant sciences	1
1.2	The structure and tissues of the mature <i>Arabidopsis thaliana</i> root	2
1.3	The plant hormone Auxin	6
1.3.1	The discovery of auxin and it's functions	6
1.3.2	Auxin Biosynthesis	6
1.3.3	Polar Auxin transport	7
1.3.3.1	Auxin influx	7
1.3.3.2	Auxin efflux and the PIN transporters	8
1.4	The plant hormone Ethylene	11
1.4.2	Ethylene Biosynthesis	12
1.4.3	Ethylene transport	12
1.4.4	The ethylene signalling pathway	12
1.5	Phytosterols	13
1.5.1	What are phytosterols?	13
1.5.2	The sterol biosynthesis pathway in plants	15
1.5.3	Sterol concentrations in plants	16
1.5.4	The functions of sterols in plants	17
1.5.5	Brassinosteroids	17
1.6	The <i>hydra</i> mutants of <i>Arabidopsis</i>	18
1.6.1	The isolation of the <i>hydra</i> mutants	18
1.6.2	The <i>hydra</i> phenotype	19

1.6.4	The sterol pathway and the <i>hydra</i> mutants	22
1.6.5	Research into the <i>hydra</i> mutants: the findings so far:	22
1.7	Molecular tools	26
1.8	Project aims and objectives	27
2.1	Materials	29
2.1.1	Molecular Biological and Chemical Reagents	29
2.1.2	Molecular Biology Kits	29
2.1.3	DNA Sequences and Maps	29
2.1.4	Media and Cell Culture Conditions	29
2.1.5	Plasmid Vectors	31
2.1.6	Plant lines	31
2.1.7	Greenhouse Growth Conditions	32
2.2	Method	32
2.2.1	Crossing	32
2.2.2	Sterile Plant Culture	33
2.2.3	<i>hydra</i> Screening	34
2.2.3.1	Embryo screening	34
2.2.3.2	Genotyping	34
2.2.4	GFP screening	35
2.2.4.1	Screening for crossing	35
2.2.4.2	Screening for experimental seed	35
2.2.5	Root Length Analysis	36
2.2.5.1	UAS lines	36
2.2.5.2	<i>PLS</i> and <i>DR5</i> lines	36
2.2.6	Root (Lugol) Staining	36
2.2.7	Confocal Microscopy	36
2.2.7.1	Root patterning and cellular structure	37
2.2.7.2	Shoot patterning and cellular structure	37
2.2.7.3	Petal DAPI staining	37

2.2.8 DNA Extraction	37
2.2.9 Genotyping	38
2.2.10 Colony PCR	41
2.2.11 Gel Electrophoresis	42
2.2.12 Cloning the <i>HYDRA2</i> promoter	43
2.2.13 Cloning into TOPO	43
2.2.14 Cloning into Δ p _{circe-gus}	45
2.2.15 Transformation into XL1 blue cells	46
2.2.16 DNA sequencing	46
Results	47
3.1 Generating the genetic crosses	47
3.2 Genotyping	48
3.3 GFP expression	49
3.3.1 GFP expression in wild type <i>ws</i> and <i>Col-0</i> lines	49
3.3.1 Comparison of GFP expression in <i>Ws</i> and <i>Col-0</i> lines	48
3.3.2 GFP expression in the <i>hydra</i> mutant background lines	51
3.3.3 Expression of HYDRA1 in the endodermis	52
3.3.4 GFP expression in the shoot	52
3.3.5 The cortex and vascular tissue UAS lines	54
3.4 The <i>hydra</i> phenotype and the phenotypic deviations that indicate rescue	55
3.5 Rescue in the <i>DR5</i> promoter driven lines	57
3.5.1 Overview of phenotypic rescue in <i>DR5::HYDRA1</i> x <i>hydra1</i>	58
3.5.2 Root Growth in <i>DR5::HYDRA1</i> x <i>hydra1</i>	58
3.5.3 Lugol staining in <i>DR5::HYDRA1</i> x <i>hydra1</i>	59
3.5.4 Flowers of the <i>DR5::HYDRA1</i> x <i>hydra1</i> lines	60
3.6 <i>DR5::HYDRA2</i> x <i>fk^{hyd2}</i>	61
3.6.1 Overview of phenotypic rescue in <i>DR5::HYDRA2</i> x <i>fk^{hyd2}</i>	61
3.6.2 Phenotypic rescue at post 21 dpv in <i>DR5::HYDRA2</i> x <i>fk^{hyd2}</i>	61
3.6.3 Lugol staining in <i>DR5::HYDRA2</i> x <i>fk^{hyd2}</i>	64
3.7 <i>PLS::HYDRA1</i> x <i>hydra1</i>	66
3.7.1 Overview of phenotypic rescue in <i>PLS::HYDRA1</i> x <i>hydra1</i>	66

3.7.2	<i>polaris</i> (<i>PLS</i>) expression	66
3.7.3	Root growth in <i>PLS::HYDRA1</i> x <i>hydra1</i>	67
3.7.4	Lugol staining in <i>PLS::HYDRA1</i> x <i>hydra1</i> lines	68
3.7.5	Petal shape in the <i>PLS::HYDRA1</i> x <i>hydra1</i> and <i>PLS::HYDRA2</i> x <i>fk^{hyd2}</i> lines.	69
3.8	<i>PLS::HYDRA2</i> x <i>fk^{hyd2}</i>	73
3.8.1	Overview of phenotype rescue in <i>PLS::HYDRA2</i> x <i>fk^{hyd2}</i>	73
3.8.2	Root growth in <i>PLS::HYDRA2</i> x <i>fk^{hyd2}</i>	73
3.8.3	Lugol staining in <i>PLS::HYDRA2</i> x <i>fk^{hyd2}</i>	74
3.9	<i>UAS::HYDRA1</i> x <i>hydra1</i> (epidermis/pericycle/endodermis)	75
3.9.1	Overview of phenotypic rescue	75
3.9.2	Root growth in <i>UAS::HYDRA1</i> x <i>hydra1</i> (epidermis/pericycle/endodermis)	75
3.9.3	Lugol staining in <i>UAS::HYDRA1</i> x <i>hydra1</i> (epidermis/pericycle/endodermis)	81
3.9.4	Petal shape in <i>UAS::HYDRA1</i> x <i>hydra1</i> (epidermis/pericycle/endodermis)	81
3.10	Cloning of the <i>HYDRA2</i> promoter	82
4.0	Discussion	84
4.1	Survey of GFP expression	84
4.2	Phenotypic rescue in root length	84
4.3	Extent of rescue in cellular patterning in the columella and root cap	85
4.4	Extent of rescue in the shoot	86
4.5	<i>hydra1</i> rescue compared with <i>fk^{hyd2}</i> rescue	86
4.6	Sterols as a signalling molecule essential for development	87
4.7	Auxin fountain model and phenotypic rescue	88
4.8	Summary of main findings	89
4.9	Conclusion	89
4.10	Further work	90

Appendix 1	91
Appendix 2	96
References	98

Abbreviations

bp	base pair (length of a nucleotide)
dNTPs	2'-deoxynucleotide 5'triphosphates
dpg	days post germination
DR5	auxin responsive promoter
EDTA	ethylenediaminetetraacetic acid
<i>fk^{hyd2}</i>	<i>fackel/hydra2</i> homozygous
GFP	green fluorescent protein
GUS	β-glucuronidase
<i>hydra1</i>	<i>hydra1</i> homozygous mutant
kb	kilobase (length of 1000bp)
KOH	potassium hydroxide
MgCL₂	Magnesium Chloride
mM	millimolar
NaCl	Sodium Chloride
pM	picomolar
PLS	<i>polaris</i> gene promoter
SDS	sodium dodecyl sulphate
T-DNA	transferred DNA
Tris-HCl	tris (hydroxymethyl) aminomethane-hydrochloric acid
rpm	revolutions per minute
UAS	upstream activation sequence promoter
μl	microlitre
μg	microgram
(w/v)	weight per volume

Acknowledgements

First I would like to give thanks to Prof. Keith Lindsay and Dr. Jennifer Topping for their support and supervision during this MSc.

Thanks to Dr. Eleri Short and Dr. Gul Ulke for providing the transgenic construct lines.

Grateful thanks go to Dr Nick Clark for his support and all the hours he spent discussing methods and supervising in the confocal microscope suite.

I would like to thank Mrs DLC Kumari and Ms Saher Mehdi for being such fun to work alongside.

Thanks must also go to the Hussey lab (Dr Mike Deeks, Dr Tim Hawkins and Ms Lizzy Ingle) for their advice, their friendship and for allowing me to 'borrow' everything in sight!

I must thank and acknowledge Dr Eileen Grey, Mrs Mary Ledger and all at DUSSD for their support, for teaching me what's important in life and for dealing with the ton of DSA paperwork!

Thanks must also go to Dr Beverley Glover at the University of Cambridge for her time, suggestions and insights.

Thanks are not enough for Dr Liz Burd, but she gets them anyway for sorting out one admin disaster after the other, for pointing out talents I hadn't realised I had and generally being an inspiration. Oh and for all the coffee!

Finally thanks to my mother for encouraging me to follow what I enjoy and chase my dreams-however unconventional and over ambitious they may be.

Introduction

1.1 *Arabidopsis thaliana*-a model system for plant sciences

Arabidopsis thaliana has been adopted as the model plant of choice for research in the plant sciences and crop genetics since the 1980s. Taking a close look at the *A. thaliana* lifecycle and genetic make-up it is easy to discern why. The mature *Arabidopsis* plant is of small stature (~15 cm tall), it does not produce vast roots and up to 10,000 seeds can be harvested per plant (Glover, 2007). *Arabidopsis* has a rapid life cycle, which can be completed in 6 weeks, and predominantly self-fertilises, as well as tolerating cross-pollination with selected plant lines (Topping and Lindsey, 1997). *Arabidopsis*'s size ensures large numbers of plants can be grown without requiring a large greenhouse space without problems with overcrowding and competition dynamics affecting the plant's development (Somerville and Koornneef, 2002; Figure 1.1).



Figure 1.1: Mature *Arabidopsis thaliana* (left) and close up of flowers with developing siliques (right). (Pictures taken by the Durham Photography Unit, Durham University, U.K.)

Several ecotypes of *Arabidopsis* are available, each with slight differences in morphology, development and stress resistance. *Columbia* (*Col-0*) is the most commonly used and was the ecotype of the *Arabidopsis* Genome Initiative sequencing project (Chang *et al.*, 2001). However for this project all the plants are in the *Wassilewskija* (*ws*) background to allow comparisons between *hydra* mutants.

Other advantages to working with *A. thaliana* are at the molecular level. The genome of *A. thaliana* is small (~130 Mb) and due to the success of the *Arabidopsis* Genome Initiative sequencing project there is ample information available for molecular work (Federspiel, 2000; Parinov and Venkatesan, 2000). Furthermore gene transformations in *Arabidopsis* are easily achievable using a derivative of the *Agrobacterium tumefaciens* bacterium and the dipping method (Clough and Bent, 1998; Pereira, 2000). Finally at the cellular level particularly in the root, the main focus of this work, *Arabidopsis*, cellular structure is relatively simple and alterations in the structure can be clearly seen and categorised (Malamy and Benfey, 1997).

1.2 The structure and tissues of the mature *Arabidopsis thaliana* root

The *Arabidopsis* root has a simple structure with easily discernible layers of differentiated cells along the longitudinal axis and distinct rings of tissue along the radial axis (Casson and Lindsey, 2003; Petricka and Benfey, 2008; Figure 1.2).

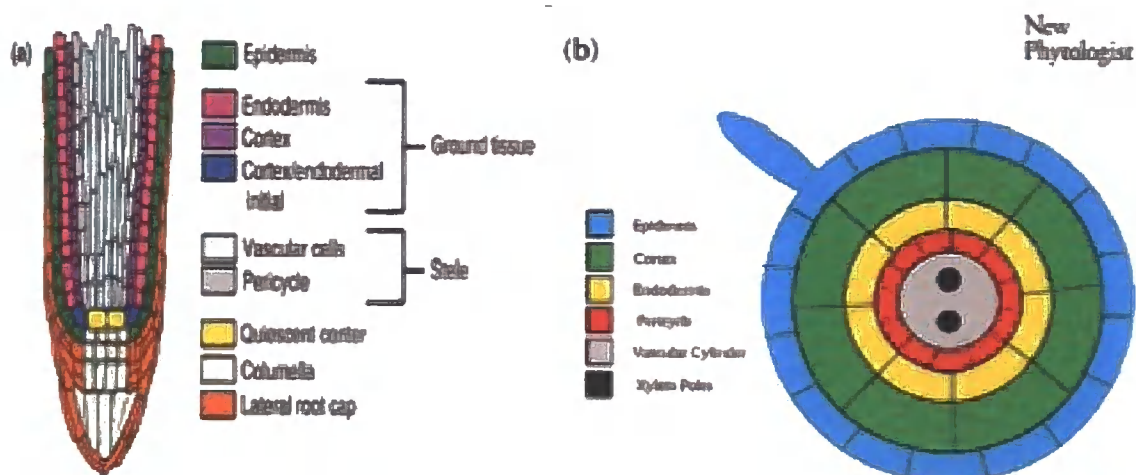


Figure 1.2: (a) diagram of differentiated root tissues on the longitudinal axis (Petricka and Benfey, 2008). (b) diagram of rings of differentiated tissue along the radial axis (Casson and Lindsey, 2002)

The tissue structure of the root can be divided into three sections: the root cap and associated tissues, the stele tissues and the ground tissues. The central root cap includes a quiescent centre (Q.C.) situated between the cortex initial cells. The Q.C. is a small number of cells (four in *Arabidopsis*), which are surrounded by highly mitotically active undifferentiated stem cells that are the source of all cells in the root (Dinneny and Benfey, 2005). From the stem cells daughter cells arise and these daughter cells further divide before elongation. Differentiation into specific cell types takes place as the cells move into position in the correct tissue layer (Hardtke, 2006; Petricka and Benfey, 2008).

Below the Q.C. are four layers of columella cells to the base of the root (Dinneny and Benfey, 2005) with a separate tissue layer termed the lateral root cap enclosing the root (Petricka and Benfey, 2008). The columella cells contain a large number of starch granules that are essential for the correct gravitropic response in the root (Vitha *et al.*, 2007).

Proximal to the Q.C. is the main root body. The main root body comprises the vascular tissue containing the xylem and phloem located centrally and surrounded by the pericycle tissue. The endodermis forms a layer outside the pericycle, protecting the fragile vascular tissues and controlling water movement. Surrounding the endodermis is the cortex tissue and the outermost layer is the epidermis (Casson and Lindsey 2003, Dolan *et al.*, 1993). Currently there is insufficient detailed knowledge of the functions of specific root tissues and internal and intracellular signalling activity, although recently microarray profiling of different cell populations has increased knowledge of gene expression in the different tissues (Petricka and Benfey 2008).

The epidermal tissue layer presents a barrier to protect the root and is the site of root hairs whose major role is in promoting the uptake of water and nutrients from the soil (Bengouch *et al.*, 2006). All epidermal cells originate from initial cells and further differentiate into either a root hair cell (RH) or a non-hair cell (NH). A key feature of the mechanism regulating this differentiation process is the position of the cell. If an epidermal cell is located in a position where the lower cell wall is in contact with two cortex cells in the layer below, that epidermal cell differentiates into a root hair cell. An epidermal cell whose cell wall is in contact with only a single cortex cell in the layer below differentiates into a non-hair cell. Laser ablation experiments in which single cells were precisely eradicated, found cells that move position into the

space left by the obliterated cell then differentiated into the appropriate cell fate (van den Berg *et al.*, 1995; Casson and Lindsey 2003; Ueda *et al.*, 2005). For example if a non-hair cell moves into a space where it is now in contact with two cortex cells in the layer below, it undergoes differentiation into a root hair cell. Though there is still some controversy over NH and RH cell fate (Petricka and Benfrey, 2008) there is evidence from studies of gene expression, the transcription factors listed in Table 1.1 play significant roles in the processes involved (Ishida *et al.*, 2008).

Table 1.1: Transcription factors involved in NH and RH cell specification (Ishida *et al.* 2008)

Transcription factors specifying NH cells	Transcription factors specifying RH cells
GLABRA 2 (GL)	CAPRICE (CPC)
GLABRA 3 (GL3)	TRITYCHON (TRY)
ENHANCER OF GLABRA 3 (EGL3)	ENHANCER OF TRITYCHON
TRANSPARENT TEST GLABRA (TTG)	CAPRICE (ETE)
WEREWOLF (WER)	

Current research proposes a TTG/GL3/EGL3/WER transcriptional complex, which binds to the GL2 promoter resulting in a repression of RH cell fate. Simultaneously the complex induces the expression of CPC in NH cells, which is then transported into the neighbouring epidermal cell, repressing GL2 expression creating an RH cell (Ishida *et al.*, 2008). Evidence to support this model was discovered when a GL2 expression modulator, GEM1, was over expressed in *Arabidopsis*. This resulted in increased root hair density correlating with reduced GL2 mRNA (Caro *et al.*, 2007).

Two further candidates expected to play roles in epidermal cell differentiation are the TRANSPARENT TEST GLABRA 2 (TTG2) and TRY. Experimental data had implied that TTG2 is able to switch on expression of itself, GL2 and CPC independently of the TTG/GL3/EGL3/WER transcriptional complex. However it later transpired through promoter deletion and hybrid analysis, TTG2 is activated by WER binding to a MYB regulatory element, which then activates GL2 (Ishida *et al.*, 2007). Both *ttg2* and TRY mutants have normal epidermal cell patterning but studies of gene

expression pattern in these mutants indicate TRY is part of a regulatory loop where in TRY represses GL2 expression in RH cells and GL2 promotes TRY expression in NH cells (Simon *et al.*, 2007). Further work on the CPC chimera protein has supported a view of competition between WER and CPC in transcriptional complexes that regulate GL2 expression related to epidermal patterning (Tominaga *et al.*, 2007).

The vast majority of research on root tissues has focused on the increasingly complex mechanisms of gene expression and cellular positioning behind the root hair. For cell differentiation however more is becoming known about the other root tissues.

A study on the endodermis and shoot growth found a potential signalling link between sterols and root cell patterning where expression of a brassinosteroid biosynthetic enzyme rescued a dwarf phenotype. The authors proposed the endodermis both promoted and restricted shoot growth through playing a role in the conduction of signalling molecules needed for correct growth (Savaldi-Goldstein *et al.*, 2007). Further work in this area revealed the transcription factor BREVISRADIX (BRX), which is believed to mediate feedback between brassinosteroids and auxin (Mouchel *et al.*, 2006).

Work on SHR and SCR in the endodermis found a SHR/SCR dependent positive feedback loop for transcription of SCR. A key part of this loop concerns SCR restricting the movement of SHR by transferring it into the nucleus. The effect of transcription of SCR then specifies the endodermal cells (Cui *et al.*, 2007). Interestingly auxin does not seem to be involved in this SHR/SCR feedback loop or in the specification of the endodermal cells despite evidence that auxin is involved with developmental or differentiation of cells in the stele tissues and the Q.C. (Petricka and Benfey, 2008).

In the stele tissues, lateral roots are formed from the mature pericycle cells in the basal area of the primary root. The pericycle cells have the ability to re-enter the cell cycle and the resulting daughter cells form the lateral root primordial cells from which the lateral root develops (Hardke, 2006).

The plant hormone auxin has been shown to accumulate in both the columella root cap and the Q.C. and has an effect on cellular patterning. The cellular patterning of the root changes when exogenous auxin is applied to it. Changes in cellular patterning were also observed when an auxin inhibitor was applied (Ueda *et al.*, 2005). Auxin's prominent role in cellular patterning is mediated in part by the action of PIN auxin transporters in the stele tissues. There is also evidence of an auxin 'sink'

situated below the Q.C. which controls an auxin gradient which is essential for auxin distribution and patterning (Friml *et al.*, 2002).

1.3 The plant hormone auxin

1.3.1 The discovery of auxin and its functions

Though a powerful growth stimulating substance in plants had been theorised and studied experimentally by both Charles and Francis Darwin in 1881, it was 1931 before Kögl and Haagen-Smit gave it the name auxin (Callis 2005; Paciorek and Friml, 2006). Today, 128 years later and despite great strides forward in this area of research, many details of auxin biosynthesis, functions and interactions within the plant are still poorly understood.

Extensive research has found that auxin is involved (either directly or indirectly) at all stages of plant growth and development. The functions of auxin include: the regulation of floral organ formation and patterning in the vascular tissues (Cheng *et al.*, 2006), embryo development, root patterning, apical hook formation (Paciorek and Friml, 2006), cell division and elongation (Zhao *et al.*, 2002) and establishment of the primary, apical-basal axis (De Smet and Jürgens, 2007). Auxin also may have a role in light perception in plants through regulation by light perception cryptochromes (Imaizumi *et al.*, 2002).

1.3.2 Auxin Biosynthesis

The sites of auxin biosynthesis are believed to be in the seed of the plant and in young roots and shoots (Benjamin *et al.*, 2005) though the molecular mechanisms driving biosynthesis remain largely unknown (Cheung *et al.*, 2006). There is evidence that two pathways are involved in the auxin biosynthesis process (Cohen *et al.*, 2003, Zhao *et al.*, 2002). Of these two pathways one is dependent on a tryptophan (Trp) precursor whilst the second pathway is Trp independent (Normanly and Bartel, 1999; Benjamin and Scheres, 2008). Trp-dependent auxin biosynthesis occurs during the earliest stages of plant development, particularly during embryogenesis and germination; whereas Trp-independent biosynthesis starts in late embryogenesis and continues during vegetative growth (Normanly and Bartel, 1999). One candidate for

involvement in the Trp dependant pathway is Cytochrome P450. Cytochrome P450 can convert Trp into the auxin intermediate indole-3-acetaldoxime (IAO_x). Cytochrome P450 is expressed in young leaves and flowers - predicted sites of auxin biosynthesis (Zhao *et al.*, 2002). The *YUCCA* gene is known to be involved in the Trp-dependent pathway at the point of conversion of tryptamine into N-hydroxyl-tryptamine. *YUCCA* genes are expressed in meristems, young leaf primordia, vascular tissues (Cheung *et al.*, 2006) – all of which are suggested to be sites of auxin synthesis. The Trp-dependent pathway also includes a tryptophan-dependent decarboxylase to convert tryptophan into tryptamine. Aldehyde oxidase is likely to be involved in the last stage of auxin production. Whereby indole acetaldehyde is converted to IAA (Zhao *et al.*, 2001).

Auxin mutant analysis has been used to characterize the biosynthetic pathways. Examples of these mutants include the *superroot* (*sur*) mutants, which over accumulate auxin. *SUR1* encodes a protein similar to tyrosine aminotransferase and could be involved in both trp-independent and -dependent pathways. The similar *sur2* high auxin mutant has been found to be defective in the cytochrome P450, CYP83B1, which causes the oxidation of indole-3-acetaldoxime (IAO_x) in indole glucosinolates biosynthesis (Barlier *et al.*, 2000; Delarue *et al.*, 1998; Mikkelsen *et al.*, 2004).

Research into auxin biosynthesis is hampered by two factors. Firstly genes affecting biosynthesis may not be directly involved in auxin biosynthesis, but instead they may influence auxin accumulation. Secondly IAA exists in its free active form in the plant as only 1% of the total auxin, while the majority exists in an inactive conjugated form with amino acids and sugars (Pollmann *et al.*, 2002; Zazimalova and Napier, 2003); this creates further problems in experimental methodology and in interpreting results.

1.3.3 Polar Auxin transport

1.3.3.1 Auxin influx

Auxin in the form of IAA is a weak acid and therefore its main route of entry to the cell is via passive diffusion. It is subsequently trapped inside the cell owing to the higher pH of the cytosol, in contrast to the apoplastic deionisation of the IAA.

When auxin is entering against a diffusion concentration gradient or where there is a need to prevent diffusion into neighbouring cells, AUXIN RESISTANT 1 (AUX1), an auxin import carrier is used (Bennett *et al.*, 1996; Swarup *et al.*, 2002). AUX1 also functions to support auxin delivery to the root apex and expression of AUX1 in the root is necessary for the root gravitational response (Swarup *et al.*, 2005). Once IAA has entered the cell, active efflux transporters are therefore necessary to facilitate the movement of auxin out of the cell to overcome the disparity of pH.

1.3.3.2 Auxin efflux and the PIN transporters

The “inverted fountain” model (Figure 1.3) of auxin efflux presents the direction in which auxin is believed to be transported in the root. Auxin reaches the root through the vascular tissues of the stele and is then transported around the tip and back up towards the shoot through the ground tissues. It is proposed that auxin also crosses through the ground tissue back to the stele at periodic intervals to ensure that a steady level of auxin is maintained in the root tip (Petricka and Benfey, 2008). What makes the auxin transport system different and inspires such continued interest is the localization of the efflux and influx proteins. This localization creates polarity in the cell, hence auxin transport is often referred to as polar auxin transport and it allows the direction of the auxin signal to be maintained over long cellular distances (Benjamin and Scheres, 2008).



Figure 1.3: Diagram of “inverted fountain” auxin efflux model (Petricka and Benfey, 2008)

The driving force of the “inverted fountain” model is membrane bound efflux transporters. These efflux transporters include the PIN-formed (PIN) protein family, which either mediates or actively transports auxin out of the cell. PINs are predicted to contain 6-10 transmembrane domains, are expressed in auxin transporting tissues and are asymmetrically localized in the plasma membrane of cells. Known PINs are numbered 1-8 (Benjamin and Scheres, 2008). PIN1 is involved in both embryogenesis and organogenesis (Papanov *et al.*, 2005). PIN1 localizes to the lower side of the cells (the predicted direction of auxin transport). PIN1 expression is mainly in the stele tissue cells of the plant root and stem, important conductors of auxin, and is involved in organogenesis (Galweiler *et al.*, 1998; Panpanov *et al.*, 2005). In the epidermal layer, PIN2 is localized to the upper side of the cells, and in the lateral root cap cells it maintains the same position; in the cortex cells it localizes to the lower side of the cell (Blilou *et al.*, 2005; Muller *et al.*, 1998). Interestingly, in the elongated epidermal cells PIN2 localizes to the inner lateral membrane where the stability of the PIN2 is essential for correct functioning. PIN2 is involved in the gravitropic response, in

which elongated cells play a role in root curvature (Abas *et al.*, 2006; Sieberer *et al.*, 2000). PIN3 is also involved in the control of gravity growth responses and is expressed in following tissues; the root pericycle, the columella, the hypocotyl, the endodermis and the apical hook (Friml *et al.*, 2002; Papanov *et al.*, 2005). PIN3 is widely expressed (no polarity) in tiers 2 and 3 of the columella cells only and localizes to the lower side of vascular cells and to the lateral side in pericycle cells (Bliliou *et al.*, 2005). PIN4 is involved in embryogenesis and the stabilization of a local auxin maximum gradient in the root meristem and in generating the auxin sink below the columella (Friml *et al.*, 2002b; Sabatini *et al.*, 1999). PIN4 therefore localizes around the auxin maximum in the root meristem. PIN7 is involved embryogenesis through a role in auxin-mediated control of embryonic axis formation (Friml *et al.*, 2003). No functional analysis of the PINs 5,6 or 8 genes have yet been published (Benjamin and Scheres, 2008).

PINs are assumed to be the efflux carriers on the basis that they are a rate limiting step in auxin efflux (Petrásek *et al.*, 2006). However there is no absolute evidence PINs are the actual efflux carriers. An alternative hypothesis proposes the PINs could have an associated protein which transports the auxin across the membranes (Blilou *et al.*, 2005). There is evidence of alternative efflux protein facilitators, which further complicates the issue, in the form of the MULTIDRUG RESISTANCE (MDR)-P-GLYCOPROTEIN (PGP) family of membrane proteins. This family includes MDR1, PGP1, PGP2, PGP4, PGP19 and mutant studies have shown that polar auxin transport is severely reduced in *mdr1* mutants and double mutants *mdr1pgp1* (Gil *et al.*, 2001; Murphy *et al.*, 2002; Noh *et al.*, 2001). PIN1 has been shown to interact with PGP1 and PGP19 and this provides evidence that PINs could guide the activity of several of the MDR transporters, which transport the auxin out of the cell. PIN2 did not present the same interactions suggesting there could be specific interactions between each of the PINs and MDR transporter proteins (Blakeslee *et al.*, 2007). It is expected that resolving the crystal structures of PINs will assist with resolving this controversy (Benjamin and Scheres, 2008).

After IAA has reached its cell destination, it is sequestered into the nucleus (Paciorek and Friml, 2006) where it binds to the TIR1 receptor (or to a related AFB receptor). TIR1/AFB is a leucine-rich repeat F box protein which forms part of a SCF-type E3 ubiquitin ligase. After IAA binding, the receptor then recruits an E2 ubiquitin-conjugating enzyme which affixes ubiquitin to AUX/IAA proteins.

AUX/IAA proteins are bound to the Auxin Response Factors (ARF), Ubiquitin degrades the AUX/IAA proteins which then bind to the IAA modified TIR1/AFB, releasing the repression of the ARF. ARFs bind to a specific TGTCTC sequence or auxin response element in promoters of the target gene, causing gene expression to take place (Guilfoyle and Hagen, 2007).

A link has been theorized and some evidence presented between the *PLETHORA* genes *PLETHORA1 (PLT1)* and *PLETHORA2 (PLT2)*, PINs and therefore auxin distribution. *PLT* genes are involved with the maintenance of stem cells in the root. Mathematical models based on spatial localization of the PIN family (which took into account only passive auxin distribution) proposed a specific auxin gradient in the root (Grieneisen *et al.* 2007). *PLT* genes are expressed in a pattern which closely follows the auxin maximum gradient in the root. Auxin is known to influence the position of the stem cell niche in the root, and transcription of *PLT* genes is activated by high levels of auxin accumulation in the root tip (Aida *et al.*, 2004; Galinha *et al.*, 2007; Grieneisen *et al.*, 2007). Further evidence of this connection comes through studies of double and triple *plt* mutants; both of which had reductions in *PIN* expression (Aida *et al.*, 2004).

Throughout the complexity of the auxin biosynthesis and transport system, it would appear regulation of auxin transport and gene expression depends on more than the auxin transport mechanisms. Without the correct cellular membrane structure and the membrane composition it is hard to perceive how the intricate complexes and array of proteins involved in auxin transport would function correctly.

1.4 The plant hormone ethylene

Ethylene has a simple structure and is unique in the class of plant hormones by existing in a gaseous form (Guo and Ecker, 2004). It has multiple roles in plant development and interactions with the environment. Ethylene is well known for its involvement in fruit ripening but it also plays a vital role in root elongation, root hair formation (Stepanova *et al.*, 2007), seed germination, seedling growth, floral initiation, leaf and flower senescence, stem cell division and it has been linked to stress responses (Zhu and Guo, 2008). Previously the bulk of plant research into ethylene has focused on aspects of the triple response, where a plant grown in the dark

in the presence of ethylene exhibits a shortened wider hypocotyl, shortened roots and a prominent apical hook (Stepanova and Ecker, 2000).

More recently attention has turned to the potential interactions between ethylene and other signalling molecules (including auxin) and how these interactions may explain some of the unanswered questions concerning plant development (Vandenbussche and van der Straeten, 2007).

1.4.2 Ethylene Biosynthesis

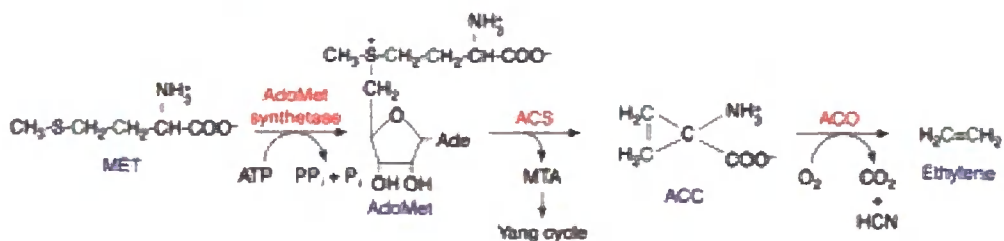


Figure 1.4: Ethylene biosynthesis (Chae and Kieber 2005)

Ethylene biosynthesis in higher plants starts with the amino acid methionine. The rate limiting step occurs early in the process, where S-adenosyl-L-methionine (AdoMet) is converted to 1-aminocyclopropane-1-carboxylate (ACC) by ACC synthase (ACS). The final step is oxygen-dependent and consists of the conversion of ACC by ACC oxidase into ethylene (Chae and Kieber, 2005; Fukao and Bailey-Serres 2007; Figure 1.4).

1.4.3 Ethylene transport

Ethylene in its gaseous form can diffuse passively into the plant through cellular membranes or through intracellular spaces or symplast (Alonso *et al.*, 2004; Cameron and Yang 1982). When long distance transport is required the precursor ACC is released into the vascular tissue and transported to the required site of action before being converted to ethylene (Colmer, 2003).

1.4.4 The ethylene signalling pathway

Whilst the full ethylene signalling pathway(s) has yet to be discovered, evidence is emerging of several pathway components of this pathway and their roles.

The ethylene molecule is bound (with a copper co-factor) by integral membrane receptors. Five such receptors have been identified in *Arabidopsis*; ETHYLENE RECEPTOR1 (ETR1), ETHYLENE RECEPTOR2 (ETR2), ETHYLENE INSENSITIVE4 (EIN4), ETHYLENE RESPONSE SENSOR1 (ERS1) and ETHYLENE RESPONSE SENSOR2 (ERS2) (Guo and Ecker, 2004). The receptors are two component systems in that the ethylene molecule binds to the N terminus of the receptor, which acts as a sensor and activates the intracellular protein kinase domain (Chang *et al.*, 1993; Stepanova and Ecker 2000). The binding action inactivates the receptor sensors and inhibits CONSTITUTIVE TRIPLE RESPONSE1 (CTR1), a further negative regulator of the signalling pathway. Transduction of the ethylene signal is believed to take the form of a phosphorylation cascade similar to (MAPK), though this is still under debate (Kendrick and Chang 2008; Hahn and Harter, 2008). EIN2, EIN3, EIN5 and EIN6 function downstream of CTR1 and are positive regulators of the pathway, though their exact function and positions in the pathway are unclear. There is evidence that the signal interacts with the integral membrane protein, EIN2. EIN3 acts downstream of EIN2 where it binds to the EBS element contained in the ERF1 gene. ERF1 expression is activated and it then interacts with and activates the GCC-box of ethylene response genes (Stepanova and Ecker, 2000).

1.5 Phytosterols

The focus of the work described in this thesis is on mutants, which are defective in sterol biosynthesis, the *hydra* mutants. Before considering their mutant phenotypes, I will describe the roles of sterols in plant biology.

1.5.1 What are phytosterols?

The nomenclature of plant sterols, also known as phytosterols, is not precisely defined due to complications in gaining an international consensus over the standard to use and the variation in structure of the high number of phytosterols known (Moreau *et al.*, 2002). The simplest definition is a steroid bearing a hydroxyl group at the C3 position and a lipophilic character (Nes, 1977).

The sterols in plants all contain a basic nuclear structure (Figure 1.5):

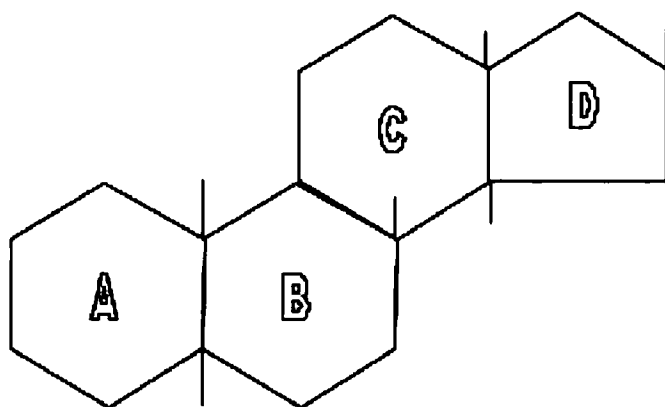


Figure 1.5: Basic nuclear structure of a phytosterol.

All sterols are structurally very similar regardless of their position in the biosynthesis pathway and are easily recognisable from the central structure (Figure 1.6):

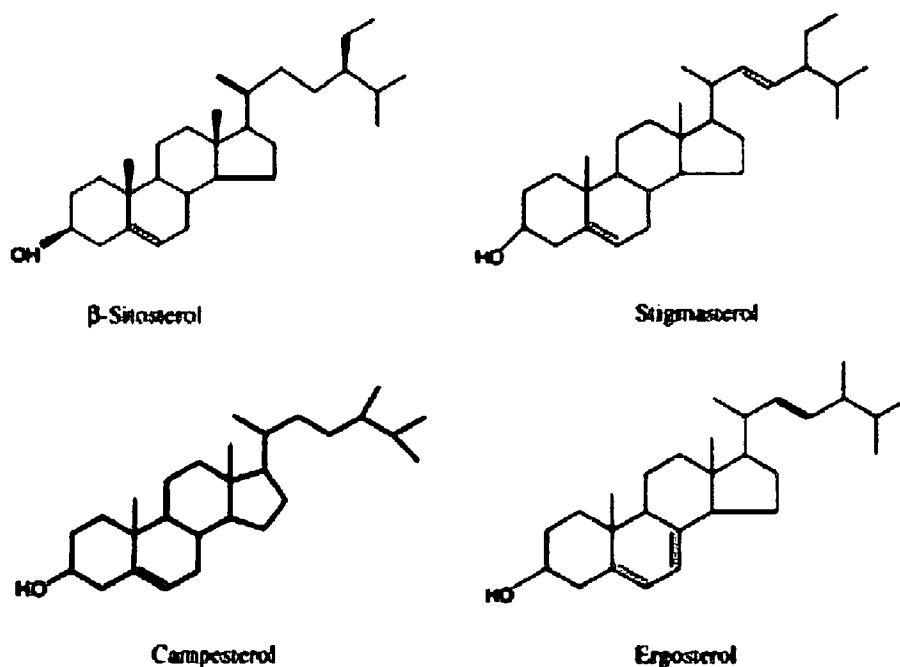


Figure 1.6: Examples of the structure of typical phytosterols (Fernandes and Cabral, 2007)

Phytosterols belong to the over 4000 member strong triterpene natural product family, and over 100 of the triterpenes are phytosterols (Moreau *et al.*, 2002). However the lipophilic nature of sterols makes recovery of sufficient quantities for research from natural sources problematic and this has resulted in slow progress in

research in this field, although recent technological improvements in phytosterol extraction are expected to correct this (Fernandes and Cabral., 2007) .

1.5.2 The sterol biosynthesis pathway in plants

The sterol biosynthesis pathway in plants can vary between different species, seen as the presence of different products and enzymes creating particular sterol profiles for individual species (Kircher and Rosenstein 1973; Lindsey *et al.*, 2003). However the general route for sterol biosynthesis starts with squalene, a product arising from Farnesyl-PP in the steroid biosynthesis pathway. From squalene, squalene-2,3-oxide is produced. Squalene-2,3-oxide cyclises to cycloartenol which is isomerised to obtusifoliol. Demethylation creates 4 α -methyl-5 α -ergosta-8,14,24-trien-3 β -ol which is reduced to 4 α -methylfecosterol. Isomerisation of the Δ 8(9) double bond to Δ 7(8) creates 24-methylenelophenol that is demethylated to episterol. Episterol is dehydrogenated to 5-dehydroepisterol and hydrogenated to 24-methylencholesterol. Isomerization of the Δ (24)28 double bond to Δ 4(25) produces 24-methylidesmosterol (Lindsey *et al.*, 2003; Schrick *et al.*, 2002; Zullo and Adam, 2002). 24-methylidesmosterol is a branch point in the sterol pathway and two products arise from it. One product is campesterol; the start point for the brassinosteroid pathway. The second product is 24-ethylidenelophenol, which leads the remainder of the phytosterol pathway to the end product of stigmaterol (Li and Chory, 1999; Figure 1.7).

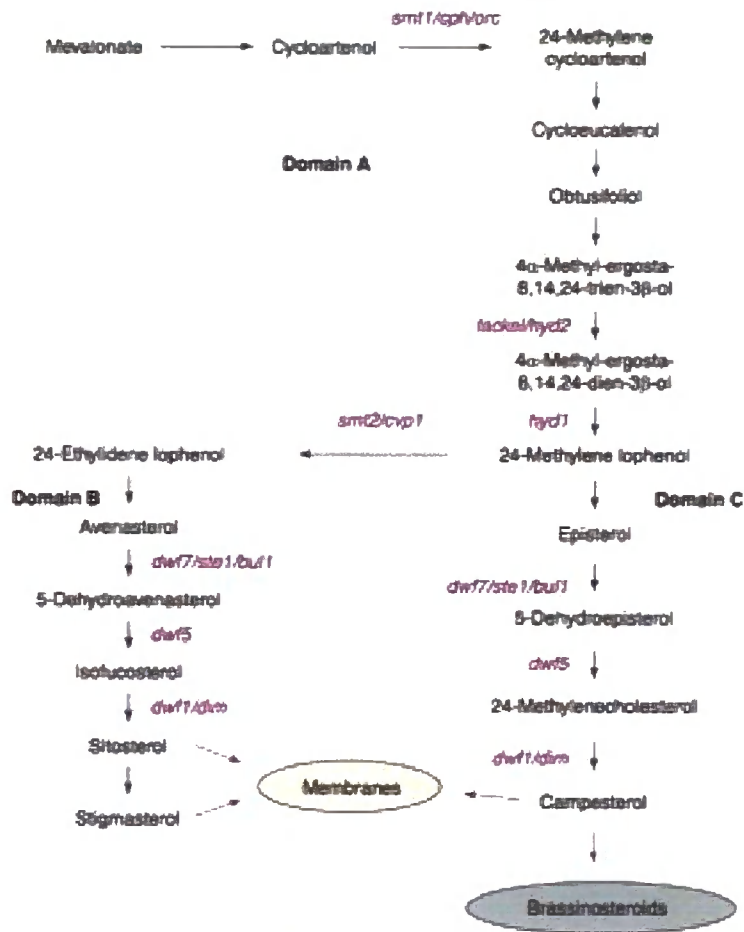


Figure 1.7: The sterol biosynthesis pathway in *Arabidopsis* (Lindsey *et al.*, 2003)

1.5.3 Sterol concentrations in plants

Sterols are present in plants in low concentrations (0.01-0.1% of wet weight on average). However dry tissue and organs such as pollen and seeds can contain 1% sterol. Within these percentage figures are two distinct groups of sterols; the dominant sterols and the trace sterols. Dominant sterols make up 90% of the total sterol content of a plant and are principally composed of 4,4,14-trimethyls. Examples include sitosterol and campesterol.

Trace sterols make up the remaining 10% of sterol content and are of two possibly structures:

- 1) Sterols bearing one or more of 5 methyl groups on the C4, or
- 2) Sterols with an $\Delta 7$, $\Delta 8$ or $\Delta^{24(28)}$ bond.

Examples of trace sterols include cycloartenol and $\Delta 7$ -avenaserol (Moreau *et al.*, 2002; Nes, 1977).

1.5.4 The functions of sterols in plants

The main function of sterols is one of huge structural importance to all living organisms as sterols represent a key component of cellular membranes. The cell membrane provides architectural support to the cell and due to the hydrophylic and hydrophobic nature of sterols in the membrane allows for free trafficking of molecules in and out of the cell with the concentration gradient; and against the concentration gradient with the aid of a protein transport mechanism embedded in or attached to the membrane itself (Hac-Wydo *et al.*, 2007; Thole and Nielsen, 2008).

Sterols are considered to be involved in stabilizing membranes. However evidence has emerged which suggests that some sterols, particularly stigmasterol can de-stabilize the membranes (Moreau *et al.*, 2002). Research, which looked at interactions between several phytosterols, indicated that the structure of the phytosterol does not affect the stoichiometry of complexes formed between phospholipids but can influence the stability of complexes formed through weaker interactions between the components (Hac-Wydo *et al.* 2007). Sterols also act as precursors of the signalling hormones brassinosteroids.

1.5.5 Brassinosteroids

Since the 1930s, considerable interest has been shown in a class of plant hormones that cause often dramatic effects on plant growth and growth regulatory activity (Zullo and Adam, 2002). Brassinosteroids are known to induce stem elongation, the growth of pollen tubes, root initiation, to induce ethylene biosynthesis, cause proton pump activation in membranes and have a role to play in gene expression (Li and Chong, 1999). Further research has found these hormones to be lipid based and the term brassins was assigned to a number of similar hormonal substances extracted from plant tissue. Brassin active compounds were isolated and purified from rapeseed pollen and the resulting crystalline substance was discovered to be brassinolide, the first brassinosteroid isolated (Moreau *et al.*, 2002; Noguchi *et al.*, 2000). Further experiments from research groups around the world rapidly discovered new brassinosteroids and their precursors. Brassinosteroids were found to display

variability in structure but two groups were characteristic of natural brassinosteroids and brassinosteroid analogues. Brassinosteroid analogues are compounds, which show structural similarity with natural brassinosteroids or present brassinolide activity (Zullo and Adam, 2002). Brassinosteroid synthesis starts in the sterol biosynthesis pathway where campesterol is produced. Campesterol is then reduced to campestanol and through the brassinosteroid specific pathway is converted to brassinosteroids (Nouguchi *et al.*, 2000; Souter *et al.*, 2000). Brassinosteroids therefore have a strong influence in plant growth and plant development.

1.6 The *hydra* mutants of *Arabidopsis*

1.6.1 The isolation of the *hydra* mutants

The *hydra* mutants were identified in a mutant screen for genes affecting embryo and seedling development, and are the focus of this project, being defective in genes encoding enzymes in sterol biosynthesis. The genes were cloned using insertional mutagenesis, a commonly used method to identify and isolate genes that play significant role(s) in plant growth and development. In insertional mutagenesis, the pathogenic properties of the tumour-forming bacterium *Agrobacterium tumefaciens* are exploited. A T-DNA –containing plasmid from *Agrobacterium tumefaciens* is manipulated to contain required promoters and/or marker genes (Parinov and Venkatesan 2000; LaCroix *et al.*, 2006). The host plants are ‘dipped’ into a solution containing the bacteria. The bacteria are taken up into the plant cells and the T-DNA inserts itself into the host genome, causing a mutation. This may result in a phenotypic change, which can be analysed and put through further experimental work to identify the original function and position of the disrupted gene.

hydra1-1 was initially believed to have been created from a T-DNA insert but was later found to be a point mutation in the *HYDRA1* gene. The *hydra1-2* allele (created by Ken Feldman) is a genuine T-DNA insert. The *hydra2* was also created by a T-DNA insert and was found to be allelic to the *fackel* mutant. The allelic relationship was confirmed by crossing *hydra 2*

with *fackel* mutants and *hydra1-1* with *hydra1-2* (Schrick *et al.*, 2000; Topping *et al.*, 1997). The *hydra1* mutation is in the sequence encoding the sterol $\Delta 7,8$ isomerase (Souter *et al.*, 2002) and the *hydra2/fk* T-DNA insert is in a sequence encoding the C14 reductase in the sterol pathway (Schrick *et al.*, 2000).

In this work *hydra1* is the term used to refer to the *hydra1-2* T-DNA insert mutation and *fk^{hyd2}* to refer to the *hydra 2/fackel* mutant; *hydra* refers to both mutant forms.

1.6.2 The *hydra* phenotype

hydra mutants display a distinct phenotype with short wide roots, a short hypocotyl and multiple cotyledons giving a cabbage appearance to the shoot. Overall *hydra* seedlings are dwarfed compared to wild-type seedlings of the same age at all stages of development (Topping *et al.*, 1997; Figure 1.8).

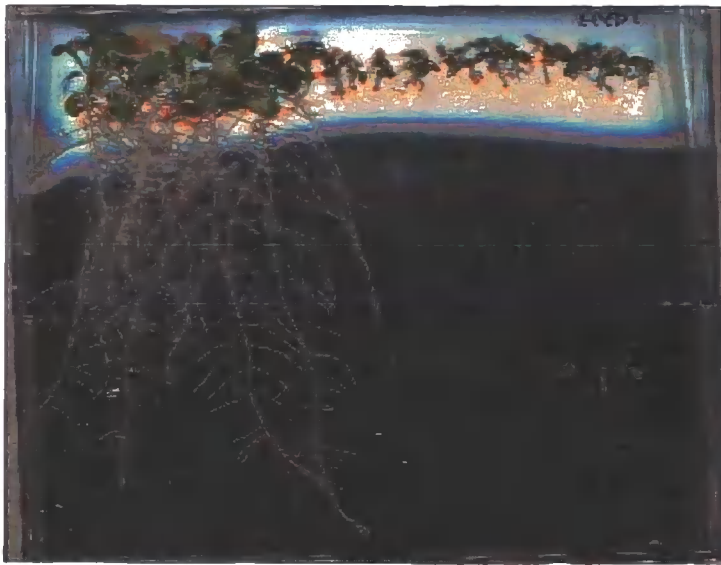


Figure 1.8: (left) wild-type *ws* seedlings, (right) *hydra1* seedlings, all 14 dpg.

hydra mutants have several other variable phenotypic defects that may not present in every seedling. These include defects in the number and placement of root hairs and trichomes on the leaf surface, erratic control of radial cell division and axial cell expansion, defects in the patterning of apical and basal structures and malformed or absent cell walls (Schrick *et al.* 2000; Souter *et al.* 2002; Souter *et al.* 2004; Topping *et al.* 1997; Figure 1.9).

Many of these defects are typical of abnormal control of auxin and/or ethylene biosynthesis or signalling.



Figure 1.9: Lugol staining of cellular patterning in *ws* (A) and *hydra1* (B) at 7 dpv

The point at which *hydra* mutants first deviate from wild type was examined by screening the embryonic contents of siliques at each stage for the first signs of *hydra* defects. Siliques were taken at various ages to follow through all the embryonic development stages. For *hydra1* mutants, no defects were observed until the globular stage, where the mutant embryos were smaller and an irregular shape. At later stages the mutant embryos had disorganised cellular structure in all tiers, no clear protoderm is present and cell component walls are positioned abnormally (Souter and Lindsey 2000; Topping *et al.* 1997). The first signs of deviation from wild type in *fk^{hyd2}* were traced back to the globular stage and the same defects observed as for *hydl*. In addition it was observed for *fk^{hyd2}* mutants the inner most cells fail to elongate and this contributed to a failure to produce daughter cells of similar sizes. In wild type embryos, cell elongation is followed by cell divisions in the inner most cells which give rise to elongated basal cells and small apical cells (Jang *et al.*, 2007; Schrick *et al.*, 2000). Neither *hydra1* or *fk^{hyd2}* mutants developed a characteristic heart shape embryo. When the wild type embryos presented the torpedo shape, both *hydra1* and *fk^{hyd2}* mutant embryos were showing a malformed heart shape caused by abnormal cell patterning and growth in the embryo (Topping and Lindsey, 1997). The mature curled cotyledon phenotype seen in wild-type is not seen in either *hydra1* or *fk^{hyd2}* mutant embryos. The mature *hydra* embryo has a misshapen

rounded basal structure and an apical structure with multiple cotyledon primordia. Transverse sections of *fk^{hyd2}* mutant embryos have revealed multiple disorganised tissue layers at this stage (Schrick *et al.*, 2000). The mutant embryos, like mutant seedlings, were consistently smaller and wider than wild type at all stages.

fk^{hyd2} mutants display a more severe phenotype than *hydra1* mutants with shorter roots, slower growth and a shorter lifespan. The *hydra1* mutant lifespan is a maximum of 40 days post germination (dpg) but root cell division may cease at 2 weeks post germination. The *fk^{hyd2}* mutant stops growth in all tissues at 10-14 days post germination and rarely survives past 21 dpg (Souter *et al.* 2002; Figure 1.10).

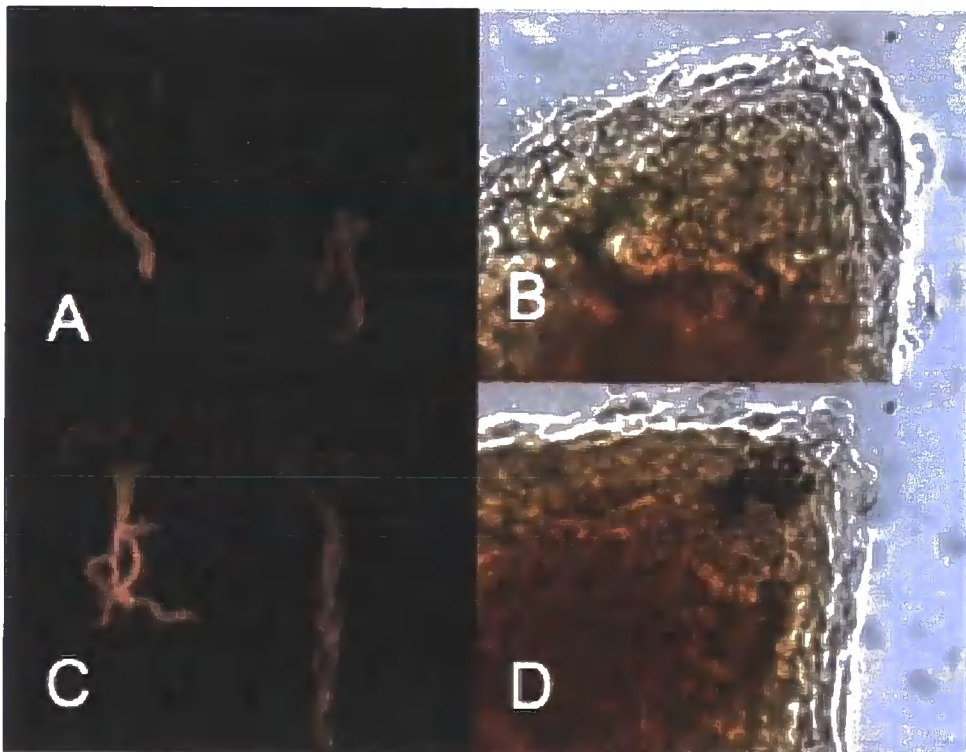


Figure 1.10: (A) *fk^{hyd2}* seedlings at 14 dpg (B) lugol stain of root showing loss of stain at 14 dpg indicating loss of cell activity. (C) *hydra1* mutants at 14 dpg (D) lugol stain of root showing abnormal but no loss of stain at 14 dpg.

Both *hydra1* and *fk^{hyd2}* homozygous mutants are seedling lethal and will not propagate on soil. An extra vernalization period of 7 days at 4°C is required in order to germinate *hydra* seeds.

1.6.4 The sterol pathway and the *hydra* mutants

Eukaryotic cell membranes are composed of sterols and the permeability and fluidity of membranes is dependent on the proportions of different of sterols, and serve as precursors for steroid signalling molecules (brassinosteroids) as described in Section 1.4 above. During the sterol biosynthesis pathway both $\Delta 7,8$ isomerase and C14 reductase are essential enzyme catalysts producing the next product in the pathway. The C14 reductase enzyme is found earlier in the main sterol pathway than $\Delta 7,8$ isomerase and both are essential for correct sterol biosynthesis (Schrick *et al.* 2000; Souter *et al.* 2004). Differences in function of the enzymes presumably explain the more severe phenotype of the *fk^{hyd2}* mutant compared to the *hyd1* mutant, and the difference in lifespan between the mutants. The function of sterols as signalling molecules and importance in controlling the properties of cell membranes could explain why hormone signalling in the *hydra* mutants is defective.

1.6.5 Research into the *hydra* mutants: the findings so far:

Previous research into the *hydra* mutants has concentrated on two areas 1) the characterisation and documentation of the *hydra* phenotype and 2) probing the hormone signalling defects to find the cause of the *hydra* phenotype. Structural features of the mutants have been described above. In addition, Souter *et al.* (2004) quantified the root growth of *hydra1* and *fk^{hyd2}* mutants compared to wildtype. Seedlings were germinated and grown on plates and the root length measured every three days post germination. As expected the wild type seedling increased at a steady rate throughout and the root growth of the *hydra* mutants was considerably reduced in comparison. The *hydra1* seedling growth showed a sharp increase at 6 days and then remained at a steady growth rate until death at ~30 days. *fk^{hyd2}* root growth was not significantly different from *hydra1* until day 9, by which time the *hydra1* roots were longer. By day 12, *fk^{hyd2}* growth declined and had ceased completely by day 18 giving further evidence to the observation the *fk^{hyd2}* mutant has a significantly more defective phenotype than the *hydra1* mutant.

Phenotypic investigation by Schrick *et al.* (2000) discovered multiple shoot meristems in some *fk^{hyd2}* by using a *KNAT2* gene promoter and GUS-reporter gene.

Some uncertainty over the presence of hypocotyl tissue in *fk^{hyd2}* seedlings existed due to the short seedling bodies. A test for the presence of hypocotyl tissue was performed consisting of germinating *fk^{hyd2}* mutants with wild type as a control, in the dark. The wild type seedlings demonstrated a standard etiolation response: apical hook formation and elongation of the hypocotyl as the plant attempted to find light. The *fk^{hyd2}* seedlings however displayed a defected response with a much reduced elongation of the hypocotyl accompanied with the development of 'callus-like' tissue. The conclusion drawn from the test was the *fk^{hyd2}* and *hydra1* mutants could sense and respond to the dark but were unable to organise the correct growth response (Schrick *et al.* 2000, Topping *et al.* 1997). This shows the mutants have defective cell elongation mechanisms.

The second area the research has focus on molecular and signalling features of the *hydra* mutants. Souter *et al.* (2004) characterized the spatial activity of the *HYDRA1* gene promoter. 2 kb of the 5' flanking region of the *hydra1* gene was cloned upstream of the *gusA* reporter gene and the resulting *pHYDRA1::GUS* construct inserted into *Arabidopsis thaliana*. Using histochemical techniques the GUS activity could be visualised. The *pHYDRA1::GUS* gene fusion was active in primary roots, lateral roots and a higher level of activity found in the root tip. Activity decreased in correlation with the increase of the age of the tissue. In the shoot promoter activity was found in the stipules but not in the shoot apical meristem. Semi-quantative RT-PCR confirmed the expression of the *HYDRA1* gene in the wild type and heterozygous seedling root. As expected no expression was found in the *hydra1* mutant as it is the *HYDRA1* gene which is disrupted by the T-DNA insert. These findings confirm that the *HYDRA1* gene has an essential function in correct root growth and/or development processes.

The bulk of the remaining research into *hydra* mutants has focused on ethylene biosynthesis or signalling. Ethylene became as a focus of the research due to the phenotype of the *hydra* mutants and the relatively unknown complex interactions between plant hormones, cytokinins, peptide

signalling molecules and sterol signalling in the control of plant growth and development (Souter *et al.*, 2002; Vandenbu and Der Straeten 2007). The activities of the plant hormone auxin which can both promote growth and inhibit growth in different tissues can be modulated by cytokinins.

Cytokinins can promote ethylene biosynthesis, therefore potentially providing a link between the activities of the two major plant hormones, auxin and ethylene, all three of which can interact with signalling regulatory molecules such as peptides and sterols (Souter *et al.*, 2004).

Given that the *hydra* mutants affect the sterol biosynthesis pathway, then this could affect membrane function or alter activity of signalling molecules residing in the membranes. This in turn could affect auxin and ethylene signalling pathways, such as through altered receptor function or hormone transport mechanisms..

Pharmacological experiments on *hydra* were carried out to characterize defects in ethylene signalling (Souter *et al.*, 2002; Souter *et al.*, 2004). Aminoethoxyvinylglycine (AVG) is an inhibitor of the ethylene biosynthetic enzyme 1-aminocyclopropane-1-carboxylic acid (ACC) synthase (Baker *et al.*, 1982). Silver ions (AgNO₃) inhibit ethylene receptors by disrupting intermolecular signalling within the receptor protein (Bayer, 1979; Binder *et al.*, 2007). *hydra* seedlings containing the *CYCA1::CBD::GUS* construct (a marker of cell division activity), were transferred to plates containing AVG or AgNO₃. By day 18, no staining was present suggesting inhibition of ethylene biosynthesis did not rescue the mutant phenotype. However cell division activity was retained in mutants treated with AgNO₃, suggesting altered ethylene signal receptors function in the mutants. Ethylene assays also showed that the *hydra* mutants do not overproduce ethylene gas (Souter *et al.*, 2002). This evidence suggests that the ethylene receptors are operating in a state of heightened activity and this is in part at least contributing to the failure of mitotic activity and hence the short lifespan of a *hydra* mutant.

Further genetic experiments used the *ethylene resistant1 (etr1-1)* mutant, which is defective in a member of the ethylene receptor family; and the *ethylene insensitive2 (ein2)* mutant which encodes a membrane-bound component of the ethylene signalling pathway that is downstream of the

receptor family. Both mutants were crossed separately with *hydra1* and both the *ein2-hydra1* mutants and the *etr1-1-hydra1* mutants showed a partial rescue of the root phenotype with significantly longer root growth than in single *hydra1* mutants. This is further evidence that the ethylene receptors in the *hydra* mutants are defective (Souter *et al.*, 2004).

The vascular patterning defects present in the *hydra* mutants suggest defective auxin transport or signalling (Mattsson *et al.*, 1999) and *hydra* exhibit enhanced responses to auxin (Souter *et al.*, 2002). Auxin regulated promoters *DR5* and *IAA2* linked to a *GUS* reporter gene are misexpressed in the *hydra* mutants. This misexpression was rescued by blocking ethylene synthesis suggesting the auxin defects are downstream of defects in ethylene signalling (Souter *et al.*, 2004). The sterol *smt1^{orc}* mutant has a disrupted gene which encodes STEROL METHYLTRANSFERASE 1 and has columella organelle positioning defects. *smt1^{orc}* presented misexpression of the auxin reporter *DR5::GUS* and membrane localization of the PIN1 and PIN3 proteins were abnormal however the AUX1 influx carrier was normally localized (Willemson *et al.*, 2003). *hydra* mutants also present defects in the columella, Immunolocalization experiments found PIN1 and PIN2 were localized normally in *hydra1* and *fk^{hyd2}* however PIN3 localization changed at 9 dpg after which point it shifted from the upper tier of the columella to the columella cell initials. By 14 dpg PIN3 had disappeared although treating seedlings with silver rescued PIN3 localization.

Finally external application of brassinosteroids has been used successfully in other mutants to rescue the phenotype (Noguchi *et al.*, 1999), however in both *hydra1* and *fk^{hyd2}* mutants this fails to rescue the phenotype (Jang *et al.*, 2000, Schrick *et al.*, 2000, Souter *et al.*, 2002) suggesting the gene disruption in *hydra* is severe; adding brassinosteroids externally should have corrected the phenotype by making available compounds the plant was lacking due to the incomplete sterol pathway. Schrick *et al.* (2000) have theorised there could be sterol based signalling molecule which is not present in *fk^{hyd2}* that regulates cell expansion. How a sterol based signalling molecule could be transported in a plant and through membranes intact is a matter of conjecture.

Although the phenotype of the *hydra* mutants has now been well documented, the reason a disruption in a sterol enzyme produces a phenotype typical of ethylene and auxin defects and the possible mechanisms and signalling pathways involved still needs to be determined.

1.7 Molecular tools

Advances in molecular biology have made cloning genes a matter of routine and continued research into *Arabidopsis* gene function has resulted in the creation or discovery of several gene promoters which can be utilised to switch genes on in a tissue specific manner.

Two of these promoters are *DR5* and the *POLARIS* gene promoter (*PLS*). *DR5* is a synthetic auxin response element which expresses in the presence of auxin and has been previously used for auxin distribution patterning experiments (Sabatini *et al.*, 1999; Mattsson *et al.*, 2003). *PLS* is a naturally occurring promoter of the *POLARIS* gene which expresses in the root cap tissues (Casson *et al.*, 2002). Another system of promoter-driven tissue specific gene expression is the GAL4 based *UAS::GFP* lines. This is a two component system originally developed in *Drosophila* and modified for use in *Arabidopsis* by Dr. Jim Haseloff and his team at the University of Cambridge, U.K (Haseloff *et al.*, 1997; Laplaze *et al.*, 2005; Figure 1.11). In a simplified form the system works as follows:

- 1) GAL4 is placed under the control of an enhancer element in one plant line.
- 2) A second line contains the chosen gene for expression under the control of an Upstream Activated Promoter (*UAS*). In the absence of GAL4 this will remain switched off.
- 3) The two plant lines are crossed together to combined the components and resulting in a section of progeny which are expressing the chosen gene in the target tissue.



Figure 1.1: Simplified diagrammatic representation of the *GAL4* based *UAS::GFP* line system. Based on Prof J Haseloff's animation

(<http://www.plantsci.cam.ac.uk/Haseloff/construction/GAL4/GALtrapscheme.html>)

ENH: plant enhancer element, *GAL4* protein expression: ● *GFP* protein expression: ● *HYDRA* gene expression: ●

This technology ensures a simple and effective way to express specific genes in specific root tissues of plants, to find evidence for the function of specific root tissues, the hormone signalling pathways involved and (in this project) indications of the role phytoosterols may have to play in correct plant development. Therefore this system is used in the current project in parallel with the *DR5* and *PLS* promoters to activate *HYDRA* gene expression and sterol biosynthesis in specific tissues in *hydra* null mutants, to investigate cell autonomy of sterol signalling effects in *Arabidopsis*.

1.8 Project aims and objectives

The overall aim of the project is to determine whether sterols function in cell autonomous or non-autonomous ways to regulate root development in *Arabidopsis*. The approach is to express sterol biosynthetic genes in specific root cell types in *hydra* null mutants, and to determine the extent of phenotypic rescue in the transgenics. Previously Dr Eleri Short had successfully made plant lines containing the following constructs : *pPLS::HYDRA1*, *pPLS::HYDRA2*, *pDR5::HYDRA1*, *pDR5::HYDRA2*, *pUAS::HYDRA1*. Dr Eleri Short contributed in the crossing process of the *PLS* and *DR5* lines into the *hydra* backgrounds. Dr Gul Ulke supplied the line containing the construct *pUAS::HYDRA2*.

Specific objectives are as follows:

1) To create, by genetic crossing, plant lines containing a copy of the respective wild type *HYDRA* gene expressed under the transcriptional control of one of the following

root tissue specific promoters: *PLS* (*polaris*), *pUAS::GFP* (epidermis), *pUAS::GFP* (endodermis), *pUAS::GFP* (pericycle), *pUAS::GFP* (vasculature tissue), *pUAS::GFP* (root cortex) or under auxin responsive *DR5*.

2) Genotyping of all plants used in experiments to confirm the presence of the transgenes in specific mutant backgrounds (*hydra* vs. wild-type)

3) To analyse the different plant lines for evidence of phenotypic rescue with particular attention to root development. This analysis will consist of:

- a) Root length measurements.
- b) Cell patterning analysis, using Lugol staining of the root to determine columella organization and light microscopy.

2.0 Materials

2.1.1 Molecular Biological and Chemical Reagents

Analytical grade reagents used in this work were supplied through Sigma-Aldrich (Poole, UK) unless otherwise stated.

IPTG was supplied by Metford Laboratories Ltd (Surrey, UK) and X-Gal supplied by Bioline (London, UK).

Taq DNA polymerase supplied with Mg⁺⁺ free 10x reaction buffer and 50 mM MgCl₂, Hyperladder I and Hyperladder IV were obtained from Bioline (London, U.K.). Oligodeoxynucleotide primers were ordered from and synthesised by MWG-Biotech (Eurofins MWG Operon, Ebersberg, Germany).

2. 1.2 Molecular Biology Kits

- 1) TOPO® TA cloning Kit with pCR2.1®-TOPO® TA vector (Invitrogen, Paisley, U.K.)
- 2) Roche Agarose Gel Purification kit (Roche Applied Science, Indianapolis, U.S.A.)
- 3) Qiagen Spin Miniprep kit (Qiagen, Crawley, U.K.)

2. 1.3 DNA Sequences and Maps

DNA sequences were supplied by Dr Eleri Short for *UAS* primer design (for sequences see Appendix 2).

Construct gene maps were supplied by Dr Jennifer Topping and reproduced in this work with minor alterations.

2. 1.4 Media and Cell Culture Conditions

Phytigel media for square 100mm x 100mm sterillin plates

(Per 1 litre of dH₂O)

Phytigel	5g
Sucrose	10g

Murashige and Skoog medium ($\frac{1}{2}$ MS₁₀) 2.2g
(pH adjusted to 5.8 with 0.1M KOH)

Soft-set Bacto-Agar for Petri dishes

(Per 1 litre of dH₂O)

Bacto-agar (Difco, UK) 5g

Sucrose 20g

Murashige and Skoog ($\frac{1}{2}$ MS₁₀) medium 2.2g

(pH adjusted to 5.8 with 0.1M KOH)

Liquid LB (Luria-Bertaini) media

(Per 1 litre of dH₂O)

Select tryptophane 10g

Select yeast extract 5g

NaCl 5g

(pH adjusted to 7.5 with 0.1M KOH)

LB plate media

(Per 1 litre of dH₂O)

Select tryptophane 10g

Select yeast extract 5g

NaCl 5g

Bacto-agar (Difco, UK) 15g

(pH adjusted to 7.5 with 0.1M KOH)

Cultures were grown in liquid LB media in test tubes (shaken at 200 rpm) or in LB media plates, incubated at 37°C.

IPTG and X-Gal and Kanamycin were added to media in the concentrations and volumes as detailed in the TOPO® TA cloning Kit instructions.

Kanamycin was added to Liquid LB media as detailed in 2.2.10.

2. 1.5 Plasmid Vectors

pCR2.1®-TOPO® TA *e.coli* vector is supplied with the TOPO cloning kit from Invitrogen (Paisley, U.K.). The vector has 3' thymine overhangs for ligation of PCR *Taq* amplified products with adenine end bases and EcoR I sites either side of the insertion site for excising the insert.

Δ pcirce-gus vector was supplied by Dr Jennifer Topping. Δ pcirce-gus is a binary vector derived from the vector pBIN19 (Bevan, 1984) which is used in *Agrobacterium*-mediated gene transfer.

2. 1.6 Plant lines

hydra plant line selection

Three lines of the *hydra1* mutant are available; *hydra1-1*, *hydra1-2* and *hydra1-3*. *hydra1-1* contains a point mutation and is in the C24 ecotype background. *hydra1-2* contains a single T-DNA insert and is in the Wassilewskia (*ws*) ecotype background. The only available line for the *fk^{hyd2}* mutant is in the *ws* ecotype, and is also an insertion mutant. Therefore *hydra1-2* was selected as the line to use for this work to allow direct comparison between the two mutants without having a possible complication in the form of natural variation between ecotypes impacting on results. *hydra1-2* was created and donated by Dr Ken Feldman and *fk^{hyd2}* by Dr Jennifer Topping and Professor Keith Lindsey. *hydra1-2* and *fk^{hyd2}* seed was supplied by Dr Jennifer Topping through Dr Eleri Short.

POLARIS (PLS) promoter lines

The *POLARIS* gene promoter is active in the root cap and the initial root vascular tissue (Topping and Lindsey, 1997; Casson *et al.*, 2002). Lines containing the constructs *pPLS::HYDRA1* and *pPLS::HYDRA2* were created and supplied by Dr Eleri Short in the *ws* background.

DR5 promoter lines

DR5 is a synthetic auxin responsive promoter (Sabatini *et al.*, 1999) and is expressed where auxin accumulates in the plant. Lines containing the construct

pDR5::HYDRA1 and *pDR5::HYDRA2* were created and supplied by Dr Eleri Short in the *ws* background.

UAS promoter construct lines

Lines containing the constructs *pUAS::HYDRA1* and *pUAS::HYDRA2* were created and supplied by Dr Eleri Short and Dr Gul Ulke respectively.

2. 1.7 Greenhouse Growth Conditions

Seedlings used for crossing or grown for seed were grown under greenhouse conditions (22°C, 16 hours light: 6 hours dark) in Gem Multi-purpose compost (Accrington, U.K.) and Gem horticultural silver sand at a ratio of 4:1. The compost-sand mix was transferred into 24 well trays and treated with Intercept systematic insecticide (Levinton Horticulture ltd, UK). 0.5g Intercept was dissolved in 1.5 ml of dH₂O and dispersed over the soil using a watering can. Seedlings were transferred from sterile plates at 10 days after germination into 24-well trays and placed on top of well watered matting. Seedlings were placed under cover for the first 7 days in the greenhouse.

Seedlings grown for seed were screened for the presence of GFP prior to planting out and (after silique development) screened for *hydra* embryos (if appropriate for the line). Mature plants positive for the relevant characteristics were bagged and watering continued until the siliques turned brown. Then the seeds were collected from the plant and dried in standard Petri dishes for 1 week before being collected into labelled seed tubes.

Method

2.2.1 Crossing

All plant crosses were performed using the 'general method' from The European Arabidopsis Stock Centre (NASC) website (http://arabidopsis.org.uk/InfoPages?template=crossing;web_section=arabidopsis). All work was performed on a Zeiss STEMI SV8 dissecting stereomicroscope (Carl Zeiss Ltd, Welwyn Garden City, Herts, U.K.).

Six plants were used for each cross, the crossed plants were labelled and placed in the greenhouse to allow silique development. Siliques were covered by seed collecting tubes at maturity to ensure no seed was lost due to unexpected shattering of the silique. The F1 seed was grown up and the resulting F2 seed grown up and analysed for evidence of a successful prior cross before crossing in the next line. The Haseloff GFP lines acquired (N9177, J0272, J3611, J0661 and J0671) were in *Columbia (Col-0)* background. As this work required all lines to be in *Wassilewska (ws)* background, the Haseloff GFP lines were each crossed 4 times into *ws*.

Each UAS line containing a construct e.g. *pUAS::HYDRA1* consisted of a further 4-6 lines all containing the same construct but with a different dipping pot origin. A result which consistently appears in all of these lines can be assumed to be genuine and not an artefact of an incomplete transformation. Each line containing the *UAS* promoter construct required crossing with the Haseloff lines. GFP positive plants were then crossed into the relevant *hydra* heterozygous background. F2 plants were genotyped and screened for rescued phenotypes.

Plants containing constructs under the control of the *PLS* or *DR5* promoter only required crossing with *hydra* heterozygotes, and F2 plants were genotyped and screened for rescued phenotypes: This seed from the final cross was used for experimental analysis through root growth experiments and observations of persistent deviations from wild type cellular patterning.

2.2.2 Sterile Plant Culture

All seeds were sterilised prior to plating out onto nutrient enhanced media to eliminate any bacterial or fungal contamination. Seeds collected from a genetic cross were sterilised through washing seed in 70% ethanol before removing the ethanol and immersing the seeds in 10% bleach with 2 drops of Tween 20 detergent as a surfactant. The seeds were washed 4 times with dH₂O in a laminar flow hood before plating out. Seeds collected from a plant grown purely to bulk up the seed numbers had not encountered the same treatment during the crossing process, which can damage tissues and allow biological contaminants to take hold. As a result bulked up seed did not require the extensive sterilization process; aliquots of seed were immersed in 70% ethanol in a 1.5 ml Eppendorf tube with 2 drops of Tween 20 detergent and shaken for 20 minutes on a shaker at 250 rpm. The tubes were taken to a laminar flow hood where

the ethanol and seeds were pipetted out onto sterile Whatson no. 1 filter paper and left to dry for 15 minutes. Once dry, autoclaved cocktail sticks were used to place seeds on square 100 mm plates (Sterilin supplied by SLS, U.K.) containing $\frac{1}{2}$ MS₁₀ Phytigel (5g/l) for root length experiments or for crossing. For Lugol staining, where avoiding damaging the root tissue was paramount, seeds were plated onto round Petri dishes containing soft-set $\frac{1}{2}$ MS₁₀ Bacto-agar (5g/l). All plates were sealed with Micropore medical tape (Industriacare Ltd, Leicestershire, U.K.).

Plates containing non-*hydra* seeds were chilled at 4°C for 72 hours to assist with germination. Plates containing *hydra* seeds or seeds resulting from a cross required an extra stratification period to encourage germination and were chilled at 4°C for 7 days. Plates were then transferred to a controlled environment culture room and grown at 22± 2°C, on a cycle of 16 hours light:8 hours dark.

2.2.3 *hydra* Screening

2.2.3.1 Embryo screening

The embryos from plants grown from the crossed seed were screened for *hydra* mutants. Siliques of ≥ 2 mm wide were removed from the plant stem and placed on a 76 x 26 mm microscope slide. Using two wire scalpels, the siliques were gently opened by making 2 cuts either side of the centre line on both sides of the silique. A drop of 0.5M KOH was added to the silique to assist with the removal of intact ovules by reducing friction between the ovule and glass and clearing the tissues.

Ovules were removed from the silique casing using the scalpels and covered with an 18 x 18 mm coverslip. The coverslip was depressed gently to uncase the embryos from the ovules. Slides were examined on an Olympus SZH10 research stereomicroscope (Olympus Optical Company Ltd., London, U.K.). Slides without at least 2 *hydra* embryos were considered non-mutant and the corresponding parent plant discarded.

2.2.3.2 Genotyping

Genotyping required an ample genomic DNA supply of the 3 controls: *ws* DNA (wild-type), *hydra* heterozygous DNA, *hydra* homozygous DNA. *ws* seeds and *hydra*

heterozygous seeds were plated out on $\frac{1}{2}$ MS₁₀ Phytigel 5g/l and kept at 4°C for 7 days before placing in the plant tissue culture room set at 22± 2°C (16 hours light:8 hours dark).

At 5 dpv, the plates were examined under a Zeiss STEMI SV8 dissecting stereomicroscope (Carl Zeiss Ltd, Welwyn Garden City, Herts, U.K.) and the *hydra* homozygous mutants identified. The *hydra* plates had the heterozygous seedlings thinned out to allow space for the *hydra* homozygous mutants to develop. The *ws* and *hydra* heterozygous plants were selected for DNA extraction at 10 days after germination. The *hydra* homozygous mutants were left on the plate for a further 7-10 days to allow the mutant to achieve its maximum size and therefore to achieve a higher DNA yield from the extraction process.

2.2.4 GFP screening

2.2.4.1 Screening for crossing

During the crossing process, seedlings required screening for the presence of GFP at several stages.

Seedlings of the Haseloff GFP lines in *Col-0* and *ws* backgrounds were screened and photographed on a Zeiss LSM510 confocal microscope (emission filter: 505-530nm and argon laser excitation: 488nm) to check the expression of GFP.

Seedlings from the crosses with the lines containing the constructs *pUAS::HYDRA1* and *pUAS::HYDRA2* were screened for GFP on a Nikon Optiphot-2 stereomicroscope (Nikon UK Ltd, Surrey, U.K.) using a BY2A (GFP) filter. The GFP positive plants were returned to the greenhouse, dried and the seed collected for the final cross with *hydra* heterozygous plants.

2.2.4.2 Screening for experimental seed

GFP screening took place after the final cross on a Nikon Optiphot-2 stereomicroscope (Nikon UK Ltd, Surrey, U.K.) using a BY2A (GFP) filter. Positive plants were returned to the greenhouse until silique development occurred. After screening for *hydra* the plants identified as positive for GFP and *hydra* were bagged for seed collection. The resulting seed was used in experiments.

2.2.5 Root Length Analysis

2.2.5.1 *PLS* and *DR5* lines

Plants containing the *PLS* or *DR5* promoter::*HYDRA* transgenes were plated out onto ½ MS₁₀ Phytigel (5g/l) media in two rows, 8 plants per row in 100 mm square plates (Sterilin). The plates were chilled at 4°C for 7 days. The plates were scanned at 7 days after germination. The roots were marked and measured after the scan to allow quantification of root growth.

2.2.5.2 *UAS* lines

Plants containing the *UAS* promoter::*HYDRA* transgenes were plated out on to ½ MS₁₀ Phytigel (5g/l) media in two rows, 10 plants per row in 100mm square plates (Sterillin, supplied by SLS, U.K.). The plates were chilled at 4°C for 7 days. Plants were photographed individually over 4 days using a Coolsnap^{cf} (Photometrics, Tucson, U.S.A.) microscope camera and images were processed using Labworks software.

2.2.6 Root (Lugol) Staining

Lugol staining was used to reveal starch-containing columella cells. Seedlings were removed from sterile plates and immersed in Lugol stain for 5 and 10 minutes. Seedlings were then rinsed in dH₂O before being fixed with a drop of Hoyer's solution onto microscope slides and covered with a 22x22mm or 22x 52mm cover slip depending on root overall length. Slides were examined on a Olympus SZH10 research stereomicroscope (Olympus Optical Company Ltd., London, U.K.).

2.2.7 Confocal Microscopy

All confocal microscope work was carried out on a Zeiss LSM510 confocal microscope, and all images were taken using the integral LSM software.

2.2.7.1 Root patterning and cellular structure

Roots were dissected from the plant and Propidium Iodide (1mg/ml) stain was pipetted onto the root tissue to act as a counter-stain for the GFP and left for 30 seconds before being rinsed off with dH₂O. The samples were then mounted in dH₂O under a 22x22 mm cover slip and examined under the microscope.

2.2.7.2 Shoot patterning and cellular structure

Seedlings aged between 5 and 7 days after germination were placed on a 76 x 22mm microscope slide. GFP counter-stain Propidium Iodide (1mg/ml) was pipetted onto the seedling and left for 2 minutes before being rinsed off with dH₂O. The samples were then mounted in dH₂O under a 22x22 mm cover slip and examined under the microscope.

2.2.7.3 Petal DAPI staining

Petals were dissected under a Zeiss STEMI SV8 dissecting stereomicroscope (Carl Zeiss Ltd, Welwyn Garden City, Herts, U.K.) using watchmaker's tweezers and a wire scalpel. Petals were placed onto a 76x22 mm microscope slide. DAPI stain (5 mg/ml) was pipette onto the petal until the tissue was completely covered. The stain was left to adsorb for 10 minutes. The sample was then rinsed with dH₂O before being mounted in the sample under a 22x22mm cover slip and examined under the microscope.

2.2.8 DNA Extraction

Extraction Buffer:

200 mM Tris-HCl pH 7.5

250 mM NaCl

25 mM EDTA

0.5% (w/v) SDS

A crude DNA extraction method based on the Edwards method (Edwards *et al.*, 1991) was used during this work.

Due to the gross inconsistencies in size between the *hydra* mutants and other plant samples, it was not possible to keep to the same size or mass of sample for each extraction. For *hydra* homozygous mutants, the entire plant was used for DNA extraction, while for other samples a piece of leaf or a young seedling of a similar size (10 mm x15 mm approx.) was used.

300µl of extraction buffer was added to a 1.5ml Eppendorf containing the sample. Using a plastic sterilised pestle the sample was ground in the tube for up to 60 seconds and then vortexed. The sample was then centrifuged for 5 minutes at 13000 rpm. The supernatant was carefully removed to a new Eppendorf and the tube containing the cell debris discarded. 300 µl of isopropanol was added to the new tube before centrifuging at 13000 rpm for a further 5 minutes to precipitate the genomic DNA. The supernatant was then removed and discarded and 100 µl 70% ethanol added to remove salts. The tube was centrifuged at 13000 rpm for a further minute before the ethanol was carefully removed and the tube left open to dry the DNA pellet. Once dry the pellet was resuspended in 50 µl of dH₂O.

n.b. Initially a small amount of quartz sand was added to the tube at the grinding stage, but this was later abandoned as higher yields were generated using just the buffer and there was a reduced chance of contaminants remaining with the pellet which would impact on the PCR reactions.

2.2.9 Genotyping

Genotyping the plants consisted of 4 sets of primers (sequences provided in Appendix 2). The first set of primers are designed to amplify *ACTIN1* and are designed to check the presence of template in a sample and the volume of template to give sufficient concentration for maximum yield of product to give a clear band.

The second set of primers amplify the promoter of the relevant plant line (*UAS*, *PLS*, *DR5*) (Figure 2.1).

Representation of sites of primers for checking the presence of the PLS/DR5/UAS promoter driven HYDRA 1 cDNA in the *hydra* 1 rescued lines.

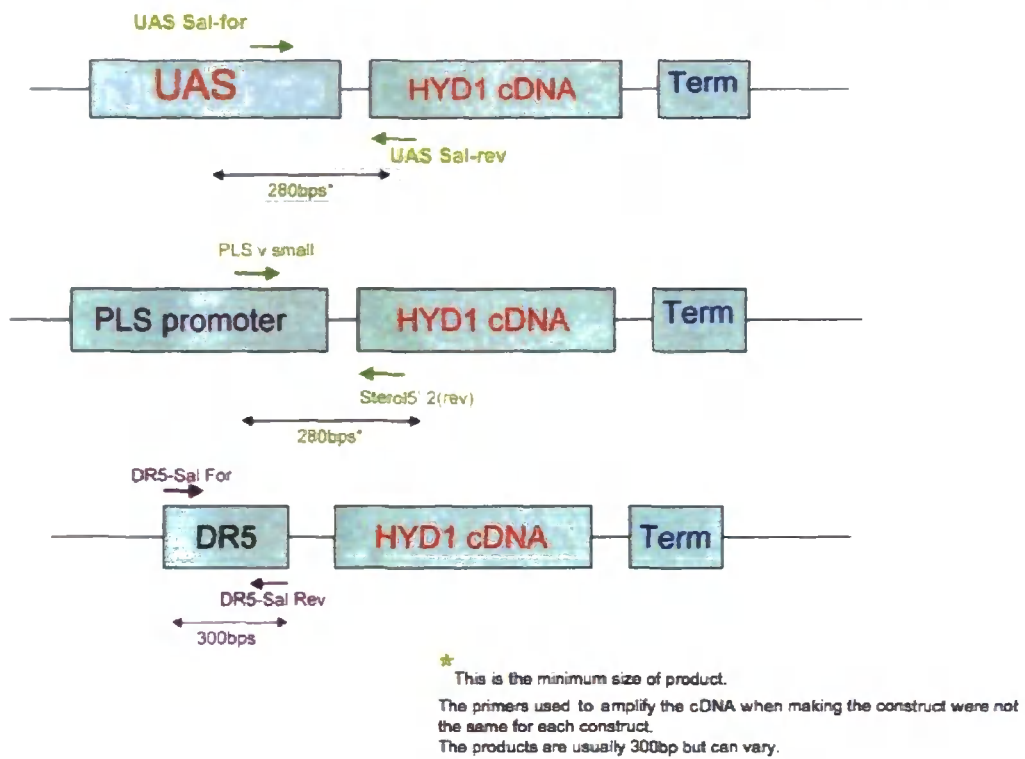


Figure 2.1 Simple gene map to show sites of primer binding and direction of amplification for the constructs *pUAS::HYDRA1*, *pDR5::HYDRA1* and *pPLS::HYDRA1*.

Representation of sites of primers for checking the presence of the PLS/DR5 promoter driven HYDRA 2 cDNA in the *hydra* 2 rescued lines.

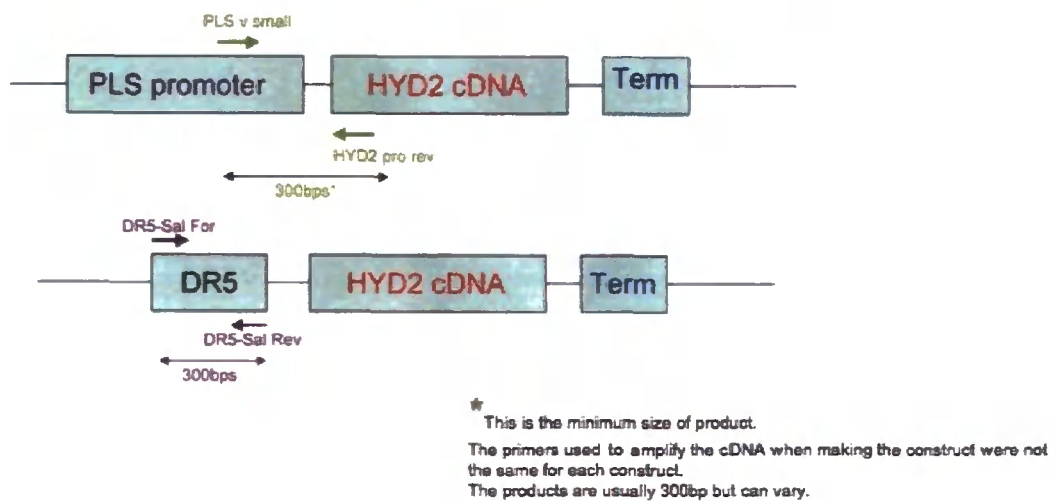
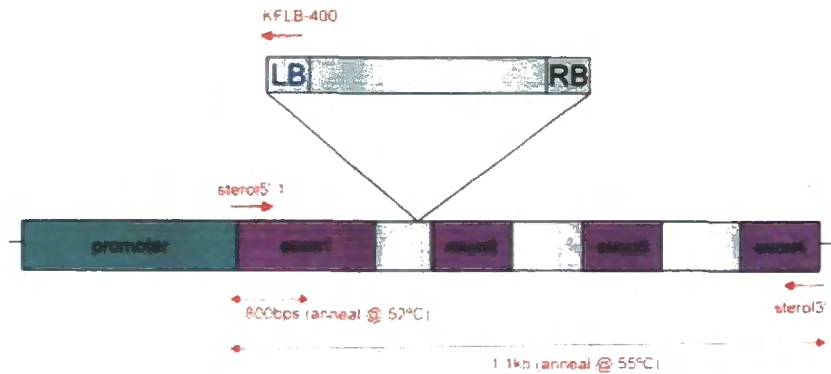


Figure 2.2 Simple gene map to show sites of primer binding and direction of amplification for the constructs *pDR5::HYDRA2* and *pPLS::HYDRA2*.

The third set of primers amplify the wild-type *HYDRA1* gene or *HYDRA2* gene (Figure 2.2) and the fourth set amplify across the T-DNA insert site in *hydra1* (Figure 2.3).

Representation of primers used to confirm *hydra* homozygous backgrounds in rescued plants.



N.B. In the *hydra* mutant, a T-DNA insert knocks out gene function, in a heterozygous background the primer pair KLB-400 and stereo 5'1 will not produce a band.

Figure 2.3 Simple gene map to show sites of primer binding and direction of amplification for the presence of the T-DNA insert present in *hydra1* homozygous or the undisrupted wild type *HYDRA1* gene.

The PCR conditions remained standard using each primer pair set.

The PCR programme used was as follows:

1)

94°C 3 mins

2)

94°C 1 min

55°C 1 min } 40 cycles

72°C 1 min

3)

72°C 10 min

4°C soak

PCR reaction recipe:

Mg ⁺⁺ free 10 x reaction Buffer	2.5µl
MgCl ₂ (50mM)	0.5 µl
10mM dNTPs mix	0.5µl
primer forward (20pmol)	0.25µl
primer reverse (20pmol)	0.25µl
DNA <i>Taq</i> polymerase	0.5 µl
genomic DNA (10-100ng)	1µl
dH ₂ O	19.5µl
total volume	25µl

Oligodeoxynucleotide primers were ordered from and synthesized by MWG-Biotech as lyophilised pellets. The lyophilised were resuspended in dH₂O to the desired concentration.

All reactions were in 0.5ml PCR Eppendorf tubes. Reactions were run using a MastercyclerR gradient (Eppendorf AG, Hamburg, Germany) or a GeneAmpR PCR System 9700 (Applied Biosystems, California, USA).

2.2.10 Colony PCR

A numbered grid was marked on a Petri dish containing Bacto-agar media to correspond to the number of colonies sampled plus a negative control. A complementary set of 0.5 µl PCR Eppendorf tubes was set up with the following reagents:

Mg ⁺⁺ free 10 x reaction buffer	2µl
MgCl ₂ (50mM)	0.5µl
10mM dNTPs mix	0.5µl
primer forward (50pmol)	0.5µl
primer reverse (50pmol)	0.5µl
DNA <i>Taq</i> polymerase	0.1µl
dH ₂ O	45.9µl

total volume

50µl

Sterilised cocktail sticks were used to transfer cells from each colony to the respective PCR tube (excepting the negative control) before scratching the surface of the corresponding marked square. The plate was sealed and incubated at 37°C overnight.

The PCR tubes were amplified using the following programme:

1)

94°C 5 min

2)

94°C 1 min

55°C 1 min } 40 cycles

72°C 2 min

3)

72°C 10 min

4°C soak

The PCR products were separated on a 1% (w/v) agarose gel to confirm the presence of the gene in the colony. Positive colonies were grown in liquid LB media containing 1 µl of kanamycin to 1 µl of LB media in flame-sterilised test tubes. Tubes were placed to shake (200 rpm) at 37°C overnight to grow. Once grown the culture were put through a mini-prep using the Qiagen Spin Miniprep kit (Qiagen, Crawley, U.K.) following the kit instructions.

The PCR products were then prepared for sequencing to confirm the gene had been correctly amplified.

2.2.11 Gel Electrophoresis

Agarose gel electrophoresis was used for visualization of PCR and ligation products. Gels varied in concentration according to the expected size of product. 1% gels were used for larger fragments (800 bp-2.5 kb) with Hyperladder I as a molecular size and approximate quantitative marker and 2% gels used for smaller products (250-

800 bp) with Hyperladder IV as a marker. All gels were made used 1x TAE buffer with 1g per 100 ml TAE or 2 g per 100 ml TAE of agarose powder. The solution was heated at full power in a microwave for 1-1.5 minutes until the powder had dissolved. After cooling to 50°C, 0.1 µg/ml of ethidium bromide was added to bind to the products and allow visualization and the gels poured and left to set for 30 minutes. After submersion of the gels in 1x TAE buffer, 2µl of loading dye pre-mixed with 5 µl of sample were loaded into each well. The gels were run at 80v for 40 minutes with a further 10-15 minutes if the products had not run far enough to perceive the band sizes clearly. Gels were visualized using a Gel Doc 1000 UV transilluminator system running the Molecular Analyst v. 2.1.1 software (BioRad).

2.2.12 Cloning the *HYDRA2* promoter

2.2.13 Cloning into TOPO

The promoter sequence was amplified using PCR initially with the primers HY2prom(+980) and HY2prom(-3530) which do not contain BamH1 linkers to ensure the correct amplification of the sequence.

1st amplification:

Buffer (with Mg)	5µl
dNTPs	1.5µl
primer forward	1.5µl
primer reverse	1.5µl
genomic DNA	2µl
dH ₂ O	38µl

+ 0.5µl of EXPAND (Roche) proof reading *taq* enzyme added at 94C in PCR program.

PCR program

1)

94°C 3 mins

2)

94°C 1 mins

55°C 1mins } 20 cycles

68°C 4 mins

3)

68°C 10 min

4°C soak

1µl of the product was used in the second reaction with the primers containing Bam H1 linkers (Hy2prom (Bam) +1127 and Hy2prom (Bam) -3490).

2nd amplification:

Buffer (with Mg) 5µl

dNTPs 1.5µl

primer forward 1.5µl

primer reverse 1.5µl

PCR product 1µl

dH₂O 39µl

+ 0.5µl of EXPAND(Roche) proof reading taq enzyme added at 94°C in PCR program.

PCR program

1)

94°C 3 min

2)

94°C 1 min

55°C 1min }30 cycles

68°C 4 min

3)

68°C 10 min

4°C soak

5 µl of the product was run on a 1% agarose gel to check product size. To A-tail the product 0.5µl of Biotin Taq was then added to the reaction and the tube incubated at 72°C for 10 minutes.

The promoter was then cloned into the TOPO vector following the instructions in the TOPO cloning TA kit.

Colony PCR was performed on cultures the correct selection colour grown from the product on kanamycin enriched Bacto-agar media to check for the correct product insert.

2.2.14 Cloning into Δ pcirce-gus

After sequencing confirmed the *HYDRA2* promoter had been successfully cloned into the TOPO vector, the promoter was then to be cloned into the Δ pcirce-gus vector. The Δ pcirce-gus vector (concentration ~ 100 ng/ μ l) was digested with BamH1 primers at 37°C for 2-3 hours.

BamH1 digest:

Δ pcirce-gus	10 μ l
BamH1 Buffer	2 μ l
BamH1	2 μ l
dH ₂ O	6 μ l

2 μ l was ran on a high quality 1% agarose gel to check product length before the remaining Δ pcirce-gus was dephosphorylated by adding 1 μ l of alkaline (shrimp) phosphatase for 1 hours at 37°C before denaturing at 65°C for 20 mins.

The TOPO vector containing the *HYDRA2* promoter was digested with Bam as above with the Δ pcirce-gus vector. After running 2 μ l of the digest on a 1% high quality agarose gel to check the product, the remaining digest was placed at 80°C for 20 mins to heat inactivate the Bam HI enzyme. A second high quality 1% agarose gel was ran with the heat-denatured digest. The gel was placed on a UV transilluminator and a razor blade used to cut out the fragment.

To find the optimum mix of vector and fragment 4 ligation reactions were set up in 0.5 ml PCR tubes as follows:

	A	B	C	D
Δ pcirce-gus vector	3	3	3	3
cloned fragment	0	1.8	3.8	4.8
DNA T4 ligase	1	1	1	1
10x buffer	1	1	1	1

H ₂ O	5	3.2	1.2	0.2
Total:	10	10	10	10

These tubes were incubated at 4°C overnight.

2.2.15 Transformation into XL1 blue cells

5 µl of each ligation reaction was added to an aliquot of XL1 cells on ice and left for 20 minutes. The tubes were heat shocked at 42°C for 30 seconds before being returned to ice for 5 minutes. 1 ml of liquid LB medium was added to each tube and incubated on a shaker at 200 rpm at 37°C for 1 hour. The tubes were spun down on a tabletop centrifuge at 13000 rpm for 2 minutes. The supernatant was removed leaving ~100 µl of media, the cells were resuspended and plated out on KAN50 plates. The plates were incubated overnight at 37°C.

The plate with the most colonies was then used to perform colony PCR for 50 samples to check for the presence of the *HYDRA2* promoter in the vector.

2.2.16 DNA sequencing

All DNA sequencing carried out using internal DNA sequencing service at the School of Biological and Biomedical Sciences, Durham University, U.K. All primers used were ordered and synthesised by MWG (for sequences see Results) and used at a concentration 3.2 pM.

3.0 Results

The main aim of this work was to ascertain if sterols are required in all cells and tissues for correct plant development or if sterols are only required in specific tissues. As detailed in this section, plant lines were created containing the wild type *HYDRA1* or *HYDRA2* genes expressing under root tissue specific promoters or cell-type specific enhancers in the *hydra1* or *fk^{hyd2}* sterol mutant backgrounds respectively. The objective was to determine whether one or more of these transgenic lines would exhibit phenotypic rescue through the activation of wild-type sterol biosynthesis in specific tissue types in *hydra* mutants. For example the line *pPLS::HYDRA1* x *hydra1* would express the *HYDRA1* gene where the *POLARIS* gene promoter expresses (the root cap) but in the other root tissues sterol biosynthesis would remain altered due to the defective *HYDRA1* gene in the *hydra1* background.

The overall project aim was therefore achieved through analysing the lines for evidence of phenotypic rescue linked to a specific tissue-specific promoter. The analysis included examination of *GFP* expression in *UAS* enhancer trap lines, quantification of root length, examining the root tip cellular structure using Lugol stain and characterization of cellular defects in mature plants using microscopy and tissue staining.

3.1 Generating the genetic crosses

There are several methods of breeding desired characteristics into lines, from simply selecting plants displaying obvious traits to more complex molecular methods where specific genes can be isolated. This project required the molecular approach to design the lines containing the construct and the more simple genetic crossing method to get the construct lines into the *hydra* background. All plant crosses were performed using the 'general method' from The European Arabidopsis Stock Centre (NASC) website

(http://arabidopsis.org.uk/InfoPages?template=crossing;web_section=arabidopsis).

This method involves removing the anthers from the plant to be fertilised and taking an anther from the plant containing the genetic marker. The pollen in the anther is then transferred onto the stigma of the first plant, fertilising the flower. The seeds collected from the flower will be the F1 generation and will be heterozygous, however

the F2 generation of seed will contain progeny containing the genetic markers in the mutant background of interest (Figure 3.1).

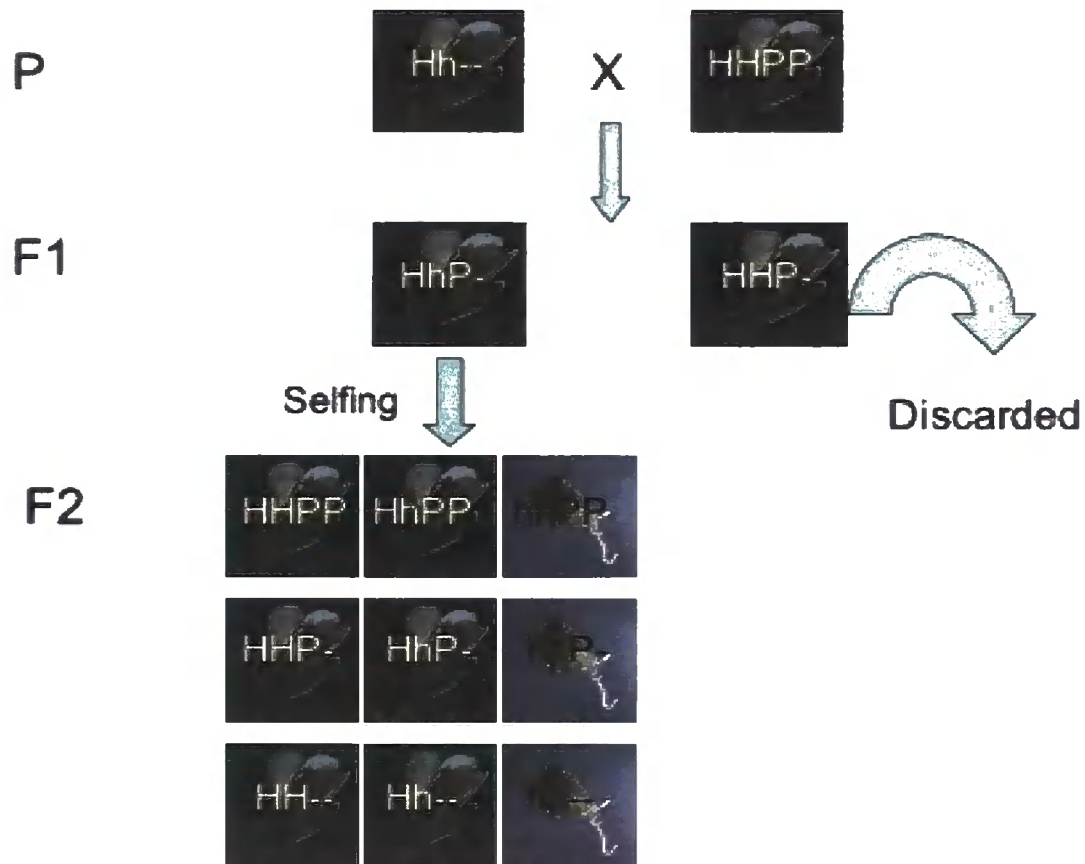


Figure 3.1: Simple representation of genetic markers in crossing process to F2 generation. PP = promoter::construct, HH =non-mutant, Hh =hydra heterozygous, hh = hydra homozygous

Plant lines were supplied containing the wild type *HYDRA1* or *HYDRA2* gene under the control of one of the following promoters: *POLARIS (PLS)*, *DR5* or *UAS*. These lines then required crossing into the relevant mutant background (*hydra1* or *fk^{hyd2}*). The *UAS* lines required further crossing with the lines containing tissue specific GFP expression genes once those lines had been back-crossed four times into *ws* from *Col-0* ecotype. After the final cross the lines were bulked up for seed and analysed. Each final line consisted of at least two lines with a different transformation dipping pot origin (i.e. the lines were independent transformants, for comparative purposes).

3.2 Genotyping

To confirm the identity of seedlings following crosses (in particular to determine whether phenotypically wild-type seedlings might be rescued mutants as

opposed to heterozygotes for the *hydra* mutations), PCR- based genotyping of each seedling was carried out.

Genotyping consisted of using 4 sets of primers to identify:

- 1) the presence of the relevant promoter;
- 2) the presence of the wild type *HYDRA* allele;
- 3) the presence of the T-DNA insert (mutant *hydra* allele).

Actin was used as a loading control, and reactions were carried out as described in the Materials and Methods. All primers used in the genotyping of seedlings are summarised in Appendix 2, and an example of the genotyping is shown in figure 3.2.

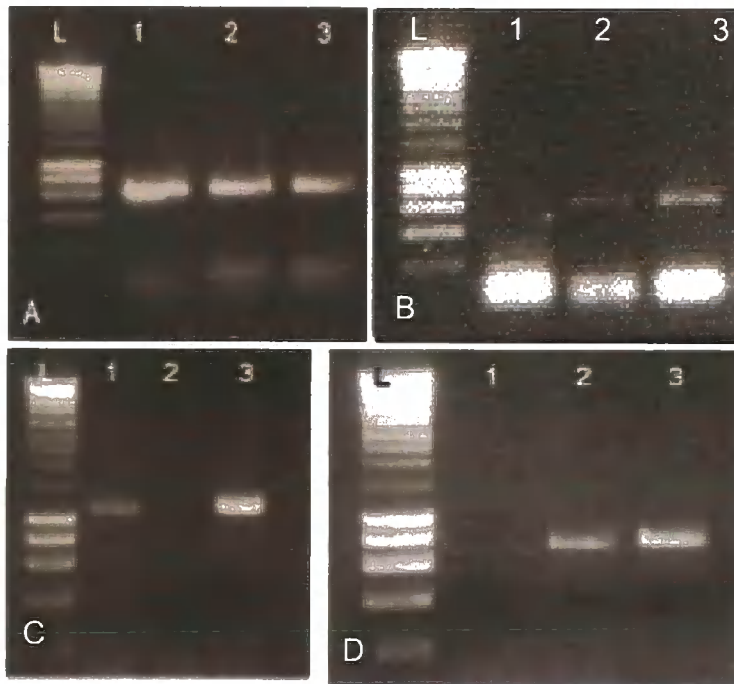


Figure 3.2: Example of genotyping process; L= Hyperladder IV (A-B) or Hyperladder I (C-D), 1= *ws* control, 2= *hydra1* homozygous, 3= *hydra1* heterozygous. A= DNA loading control (primers Act2 for and Act2-rev) B= PCR for DR5 construct (primers DR5 Sal-for and DR5 Sal-rev), C= PCR for HYDRA1 gene (primers sterol 5'1 and sterol 3'2) C=PCR for *hydra1* T-DNA insert (primers KFLB+400 and sterol 5'1)

3.3 GFP expression

3.3.1 GFP expression in wild type *ws* and *Col-0* lines

When backcrossing into a different ecotype it is important to check natural variation between ecotypes has not disrupted any characteristics of the line. This includes checking the GFP expression is expressing in the correct tissue and has a

consistent strong signal to ensure GFP expression can be easily distinguished from background autofluorescence.

After the backcrosses of the GFP expression lines were complete, the resulting F2 seed was grown up and examined. The pericycle and endodermis lines gave a strong consistent signal along the length of the respective tissues. The epidermis line gave a fragmented but consistent signal in the epidermis. GFP expression had not altered in the backcrossing process of the epidermis, endodermis, pericycle lines (Figure 3.3).

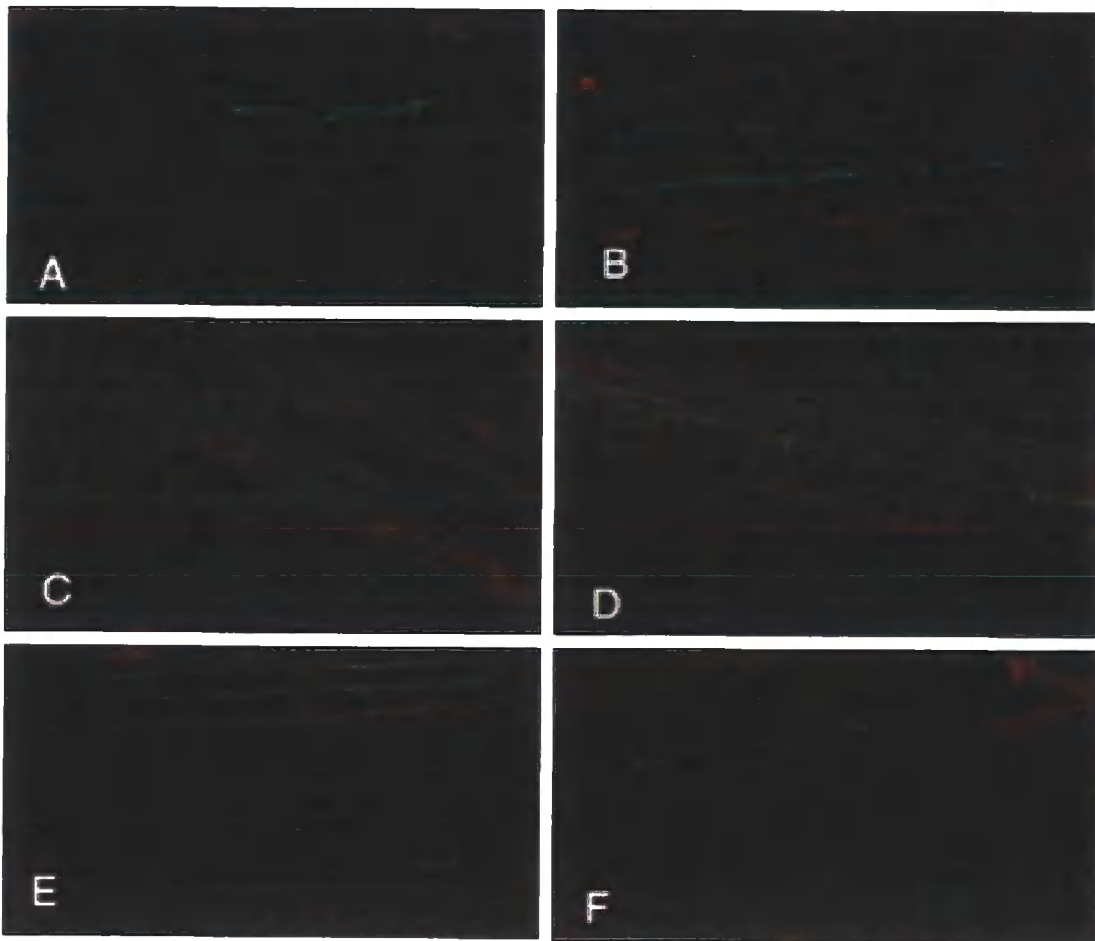


Figure 3.3: A= Endodermis expression in Col-0 background B=Endodermis expression in Ws background. C= Pericycle expression in Col-0 background D= Pericycle expression in Ws background E= Epidermis expression in Col-0 background F= Epidermis expression in ws background. Red counter-stain is Propidium Iodide (1mg/ml). (All images taken with assistance from Dr Nicholas Clark, Durham University UK.)

3.3.2 GFP expression in the *hydra* mutant background lines

The GFP lines were expressing in the correct tissue after back crossing into the *ws* from *Col-0* ecotype. However due to the *hydra* mutants' cellular disorganisation it was important to check the GFP expression again after crossing into the *hydra1* mutant background.

After crossing the *pUAS::HYDRA1::GFP* construct into the *hydra1* mutant background, the progeny were screened for GFP expression. The majority of seedlings displayed the expected GFP expression pattern, however approximately 1 in every 5 seedlings did display altered GFP expression (Figure 3.4). In the aberrant expressing individuals, the pericycle and endodermis GFP expression did not maintain in the correct tissue layer for the length of the root and expression was seen in the tissue layers on either side. In the epidermis lines, GFP was expressing simultaneously in the epidermal layer and in a separate ground or stele tissue layer. GFP expression also occurred in root hairs in the epidermis line.

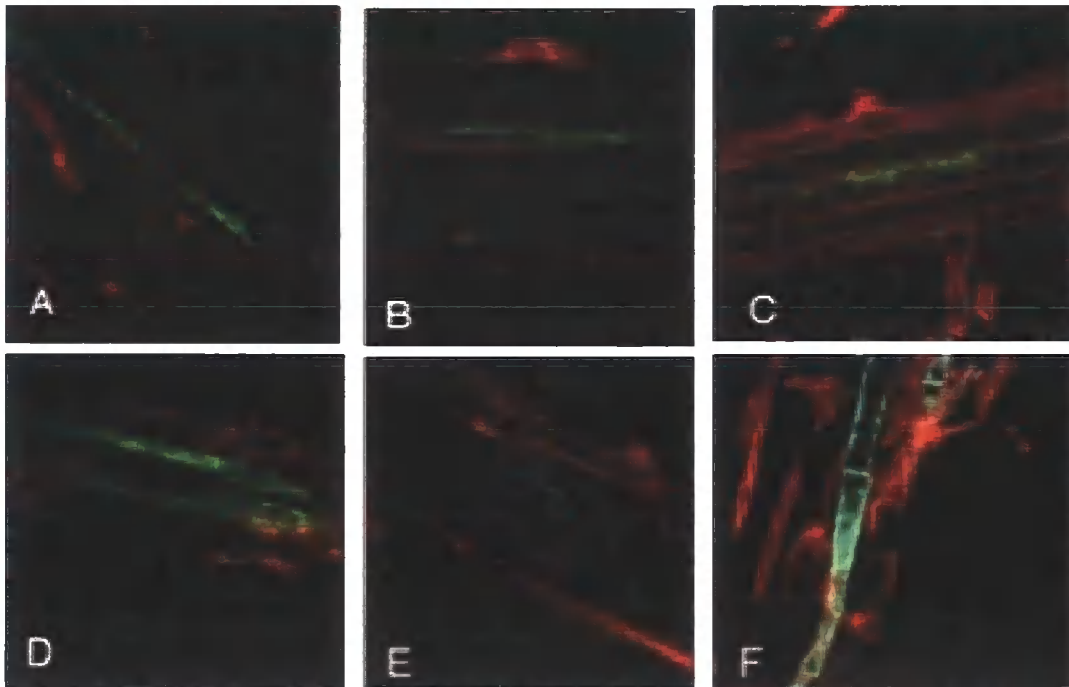


Figure 3.4: Altered GFP expression in *pUAS::HYDRA1 x hydra1* lines A=pericycle expression B=epidermis expression, C=epidermis expression, D= endodermis expression, E=pericycle expression, F= epidermis expression. Red counter-stain is Propidium Iodide (1mg/ml) (images taken with assistance from Dr Nicholas Clark, Durham University UK.)

3.3.3 Expression of HYDRA1 in the endodermis

Whilst screening the GFP lines crossed into the *pUAS::HYDRA1* x *hydra1* (endodermis) line, it was noted there was a number of seedlings of the *hydra* phenotype on the plate and these mutant phenotypes were screened for GFP expression (Figure 3.5). The expression was disordered and fragmented, however the distorted expression is likely due to the disorganised internal cellular structure of the *hydra* mutant than misexpression in the line. The non-mutant *hydra1* phenotype seedlings presented the same expression (and endodermis structure) as in the *ws* (endodermis) line (Figure 3.5 B). From this, it would appear if the endodermis is very fragmented in the mutant, expressing *HYDRA1* in the fragmented endodermis tissue layer does not rescue the *hydra* mutant phenotype.

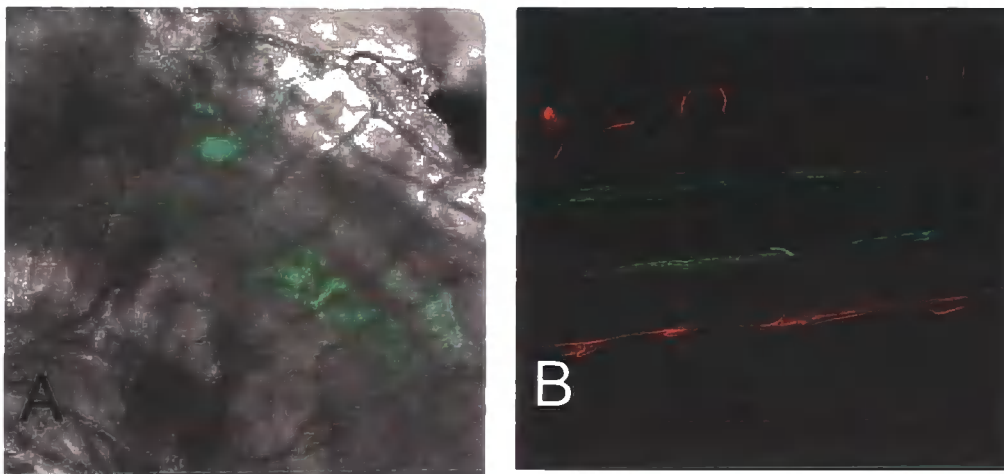


Figure 3.5: A: Expression in mutant. phenotype expressing *HYDRA1* gene in the endodermis B: Expression in *hydra1* expressing *HYDRA1* gene in endodermi, red counter-stain is Propidium Iodide (1mg/ml), (images taken with assistance of Dr Nicholas Clark, Durham University UK).

3.3.4 GFP expression in the shoot

The GFP expressing *hydra* mutant lines were expected to only express in the root (J0272, J3611, J2551;

<http://www.plantsci.cam.ac.uk/Haseloff/construction/catalogues/Jlines/index.html>).

However the shoot of *hydra1* seedlings was also surveyed for GFP expression.

It was found that the pericycle and endodermis lines both showed continued expression into the hypocotyl of *hydra1* seedlings, with only a small break in expression at the junction between root and shoot (Figure 3.6). The GFP expression

was evident in either a single or double line of cells mimicking the expression pattern in the root (Figure 3.7).

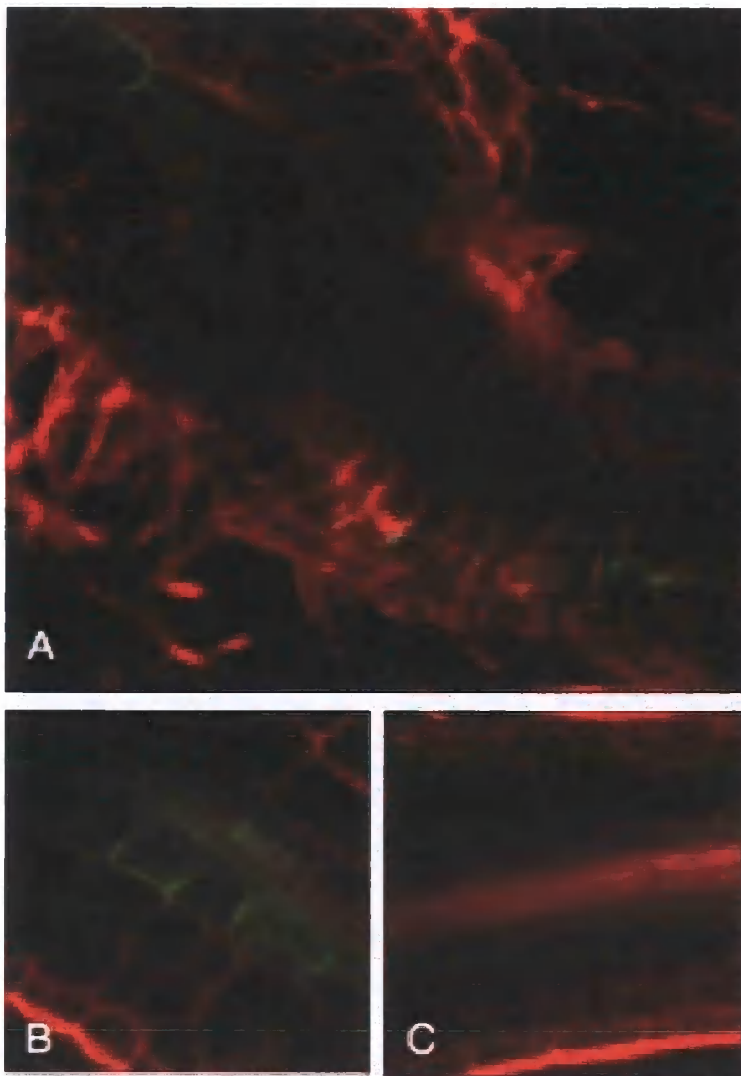


Figure: 3.6: A: Shoot-Root junction of hydra seedlings showing expression B: pericycle line expression in hypocotyls, C: pericycle line expression pattern at top of root Red counter-stain is Propidium Iodide (1mg/ml) (images taken with the assistance of Dr Nicholas Clark, Durham University UK.)

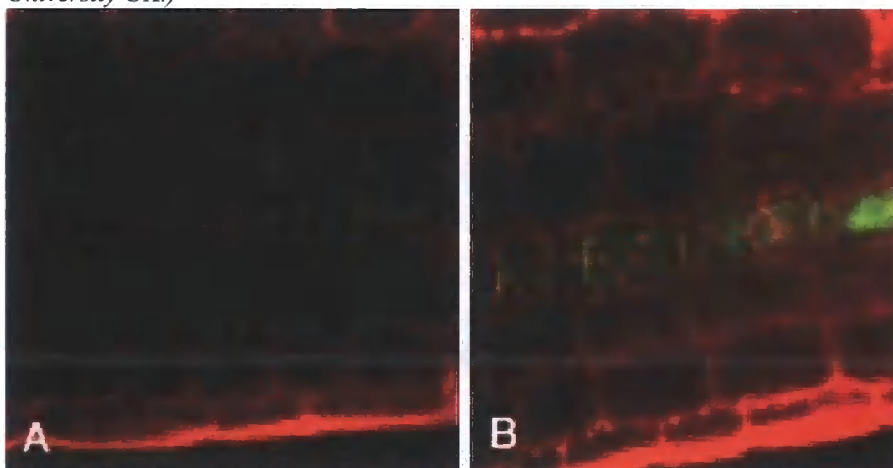


Figure 3.7: Hypocotyl expression of pericycle (A) and endodermis (B) lines. Red counter-stain is Propidium Iodide (1mg/ml), (images taken with the assistance of Dr Nicholas Clark, Durham University UK).

The GFP lines in *ws* and in *Col-0* ecotype wild-type backgrounds were then surveyed for shoot expression. The GFP (endodermis) lines in *Col-0* and *ws* and GFP (pericycle) lines in *Col-0* and *ws* all showed expression in the hypocotyls. Therefore the expression in the shoot is a feature of the UAS enhancer activity, and not a result of the cross into the *hydra* background.

Further faint expression was observed in patches of leaf pavement cells (not shown) and the SAM in the *Col-0* and *ws* wild-type backgrounds (Figure 3.8).

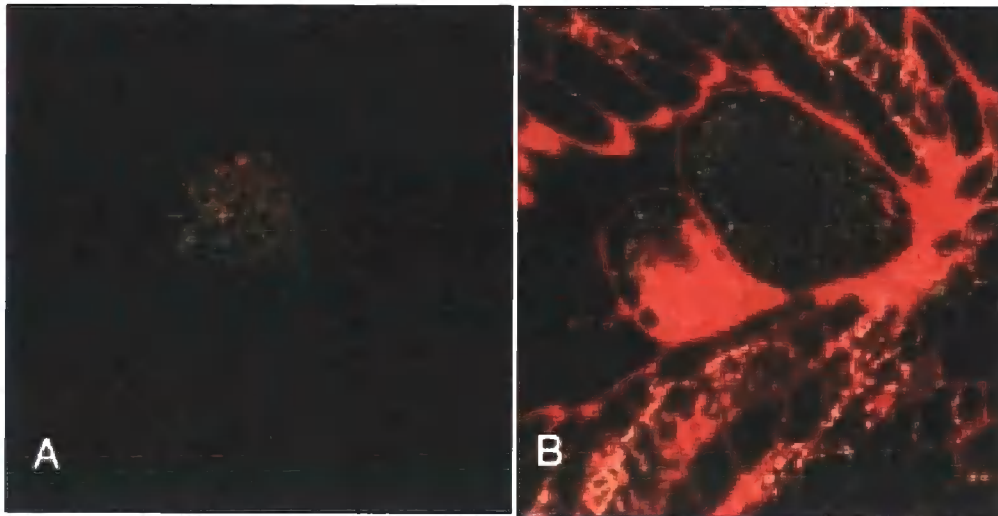


Figure 3.8: Faint expression in the SAM of the *Col-0* pericycle (A) and *ws* endodermis line (B) Red counter-stain is Propidium Iodide (1mg/ml)

3.3.5 The cortex and vascular tissue UAS lines

The *pUAS :: HYDRA1 x hydra1* x GFP root cortex line exhibited only plant background autofluorescence could be detected, there was no other GFP expression from the UAS construct detectable (Figure 3.9).

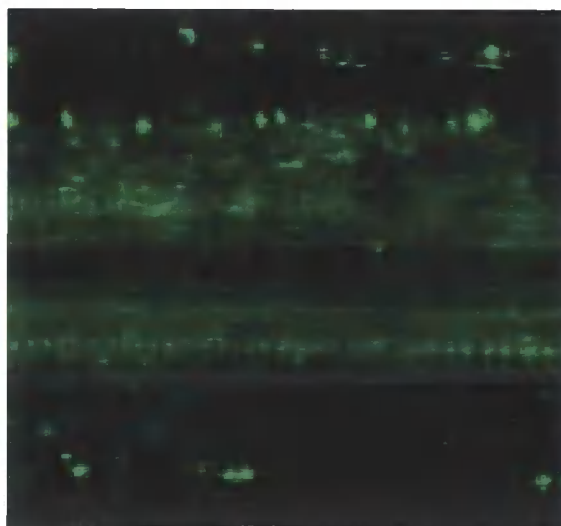


Figure 3.9: No GFP expression in cortex line (image taken with the assistance of Dr Nicholas Clark, Durham University UK.)

In view of the absence of GFP expression in the cortex line, 84 seeds of the cortex line in *ws* and *Col-0* background were plated out onto ½ MS₁₀ Phytigel (5g/l) and grown up as detailed in the Materials and Method section 2.2.2, to screen for potentially expressing individuals. At 7 dpg the seedlings were screened for GFP. The germination rates and occurrence of GFP expression is detailed in table 3.1.

Table 3.1: Germination rates of root cortex GFP line in *Col-0* and *ws*

	Col-0	Ws
Seeds plated out	42	42
No. of seeds germinating	25	27
No. positive for GFP expression in root cortex.	2	1

Due to the very low rates of GFP expression in both lines, the loss of GFP expression was unlikely to be caused by backcrossing process. However the low rates of expression made the line unsuitable for use in this research. The cortex line was therefore abandoned at this point in the project.

Due to a malfunction in greenhouse temperature and lighting control resulting in several harvest failures, the vascular tissue line and the *pUAS::HYDRA2 x fk^{hyd2} x GFP* (epidermis/endodermis/pericycle) enhancer trap lines were not analysed during this work.

3.4 The *hydra* phenotype and the phenotypic deviations that indicate rescue

As described in Chapter 1, *hydra* mutants display a distinct phenotype with short wide roots, a short hypocotyl and multiple cotyledons giving a cabbage-like appearance to the shoot. *fk^{hyd2}* mutants display a more severe phenotype than *hydra1* mutants with shorter roots, slower growth and a shorter lifespan.

The *hydra1* mutant lifespan is a maximum of 40 dpg but root cell division may cease at 14 dpg. The *fk^{hyd2}* mutant stops growth in all tissues at 10-14 dpg and rarely survives past 21 dpg. Therefore any seedlings of the promoter lines that survive past this age are an indication of a degree of rescue.

hydra mutants have very short and thickened roots of a swollen appearance (Figure 3.10) with only 2-3 lateral roots developing compared to a much larger number in wild type. An increase in root length, that is significantly longer than *hydra* controls, is therefore likely to be an indication of rescue by tissue-specific *HYDRA1* gene expression.

hydra mutants have disorganised cellular patterning in the root with misshapen cells and irregular root cell files which is very distinctive. Irregular cellular structure present in a root would be an indication of an imperfect phenotypic rescue.

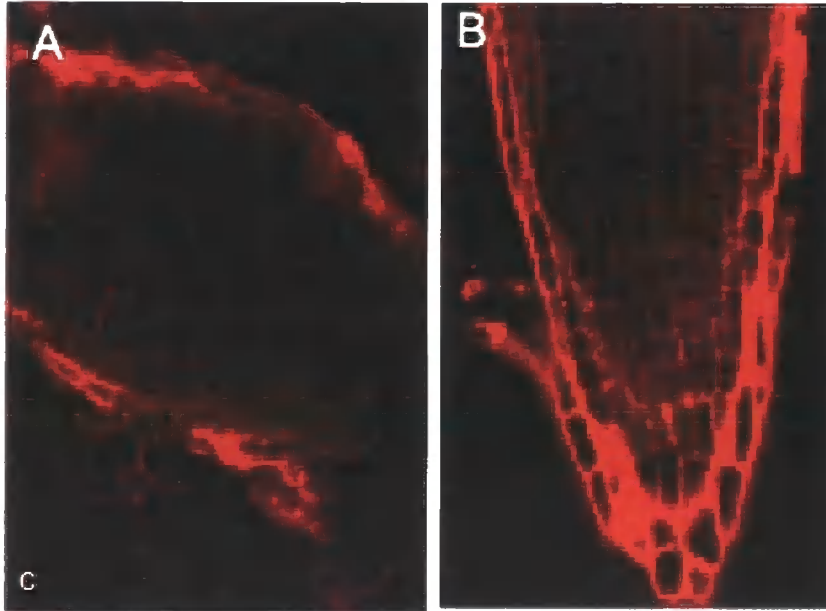


Figure 3.10: A=*hydra* root structure B= *ws* wild type root structure C= close up of section of *hydra* root. Red counter-stain is Propidium Iodide (1mg/ml), (images taken with the assistance of Dr Nicholas Clark, Durham University UK.)

hydra presents abnormal localization of starch which normally accumulates in the columella and is involved in correct gravitropic response. Lugol staining provides a quick efficient method of surveying root tips for evidence of *hydra* phenotypic rescue. The staining of the starch in the columella is distinctive in both wild type and *hydra* and light microscopy is sufficient to identify ordered wild type vs. mutant cell patterning.

Figure 3.11 shows Lugol staining patterns of *hydra* mutant and wild-type roots. *fk^{hyd2}* loses the stain, and so columella differentiation, earlier than *hydra1* due to cessation of cell division at 14dpg.

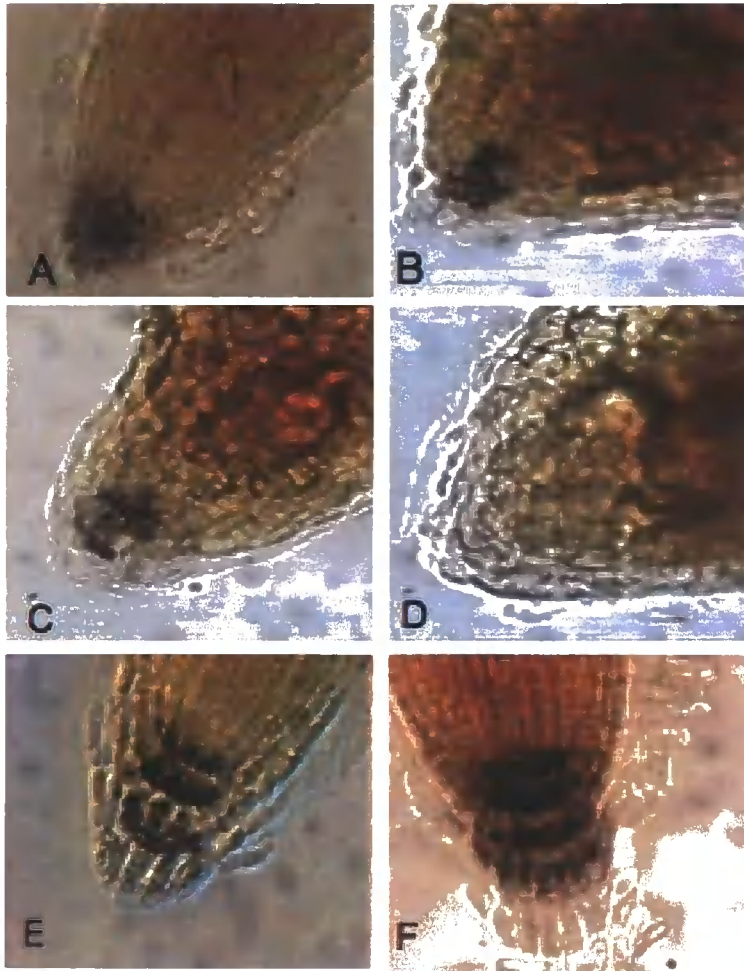


Figure 3.11: Examples of Lugol staining at 7 dpg (A) and 14 dpg in *hydra1* homozygous (B), *fkh^{hd2}* homozygous at 7dpg (C) and 14 dpg (D) and *ws* at 7dpg (E) and 14 dpg (F).

hydra mutants are seedling lethal, and so do not mature to the stage of producing flowers or seed or for the hypocotyls to mature into a stem. As previously mentioned *hydra* also do not produce morphologically normal leaves. Therefore if the lines expressing the promoter *pUAS:HYDRA1* construct produce distinct leaves or any organs or tissues produced in mature wild type plants, this will indicate phenotypic rescue.

3.5 Rescue in the *DR5* promoter driven lines

DR5 is a synthetic auxin responsive promoter which in the root expresses predominantly in the root tip where auxin accumulates. By fusing the β -glucuronidase (*GUS*) reporter gene to the *DR5* promoter, the expression of *DR5* in the root tip of *ws* seedlings can be visualised (Figure 3.12) over a time period.

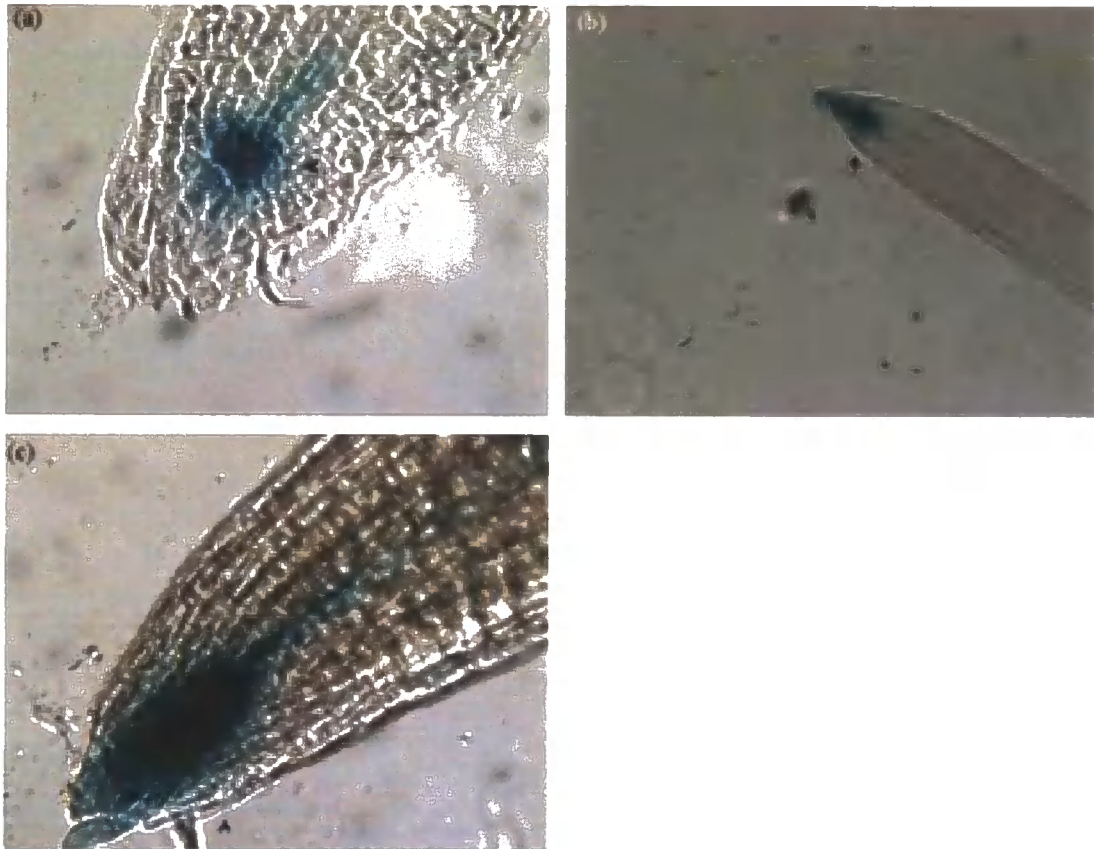


Figure 3.12: *DR5::GUS* expression a) expression at 5 dpg, b) expression at 9 dpg and c) expression at 11 dpg. (All pictures taken by Lizzie Andrews and used with permission.)

3.5.1 Overview of phenotypic rescue in *pDR5::HYDRA1* x *hydra1*

pDR5::HYDRA1 x *hydra1* had a predominantly wild-type phenotype. Cellular structure of the root was indistinguishable from *ws*, the shoot developed distinct leaves, the seedlings survived on soil and the mature plant produced viable seed. The main deviations in phenotype were a deviation in petal shape and a reduced root length at 7 dpg compared to *ws*.

3.5.2 Root growth in *pDR5::HYDRA1* x *hydra1*

In the *pDR5::HYDRA1* x *hydra1* lines the average root length was longer than in the *hydra1* homozygous mutant. However there was a clear difference between the *ws* and *hydra1* heterozygous controls and the *pDR5::HYDRA1* x *hydra1* lines (Figure 3.13). A One-way ANOVA was performed which confirmed there was a statistical difference between the average root lengths at the $p < 0.0001$ level (Table 3.2).

The average root length of *pDR5::HYDRA1* x *hydra1* is shorter than *ws* and this result suggests the root growth is not completely rescued.

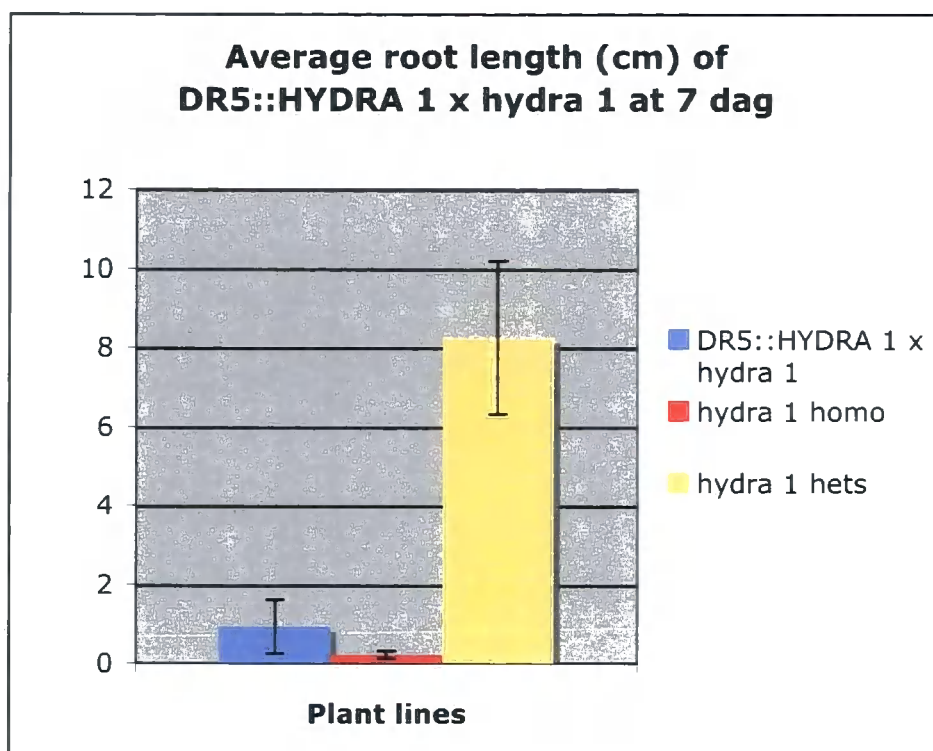


Fig 3.13: Average root length with standard error bars of *pDR5::HYDRA1 x hydra1* with controls *ws*, *hydra 1* heterozygous and *hydra1* homozygous for comparison. All roots were measured from the root tip to the start of the hypocotyl.

Table 3.2: Summary of results of One Way ANOVA. The P value, assuming the null hypothesis, is less than .0001

Variation	Sum of squares	d.f.	Mean squares	F
Between	553.9	2	276.9	197.0
Within	54.84	39	1.406	
Total	608.7	41		

3.5.3 Lugol staining in *pDR5::HYDRA1 x hydra1*

Analysis of Lugol-stained *pDR5::HYDRA1 x hydra1* crosses revealed no major differences compared to the *ws* control roots and the parent lines containing the *pDR5::HYDRA1* construct but not crossed into the *hydra* background. It would appear the *pDR5::HYDRA1 x hydra1* lines root phenotype was indistinguishable from the controls and represents a fully rescued phenotype (Figures 3.11 and 3.14).

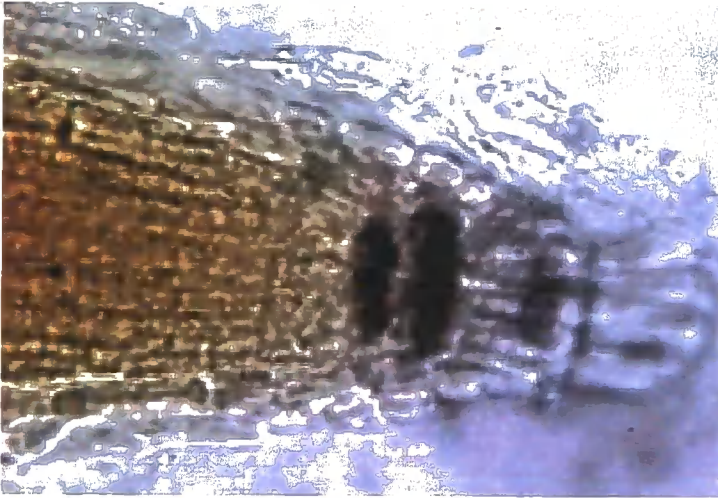


Figure 3.14: Example of *pDR5::HYDRA1 x hydra1* presenting a normal Lugol staining pattern at 14 dpg.

3.5.4 Flowers of the *pDR5::HYDRA1 x hydra1* lines

Examination of the mature *pDR5::HYDRA1 x hydra1* plants found a virtually normal phenotype except for the petals, which exhibited deviations in shape compared with wild-type (Figure 3.15). The flowers of the *pDR5::HYDRA1 x hydra1* had frilly edges, similar to the sterol mutant *fr11* (Hase *et al.*, 2000). However unlike the *fr11* mutant, the sepals were of wildtype phenotype, as were the reproductive organs.



Figure 3.15: Flower head of *ws* (L), and flower head with frilly petals in *pDR5::HYDRA1 x hydra1* (R)

3.6 *pDR5::HYDRA2* x *fk^{hyd2}*

3.6.1 Overview of phenotypic rescue in *pDR5::HYDRA2* x *fk^{hyd2}*

The *pDR5::HYDRA2* x *fk^{hyd2}* line showed significant variation in phenotypic rescue. Some seedlings had a wild type phenotype while others were indistinguishable from *fk^{hyd2}* until 21 dpv. The latter, then developed to present partial rescue in both shoot and root. The root initially presented a deceptively wild type phenotype and length by eye though Lugol staining proved this was not the case. Genotyping confirmed the presence of the *pDR5::HYDRA2* construct and the *fk^{hyd2}* homozygous background in seedlings presenting full and partial phenotypic rescue.

3.6.2 Phenotypic rescue at post 21 dpv in *pDR5::HYDRA2* x *fk^{hyd2}*

fk^{hyd2} does not normally survive to 21 dpv, however a seedling with a *fk^{hyd2}* phenotype from the line *pDR5::HYDRA2* x *fk^{hyd2}* survived to 21 dpv on ½ MS 10 Phytigel medium (Figure 3.16 A). This could have been a late germinating *fk^{hyd2}* seedling. *hydra* do not survive in soil so to test if rescue was occurring, the seedling was planted out with the other seedlings that showed a wild type phenotype from the same line. When the seedling survived, proving it was an example of partial rescue and not late germination (Figure 3.16 B), further characterisation of this partially rescued phenotype was carried out.

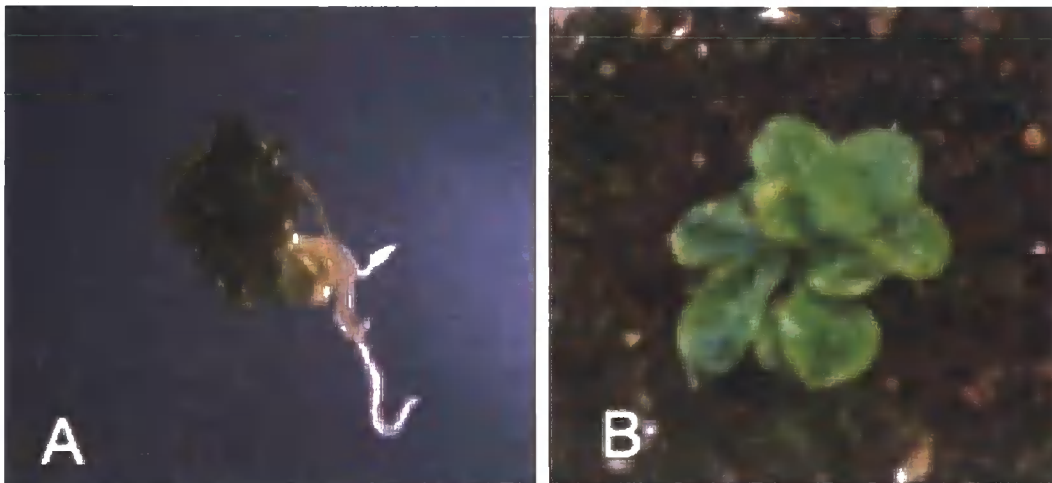


Figure 3.16: A: *pDR5::HYDRA2* x *hydra 2* at 21 dpv B: *pDR5::HYDRA2* x *fk^{hyd2}* at 40 dpv after germination.



Figure 3.17: *pDR5::HYDRA2 x fk^{hyd2}* mutant at 40dpg after germination (Left) with control (Right).

At 28 dpg germination, the shoot had achieved a partial rescue (Figure 3.15 B). Separate leaves had developed though the leaves were of much smaller size than those of other seedlings/plants of the same line (Figure 3.17). The leaf structure was also affected; leaf edges were thickened and curled over, trichomes were abundant on the leaf surface and of wild type structure, and there was no sign of any development of reproductive organs or further vegetative growth. The plant was gently removed from the soil and roots examined and appeared to be fully rescued by length and appearance comparable to *ws* control (figure 3.18). This suggests *DR5*-driven expression of the *HYDRA2* gene in the *fk^{hyd2}* mutant rescues root growth but not shoot development.

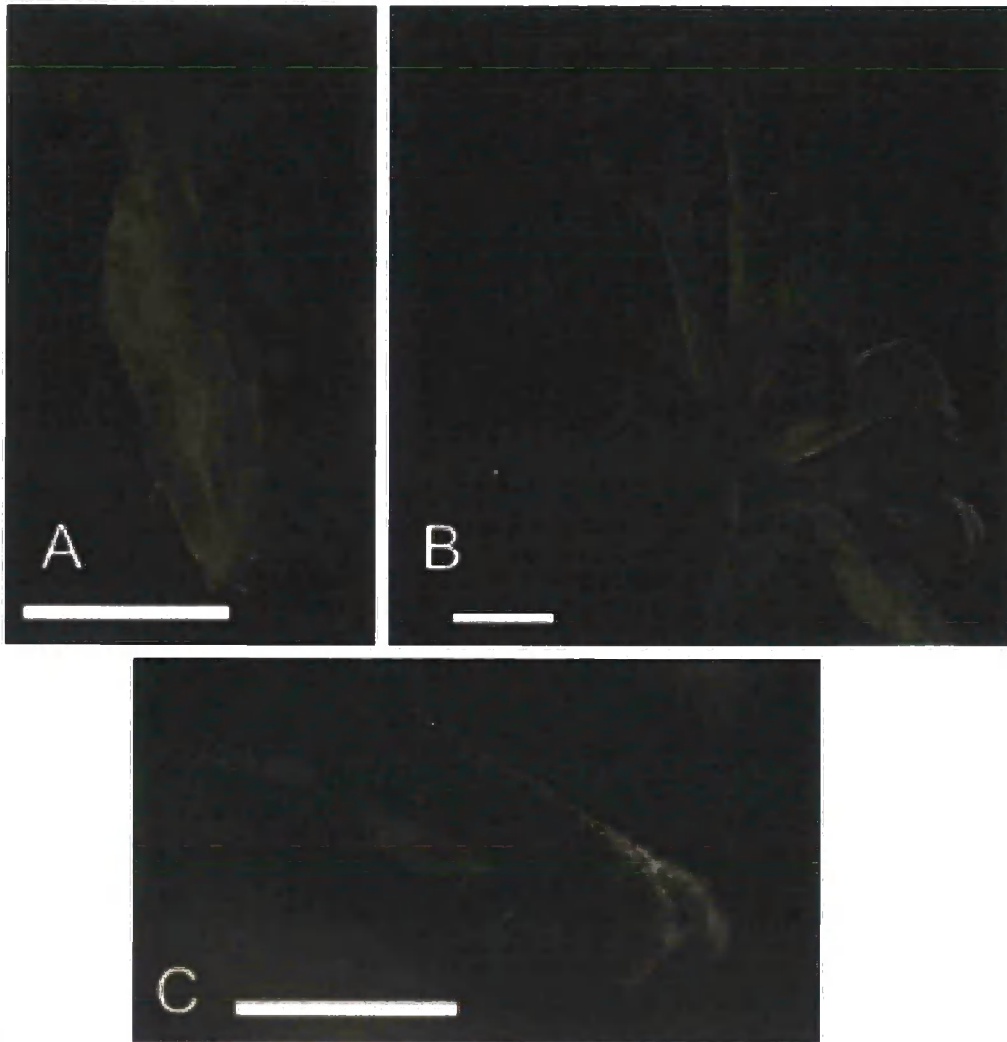


Figure 3.18: A-C close up of shoot of $pDR5::HYDRA2 \times fk^{hvd2}$. White bar is 1 cm.

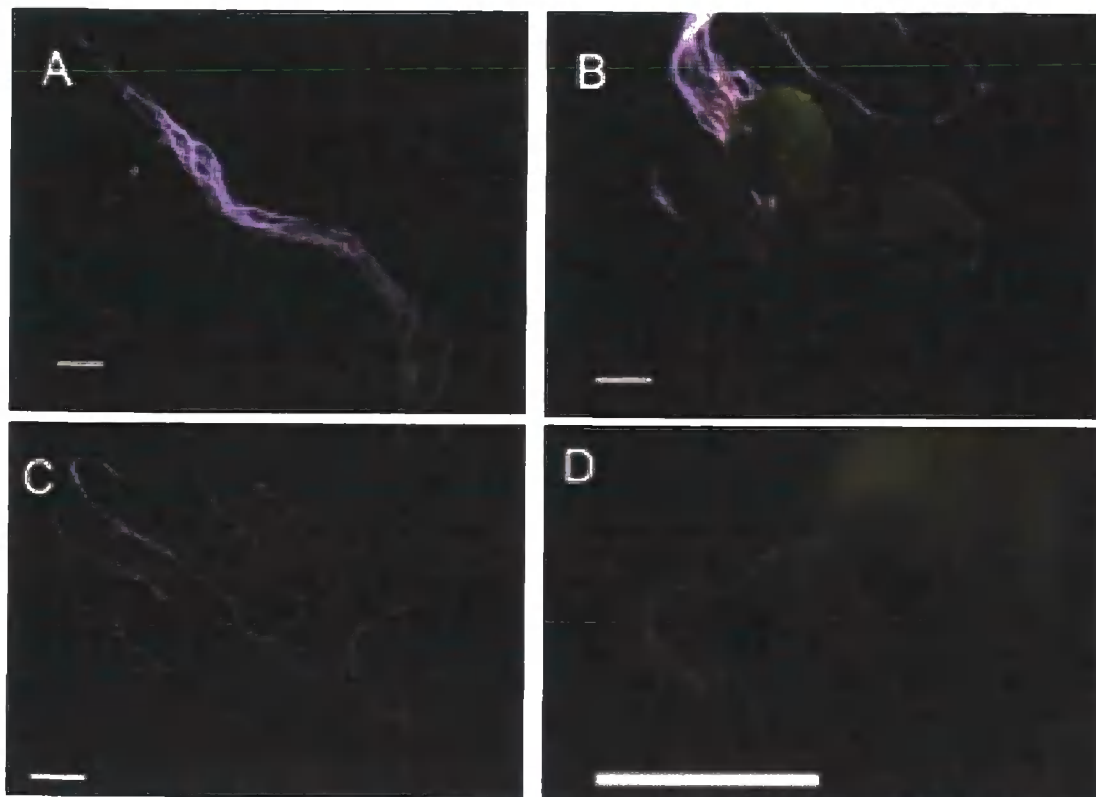


Figure 3.19: **A:** *ws* root of same age as *pDR5::HYDRA2 x fk^{hyd2}*, **B:** *pDR5::HYDRA2 x fk^{hyd2}* shoot, **C:** *pDR5::HYDRA2 x fk^{hyd2}* roots, **D:** onset necrosis in shoot of *pDR5::HYDRA2 x fk^{hyd2}* at 40dpg after germination. White bars are 1 cm.

At 40dpg when the partially rescued plant and the plants of the same line were showing clear signs of necrosis, there was still no indication of development of reproductive organs in the partially rescued plant (Figure 3.19 D). At this point the plant was again removed from the soil, the shoot photographed and the root stained with Lugol solution

3.6.3 Lugol staining in *pDR5::HYDRA2 x fk^{hyd2}*

The *pDR5::HYDRA2 x fk^{hyd2}* lines contained more *fk^{hyd2}* phenotypes (ie a lower frequency of rescued seedlings) than did the *pDR5::HYDRA1 x hydra1* seedlings. The *pDR5::HYDRA2 x fk^{hyd2}* seedlings with mutant phenotype roots stained at 7 dpg, 11 dpg and 14 dpg with the same pattern as *fk^{hyd2}* homozygous; and the rescued phenotype roots at the same age intervals stained with the same pattern as *ws* (see Figure 3.11). Nevertheless, when mature *pDR5::HYDRA2 x fk^{hyd2}* roots (40 dpg) were lugol-stained the results showed wild-type cell patterning, suggesting some of the the seedlings showing early mutant phenotypes (lack of rescue) show evidence of rescue at later stages of development (Figure 3.19).

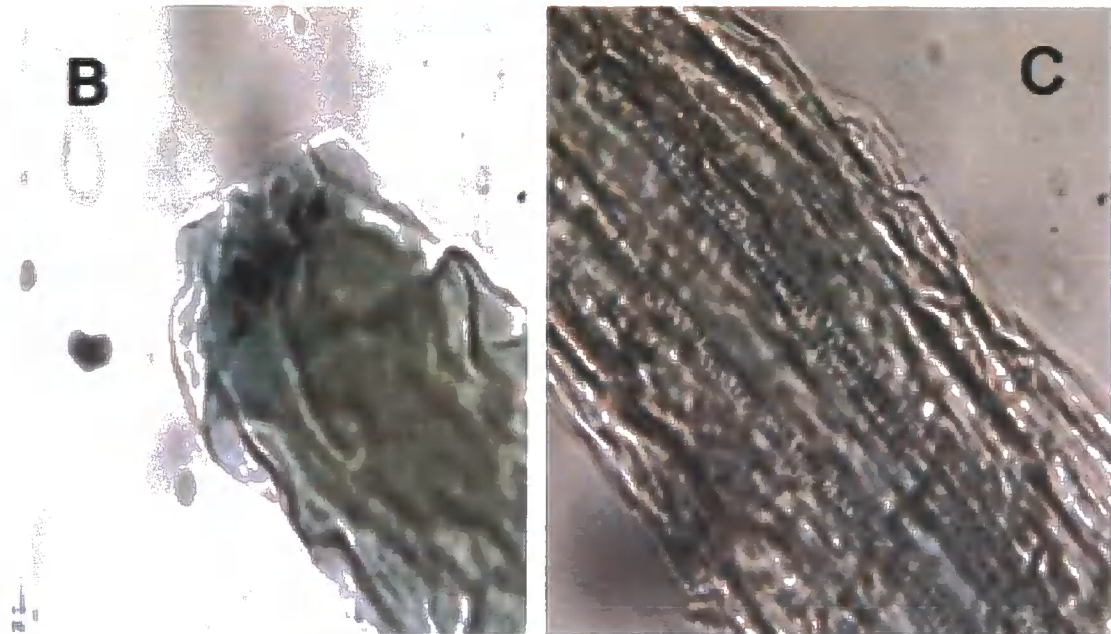


Figure 3.20: Lugol staining of $pDR5::HYDRA2 \times fk^{hyd2}$ root. **A:** Wild type phenotype root tissue at middle of root length **B:** Root tip displaying a fk^{hyd2} phenotype **C:** Wild type phenotype root tissue just before root tip.

In summary, although some roots of $pDR5::HYDRA2 \times fk^{hyd2}$ seedlings showed evidence of rescue, some did not. Despite the morphological appearance of the root of the mature $pDR5::HYDRA2 \times fk^{hyd2}$ root from the latter group, the Lugol stain provided evidence of only a partial rescue in the root in these plants. The root tip was clearly of the fk^{hyd2} phenotype (Figure 3.20 B) however the root tissue just beyond the tip and throughout the main root body was wild-type in structure with regular organised cell files (Figure 3.20 A and C). It would appear the expression of $pDR5::HYDRA2$ in fk^{hyd2} leads to only partial phenotypic rescue, and for some seedlings the rescue only becomes evident after 21dpg. The differences between the independent lines are likely to be due to position effects, as the transgenes will be

expected to have inserted at different genomic loci; the position effects will influence the level of expression of the HYDRA2 transgene.

3.7 Rescue in the *PLS* promoter driven lines

3.7.1 Overview of phenotypic rescue in *pPLS::HYDRA1* x *hydra1*

The mature plants of the *pPLS::HYDRA1* x *hydra1* line produced misshapen petals and displayed shorter roots than *ws* at 7 dpg. Aside from this, the phenotype of this line presented near perfect rescue with restored cellular patterning in the root and a restored shoot.

3.7.2 *polaris (PLS)* expression

The *PLS* gene expresses predominantly in the root cap and the base of adjoining tissues, there is very little expression of *PLS* in the aerial parts of the root. By fusing the β -glucuronidase (*GUS*) reporter gene to the *DR5* promoter, the expression of *DR5* in the root tip of *ws* seedlings can be visualised (figure 3.21) over a time period.

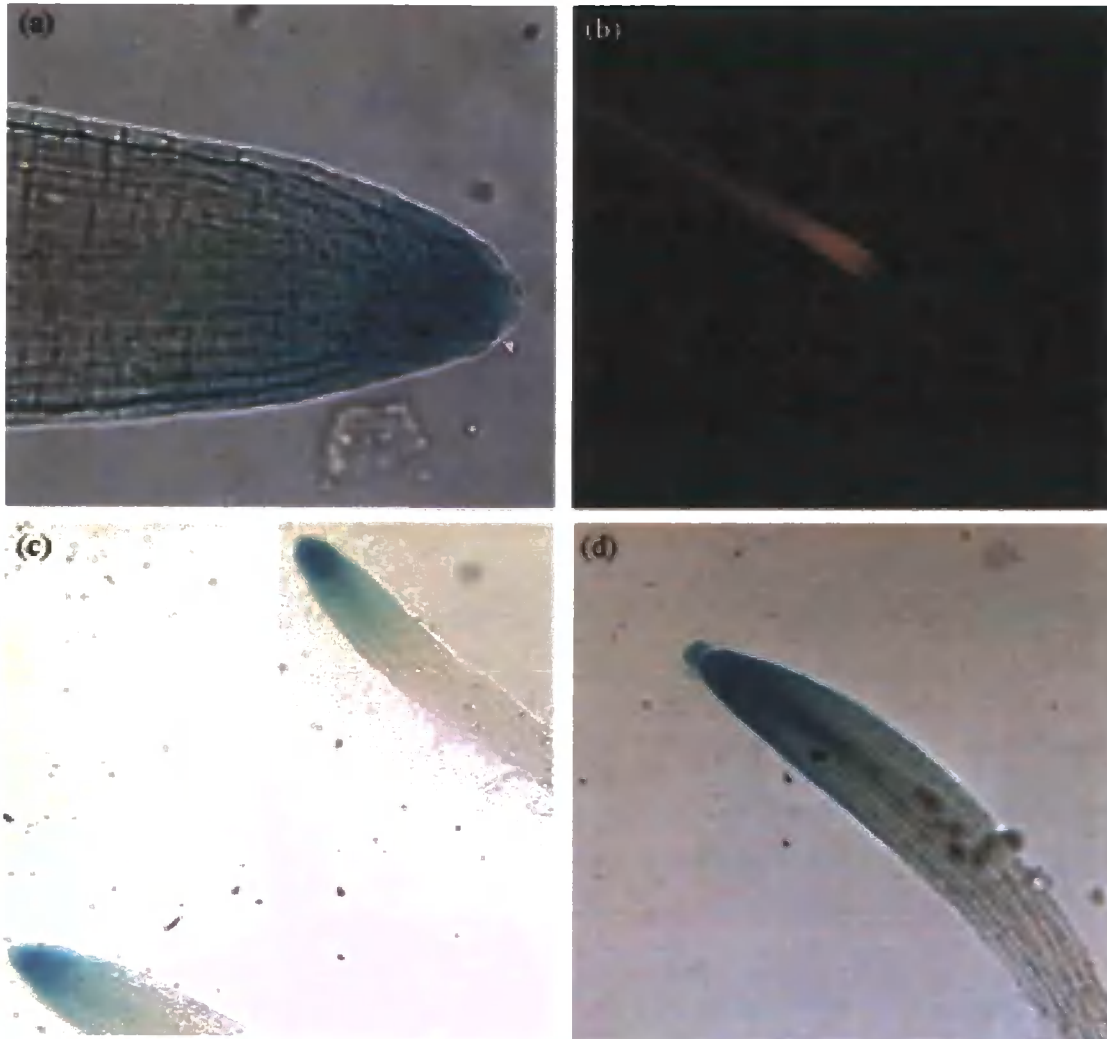


Figure 3.21: *PLS::GUS* expression a) expression at 3 dpg b) expression at 5 dpg, c) expression at 9 dpg and d) expression at 13 dpg. All images taken by Lizzie Andrews and used with permission.

3.7.3 Root growth in *pPLS::HYDRA1* x *hydra1*

Seeds of the *pPLS::HYDRA1* x *hydra1* line were plated out, germinated and cultured as detailed in Section 2.2.2. All roots were measured from the root tip to the start of the hypocotyl. The average root length of the transgenic seedlings was longer than the *hydra1* homozygous line, however there was a clear difference between these seedlings and the controls, suggesting incomplete root growth rescue (figure 3.22). One way ANOVA was performed on each set of result to confirm the differences in average root length of each line were significantly different (table 3.3). A significant difference in mean root growth between the rescued mutant lines, the *hydra1* heterozygous line and the *hydra1* homozygous line at 7 dpg was confirmed at the $p < 0.0001$ level.

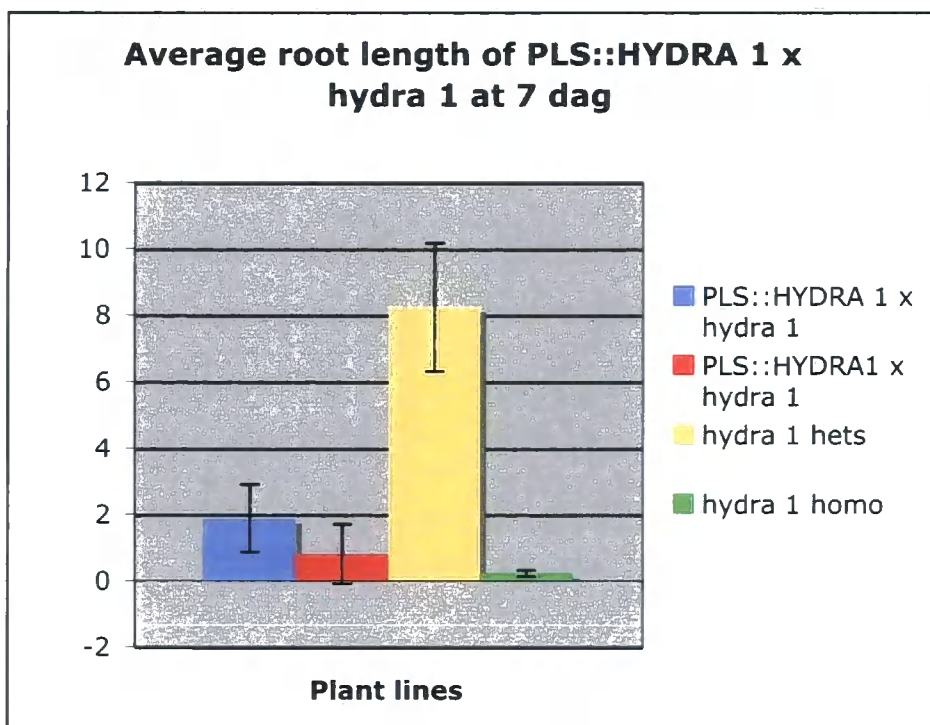


Figure 3.22: Mean root length with standard error bars of two lines of *pPLS::HYDRA1 x hydra1* with different dipping pot origins and controls *ws*, *hydra1* heterozygous and *hydra1* homozygous for comparison.

Table 3.3: Summary of results of One Way ANOVA. The P value, assuming the null hypothesis, is less than .0001

Variation	Sum of squares	d.f.	Mean squares	F
Between	577.0	3	192.3	137.7
Within	72.61	52	1.396	
Total	649.6	55		

3.7.4 Lugol staining in *pPLS::HYDRA1 x hydra1* lines

No deviations in root cellular patterning were observed for any of the *PLS* promoter lines. The *pPLS::HYDRA1 x hydra1* displayed the same patterning as in the *ws* and parent line (*pPLS::HYDRA1*) controls (Figure 3.11).

3.7.5 Petal shape in the *pPLS::HYDRA1 x hydra1* and *pPLS::HYDRA2 x fk^{hyd2}* lines.

Examination of the adult transgenic plants' morphology found a virtually normal phenotype except for the flower petals, which presented deviations in shape.

The petals of both promoter lines were first examined under the light microscope and found to contain two separate deviations in form with both present in the separate *hydra* lines:

- 1) Petals with the appearance of wild type petals apart from frilly edges (Figure 3.23) which were the same phenotype as seen in the *pDR5::HYDRA1 x hydra1* plants (Figure 3.15).
- 2) Petals presenting more severe deviations from wild type with s-bends or a thin extended shape (Figure 3.25).

Flowers either consisted of all the petals shared the same deviation in shape or consisted of four petals each presenting a different shape (Figure 3.23 and Figure 3.25), often the deviation in shape was immediately apparent from the flower as the sepals and organs were not abnormal in shape or size (Figure 3.24).

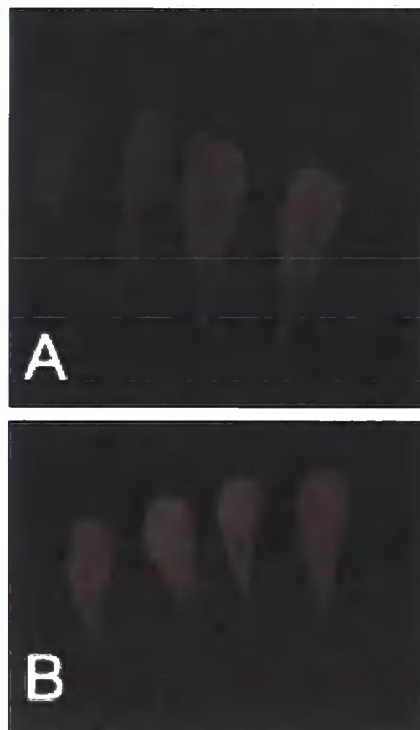


Figure 3.23: A: Petals from *ws* (L) and frilly petals from *pPLS::HYDRA1 x hydra1* (R), B: frilly petals from *pPLS::HYDRA2 x fk^{hyd2}*

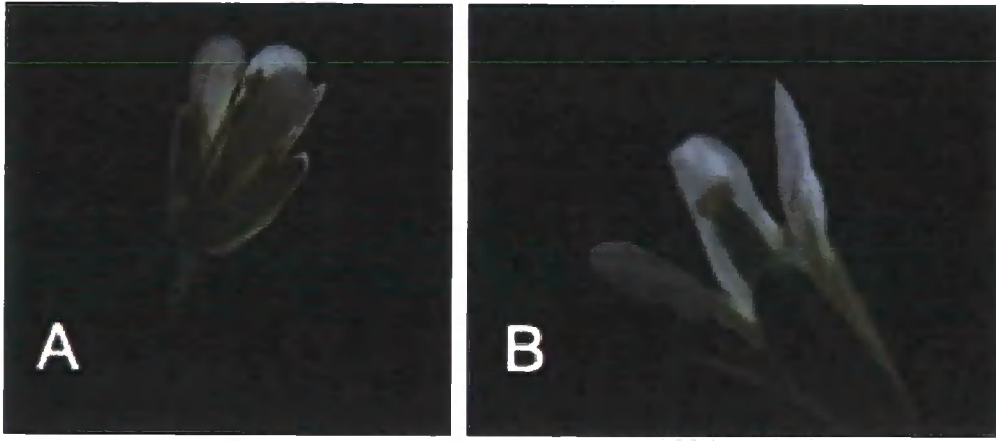


Figure 3.24: *A: flower head from pPLS::HYDRA1 lines B: Flower head from pPLS::HYDRA1 x hydra1 showing curves in petals.*

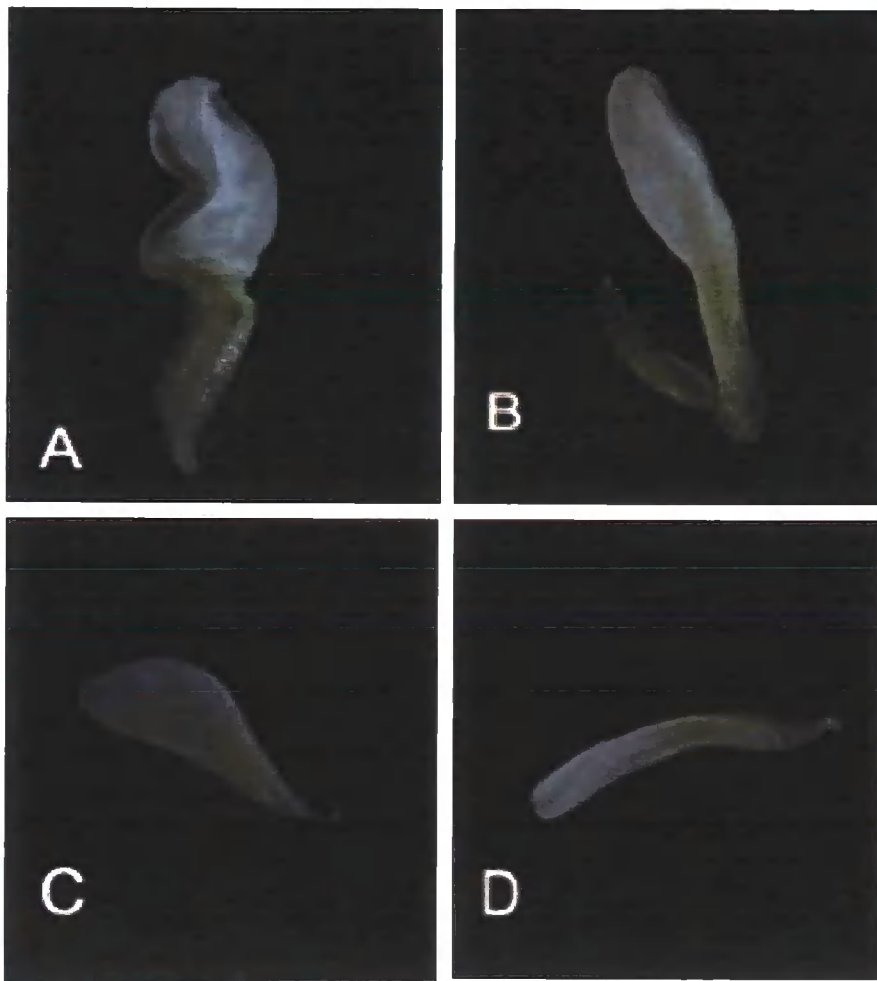


Figure 3.25: *A-D images of the variation of petal form in a single flower of pPLS::HYDRA2 x fk^{hyd2} .*

To gain a perspective at the cellular level, the petals from *pPLS::HYDRA1 x hydra1* and *pPLS::HYDRA2 x fk^{hyd2}* were DAPI stained and examined under the

confocal microscope using *ws* petals as a control. Two deviations from *ws* conical cells (Figure 3.26) were observed in lines crossed in *hydra*.

- 1) Flat regular cells in the absence of wild type epidermal conical cells (Figure 3.27 B and C)
- 2) Cells of a rounded but not conical appearance on the final cell layer on the petal edge (Figure 3.27 A).

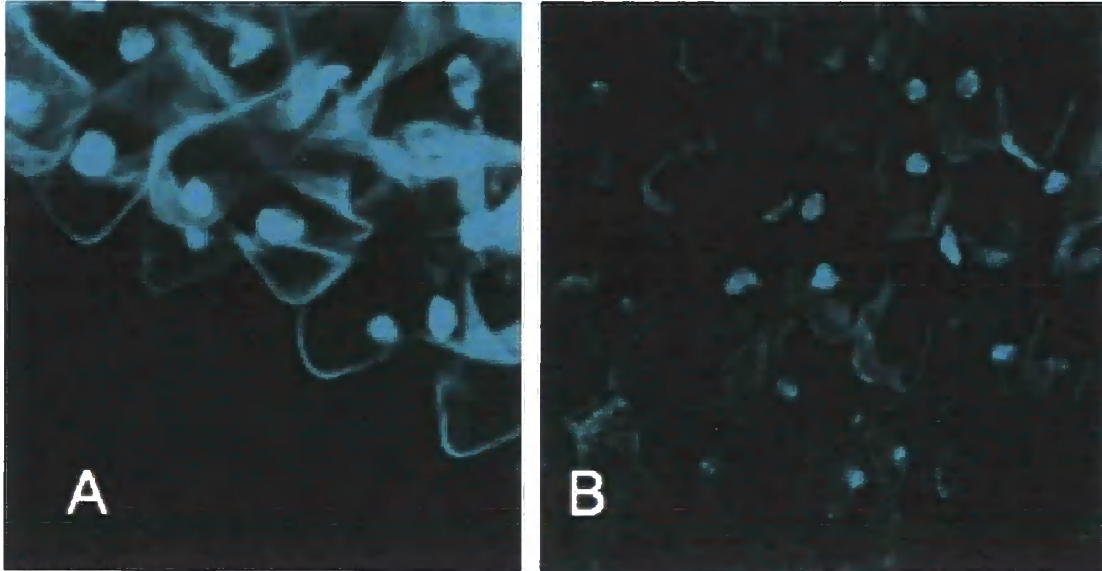


Figure 3.26: *DAPI stained epidermal petal cells A-B ws control image of DAPI stained epidermal cells on petal edges.*

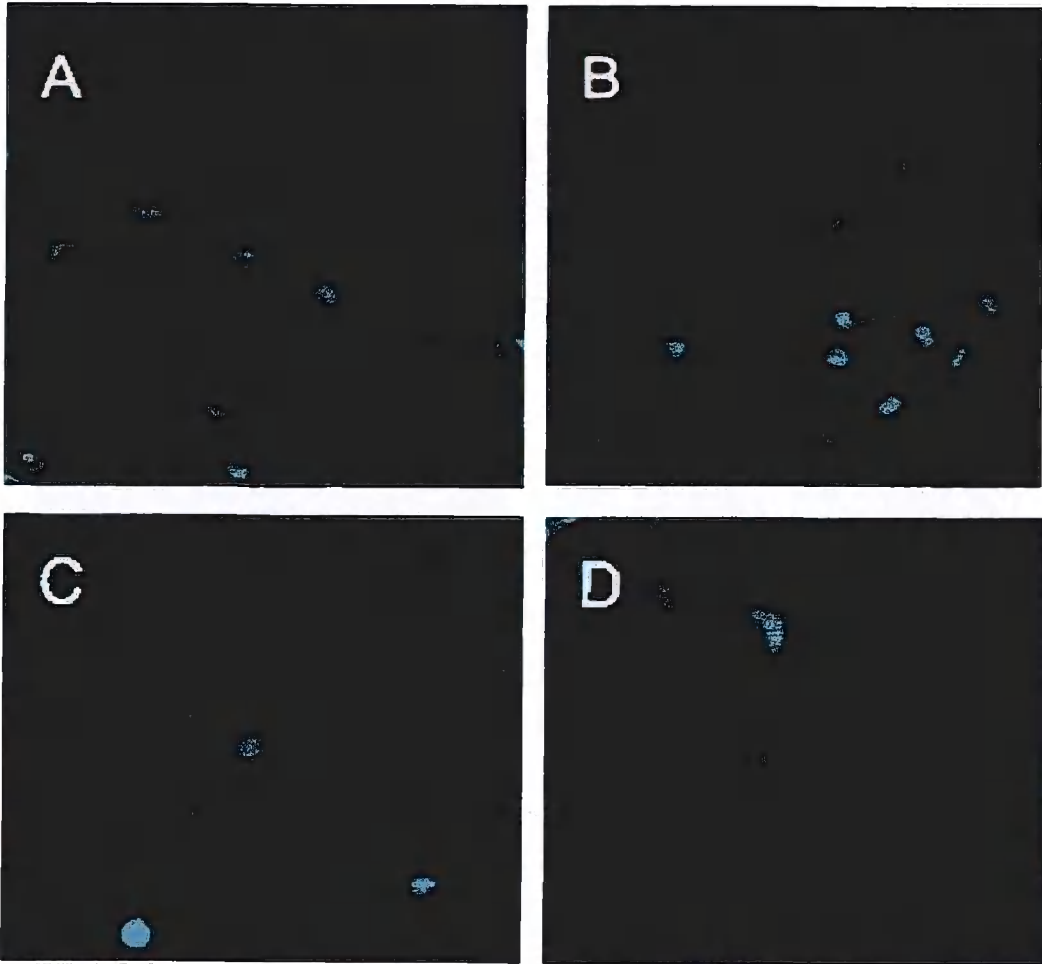


Figure 3.27: *DAPI stained epidermal petal cells A: rounded cells on edge of petal with rows of flat misshapen cells of rows behind, B: Patch of flat regular cells on petal edge C: Close up of disordered patch of flat cells D: patch of conical cells from above which lay next to B.*

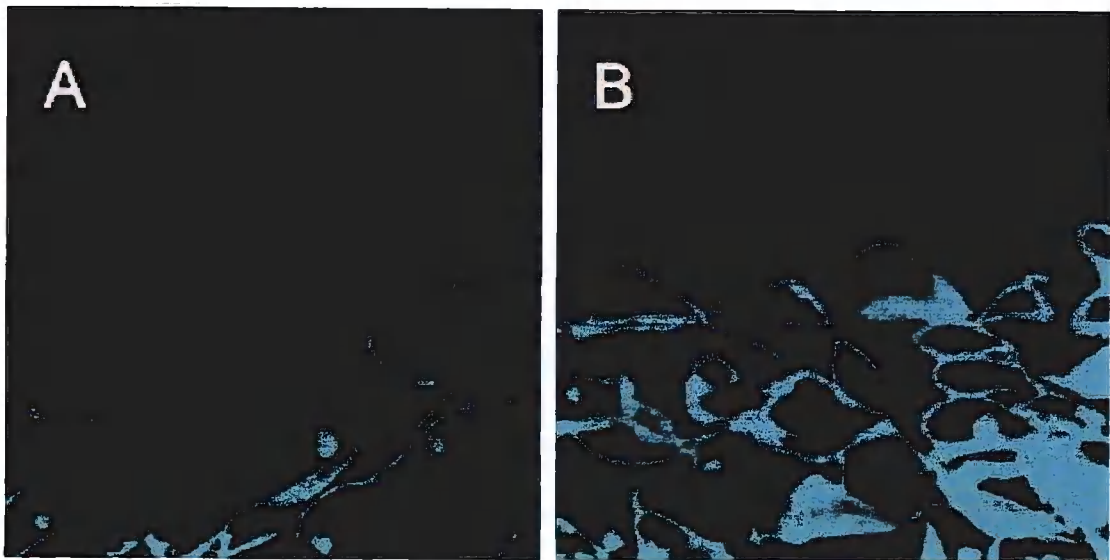


Figure 3.28: *DAPI stained epidermal petal cells A: Cells at petal edge of elongated narrow petal (see Figure 3.24 D), B: Boundary area between conical cells and flat cells showing conical cells beginning to loose shape.*

The petals with frills had flat regular cells leading up to the final cell layer at the edge which had rounded shaped cells. The combination of an unusually flat cellular surface combined with the round edge cells appeared to give the petals their frills.

The petals with s-bends contained patches of wild type conical cells next to patches of flat regular cells (Figures 3.27 B-D and 3.28 B). The contrast between the two cellular structures appeared to have created the waves and bends in the petal shape. Finally the elongated thin petals exhibited the same flat regular cell files along the entire length of the petal (3.28 A) with very few conical shaped cells at the apical end of the petal. The transgenic lines in both *hydra1* and *fk^{hyd2}* backgrounds both displayed the same deviations, suggesting no rescue of normal petal development by the respective gene expression constructs. The petal deviations therefore are likely to be a result of incomplete rescue from the *hydra* phenotype or related to a change in the plant sterol profile due to the expression of the HYDRA genes under the *PLS* (or *DR5*) promoters.

3.8 *pPLS::HYDRA2* x *fk^{hyd2}*

3.8.1 Overview of phenotype rescue in *pPLS::HYDRA2* x *fk^{hyd2}*

The phenotype of *pPLS::HYDRA2* x *fk^{hyd2}* was clearly affected by the *fk^{hyd2}* background. Root length was severely curtailed and only one line produced root lengths significantly different from *fk^{hyd2}*. The root cellular pattern was rescued but there was a loss of starch in the columella at 1 dpv. The shoot was also of wild type appearance except the petals of the mature plant were misshapen.

3.8.2 Root growth in *pPLS::HYDRA2* x *fk^{hyd2}*

For the *pPLS::HYDRA2* x *fk^{hyd2}* lines, there were observed differences in root growth between seedlings of independent transgenic lines. One line showed root growth rescued in comparison to the *fk^{hyd2}* homozygous controls, but the remaining two *pPLS::HYDRA2* x *fk^{hyd2}* lines did not exhibit a mean root length that was clearly different from the *fk^{hyd2}* homozygous mutants. The line with a noticeably longer mean root length did nevertheless exhibit a large variability in root growth, illustrated as the large standard deviation (Figure 3.29). One way ANOVA was performed to confirm there were statistically significant differences in mean root length within the set of

results (Table 3.4). A significant difference in mean root growth at 7 dpv was confirmed at the P0.0001 level. The differences between the independent lines are likely to be due to position effects, as the transgenes will be expected to have inserted at different genomic loci; the position effects will influence the level of expression of the HYDRA2 transgene.

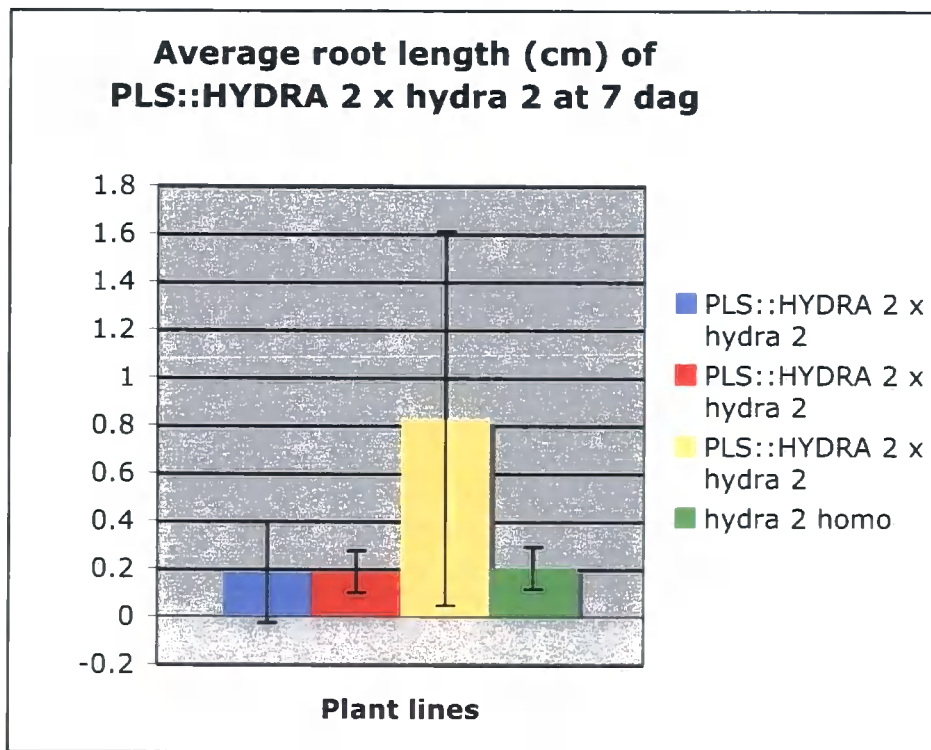


Figure 3.29 Mean root length with error bars of three independent transgenic lines of $pPLS::HYDRA2 \times fk^{hyd2}$ and controls ws and fk^{hyd2} homozygous for comparison

Table 3.4: Summary of results of One Way ANOVA. The P value, assuming the null hypothesis, is less than .0001

Variation	Sum of squares	d.f.	Mean squares	F
Between	4.240	3	1.413	8.418
Within	8.732	52	0.1679	
Total	12.97	55		

3.8.3 Lugol staining in $pPLS::HYDRA2 \times fk^{hyd2}$

No deviations in root development or cellular patterning were observed for any of the PLS promoter lines. However the $pPLS::HYDRA2 \times fk^{hyd2}$ lines exhibited an unexpected loss of staining in roots at 11 dpv despite displaying normal staining

presence at 7 dpf (Figure 3.30). This suggests incomplete phenotypic rescue of the fk^{hyd2} phenotype by the transgene.

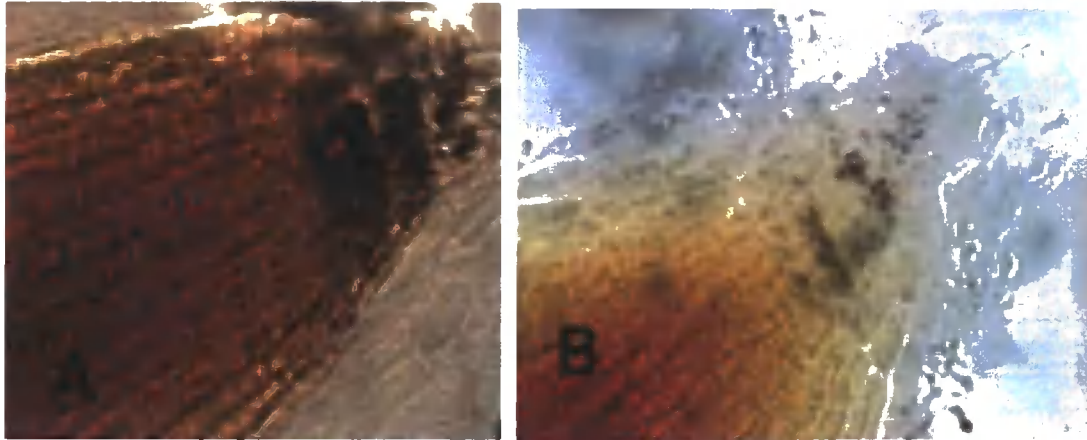


Figure 3.30: Lugol staining at 7 dpf in $pPLS::HYDRA2 \times fk^{hyd2}$ (A), loss of Lugol staining at 11 dpf in $pPLS::HYDRA2 \times fk^{hyd2}$ (B).

3.9 Rescue in the *UAS* promoter driven lines

3.9.1 Overview of phenotypic rescue

The phenotypes of the lines $pUAS::HYDRA1 \times hydra1$ (epidermis) and $pUAS::HYDRA1 \times hydra1$ (pericycle) produced phenotypes the closest to full rescue out of all the promoter lines. Cellular patterning and structure in the root were restored, there were no deviations in petal shape as had been observed in the other lines and the roots were significantly longer than *hydra1*. The phenotype of $pUAS::HYDRA1 \times hydra1$ (endodermis) presented variable results with one line showing rescued root length and the other not. Cellular structure in the root was rescued and the staining of the columella was the same as wildtype.

3.9.2 Root growth in $pUAS::HYDRA1 \times hydra1$ (epidermis/pericycle/endodermis)

Root growth was measured in seedlings of the *UAS* transgenic lines grown on vertical plates at 4, 5, 6 and 7 dpf, as detailed in Materials and Methods section 2.5. The individual *UAS*/mutant lines that were analysed for phenotypic rescue were numbered 0.1.1, 0.3.3 and 0.7.4, plus the root tissue identifier (epidermis, endodermis, pericycle), referring to the site of both *GFP* and *HYDRA1* gene expression.

All roots were measured from the root tip to the start of the hypocotyl. The mean lengths of each line showed significant differences between the *pUAS::HYDRA1* construct lines and the same lines which had been crossed into the *hydra* background (Figures 3.31-3.34). A One-way ANOVA was performed and confirmed there were significant differences between the line means at $p < 0.0001$ for each day of measurements (tables 3.5-3.8). It was again confirmed there were significant differences between the line means at $p < 0.0001$ for each day of measurements.

Some variability in the data was observed for individual lines, and there are a number of reasons for this. The *ws* control germinated very late and developed slowly, which was discovered to be a problem with the seed batch. The line *pUAS::HYDRA1 0.3.3 x hydra1*, which expresses *HYDRA1* in the endodermis, presented very low rates of germination, although those plants which did germinate developed normally. Subsequent plating out of this line (5/14, 6/14, 3/14) found low rates of germination which was not found in the parent line *pUAS::HYDRA1* (11/14, 12/14, 13/14).

The low germination rates in a few lines possibly leading to a high variation from the mean could be corrected by using larger sample sizes. However it is worth noting the *hydra* mutants typically display a wide variation in root length and other phenotypic variables (Topping et al. 1997; Souter et al. 2002).

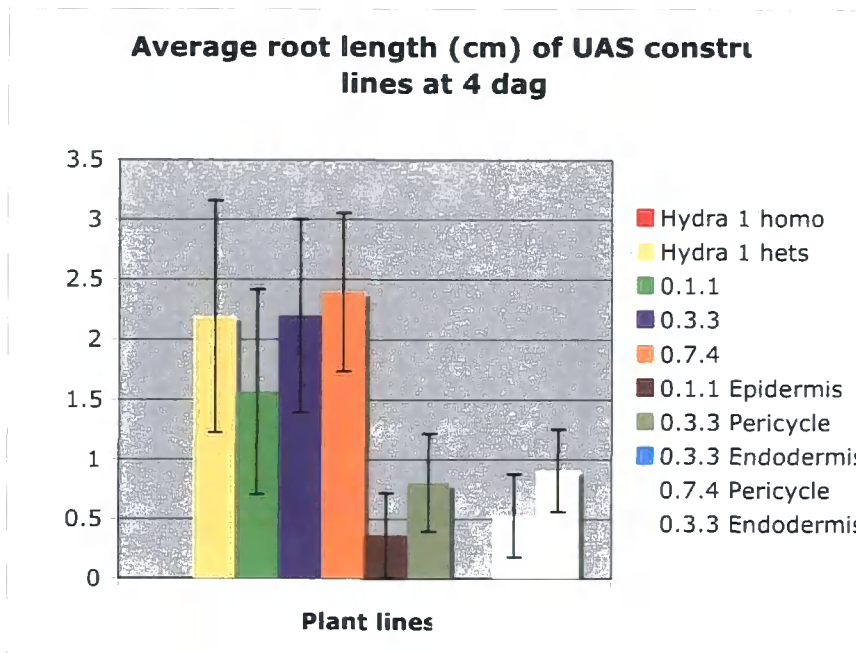


Figure 3.31: Mean root length with error bars of *pUAS::HYDRA1 x hydra1* expressing in epidermis (0.1.1), Endodermis (0.3.3 and 0.7.4) and Pericycle (0.3.3 and 0.7.4) and parent lines (*pUAS::HYDRA1* from same dipping pot origins) and controls, *hydra 1* heterozygous and *hydra1* homozygous for comparison.

Tables 3.5 : Summary of one-way ANOVA on mean root length measurements at 4 dpd $p < 0.0001$

Variation	Sum of squares	d.f.	Mean squares	F
Between	107.6	9	11.96	36.43
Within	42.67	130	0.3282	
Total	150.3	139		

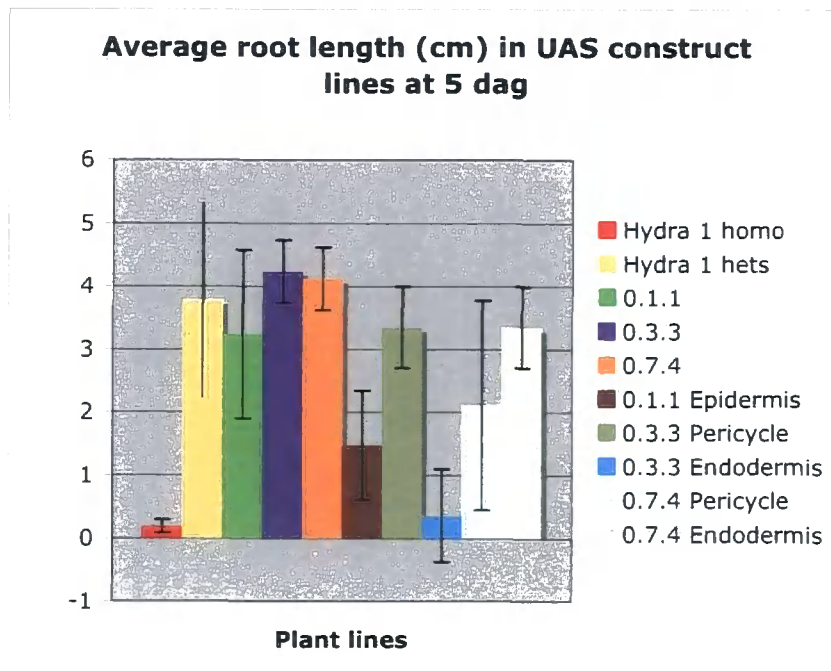


Figure 3.32: Mean root length with error bars of pUAS::HYDRA1 x *hydra1* expressing in epidermis (0.1.1), endodermis (0.3.3 and 0.7.4) and pericycle (0.3.3 and 0.7.4) and parent lines (UAS::HYDRA1 from same transformation event) and controls *hydra1* heterozygous and *hydra1* homozygous for comparison.

Tables 3.6 Summary of one-way ANOVA on mean root length measurements at 5 dpd $p < 0.0001$

Variation	Sum of squares	d.f.	Mean squares	F
Between	282.4	9	31.38	32.91
Within	124.0	130	0.9535	
Total	406.3	139		

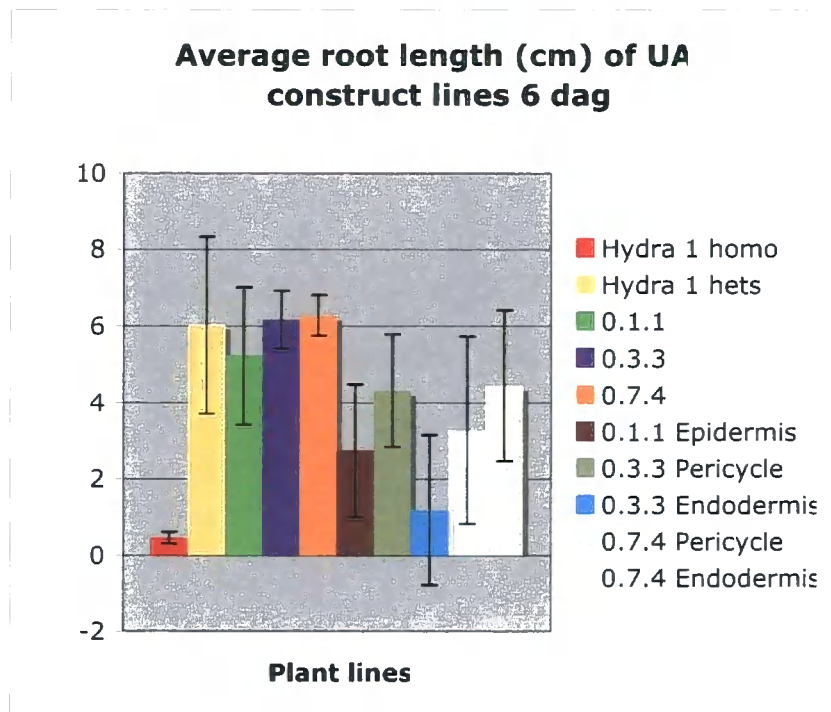


Figure 3.33: Mean root length with error bars of pUAS::HYDRA1 x *hydra1* expressing in epidermis (0.1.1), Endodermis (0.3.3 and 0.7.4) and Pericycle (0.3.3 and 0.7.4) and parent lines (UAS::HYDRA1 from same dipping pot origins) and controls *hydra1* heterozygous and *hydra1* homozygous for comparison.

Tables 3.7: Summary of one-way ANOVA on average root length measurements at 6 dpv $p < .0001$

Variation	Sum of squares	d.f.	Mean squares	F
Between	535.9	9	59.54	21.03
Within	368.1	130	2.831	
Total	903.9	139		

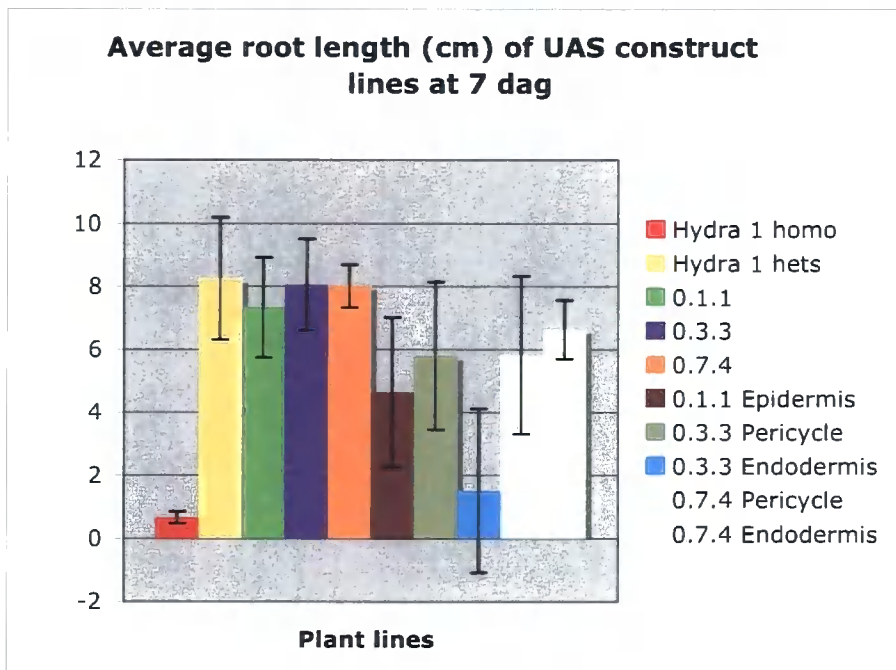


Figure 3.34: Mean root length with error bars of UAS::HYDRA1 x *hydra1* expressing in epidermis (0.1.1), endodermis (0.3.3 and 0.7.4) and pericycle (0.3.3 and 0.7.4) and parent lines (UAS::HYDRA1 from same dipping pot origins) and controls *hydra 1* heterozygous and *hydra1* homozygous for comparison.

Tables 3.8: Summary of one-way ANOVA on mean root length measurements at 7dpg. $p < 0.0001$

Variation	Sum of squares	d.f.	Mean squares	F
Between	909.6	9	101.1	29.77
Within	441.3	130	3.395	
Total	1351.0	139		

3.9.3 Lugol staining in UAS:: HYDRA1 x *hydra1* (epidermis/pericycle/endodermis)

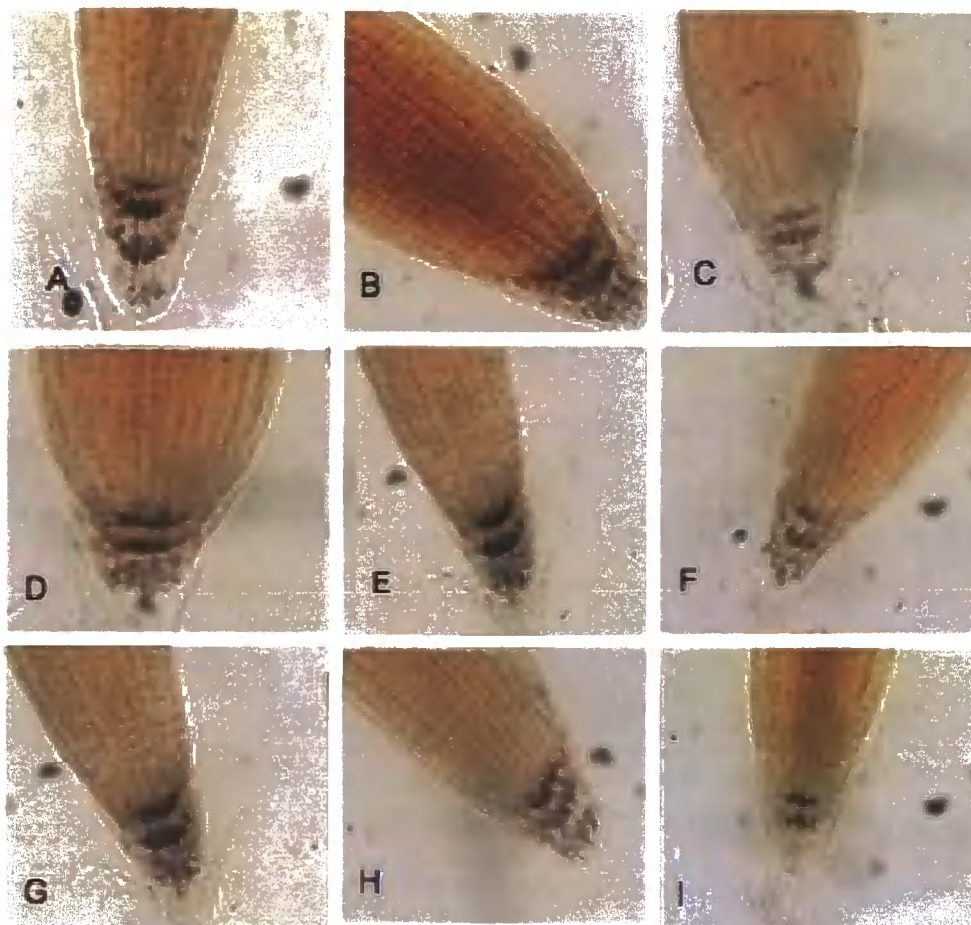


Figure 3.35: Lugol staining in *pUAS::HYDRA1 x hydra1* lines at 7, 11 and 14 dpf respectively for epidermis lines (A,B,C) endodermis layer (D,E,F) and pericycle (G,H,I).

Like the *DR5* and *PLS* promoter lines, the UAS promoter lines presented variability in staining that was also present in the parent lines and the *ws* roots. No deviation in cellular patterning typical of *hydra1* was observed (Figure 3.35).

3.9.4 Petal shape in UAS:: HYDRA1 x *hydra1* (epidermis/pericycle/endodermis)

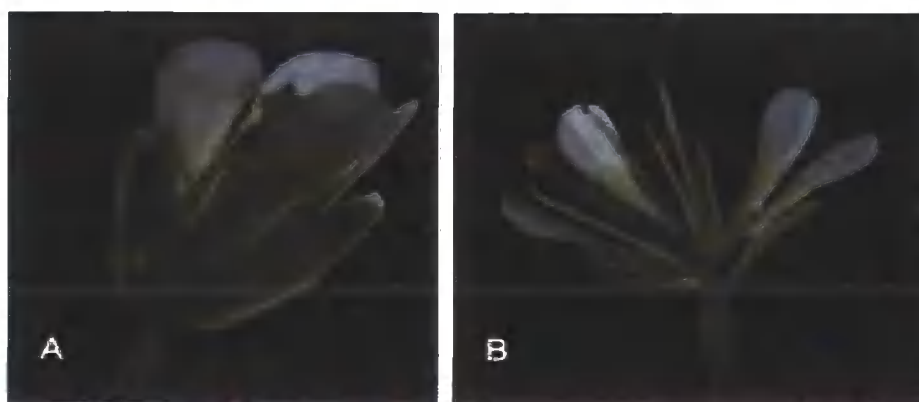


Figure 3.36: Example of typical flowers in the UAS promoter lines A= *UAS::HYDRA1xhydra1* (epidermis), B=*UAS::YDRA1 x hydra1*(pericycle) flower opened to display floral organs and petals.

Unlike the petals in the mature plants of the *DR5* and *PLS* promoter lines, the *UAS* promoter plant lines did not produce any deviation in petal shape from *ws* (Figure 3.36).

3.10 Cloning of the *HYDRA2* promoter

The sites of expression in wild type plants of the *HYDRA1* gene are already known, however the sites of expression for the *HYDRA2* gene are not clearly defined. As the *HYDRA2* gene is being expressed under different promoters, the knowledge of the sites of expression in wild type plants would be useful for interpretation of results. The cloning procedure was carried out as detailed in 2.1.5, 2.2.12, 2.2.1 and 2.2.10. The promoter was to be cloned into the TOPO vector first and the cloned sequence checked for inaccuracies before cloning into Δ pcirce-gus.

The *HYDRA2* gene promoter was successfully cloned into the TOPO vector which was confirmed first by a PCR reaction using primers (Figure 3.37; Table 3.9) for the *HYDRA2* promoter and then by sequencing the vector and checking the sequence was present and each base correct.

Further work on this was not possible due to lack of time.

Table 3.9: Primers used in the cloning of the HYDRA2 gene promoter

Primer name:	Primer sequence (5'→3'):	Product length:	Function:
HY2prom(+980)	TCC CTC ATC CTT TTC GCA GCA ACT	2.5kp	To amplify the sequence to be cloned.
HY2prom (-3530)	ACC GAG ATC CAT ATC TAG CAG		
HY2pro(Bam)+ 1127	CGG GAT CCC TTC CCC ATT GCT TCT CCA CAC CT	2.4kb	To add BAM H1 linker sites to the sequence for cloning.
HY2pro(Bam)-3490	GGG GAT CCG CAG CAT TAA GCA GAA GAA GGA TTT TC		
Hyd2proFOR	TGC TTT GTG TGG GTT ACA TGG	500bp	To check for presence of HYDRA 2 promoter in colony PCR.
Hydr2pro(mid) rev	GAT GGA CCA TAG TGG AAA AAG		



Figure 3.37: Gel electrophoresis of PCR products from bacterial colonies positive for HYDRA 2 gene promoter. L= Hyperladder I, bands resolve at 500 bp. Primers Hyd2proFOR and Hydr2pro(mid) rev.

4.0 Discussion

It is not known at the mechanistic level how the *hydra* phenotype is generated. The disruption in sterol biosynthesis and subsequent altered sterol profile may lead to a loss of sterol-based signals required for development (Schrick et al. 2000), or disruption of other hormone signalling pathways (Souter et al. 2002, 2004); or some other mechanism. To determine whether sterol biosynthesis is required in specific cell types, we expressed the wild type *HYDRA1* and *HYDRA2* genes respectively under tissue specific promoters in the relevant *hydra* backgrounds and looked for evidence of phenotypic rescue. Phenotypic rescue did occur in all lines analysed, however there were differences in the extent of phenotypic rescue under different promoters and in different independent transgenic lines. Furthermore, where the same promoters were used, there was a difference in the degree of rescue in *hydra1* to *fk^{hyd2}*. *fk^{hyd2}* displayed partial rescue under the *DR5* and *PLS* promoters whereas *hydra1* displayed almost complete restoration to wild type phenotype. *fk^{hyd2}* is known to have the more severe phenotype of the two mutants, this result may indicate the product of C-14 reductase has a particularly critical role in plant development.

4.1 Survey of GFP expression

The activity of the endodermal and pericycle *UAS* enhancers in the hypocotyl and shoot needs to be taken into account when assessing rescue. The mis-expression observed in one fifth of the seedling expressing in the epidermis, endodermis and pericycle lines after the cross into the *hydra1* background, due to the aberrant cellular patterning and specification in the *hydra* mutants, should also be taken into account.

4.2 Phenotypic rescue in root length

There was seen a clear difference in average root length between the different promoter-construct lines crossed into the *hydra* background and the controls. The lines expressing *HYDRA1* under the control of the *UAS* promoter in the epidermis, endodermis and pericycle exhibited root lengths closer to the parent lines and *hydra* heterozygous controls than the lines under the control of the *PLS* and *DR5* promoters. The difference in

root length between the UAS promoter lines and controls narrowed towards 7 dpv and in older roots the wild-types and transgenic became almost indistinguishable.

The rescue in the *HYDRA2* expressing lines was less distinct than in the *HYDRA1* lines. The root length measurements of *pPLS::HYDRA2 x fk^{hyd2}* did not present a convincing argument for rescue. If the seedlings were not of wildtype phenotype the conclusion would have been that no phenotypic rescue had occurred. However genotyping (in collaboration with Jia Hashmi) has confirmed the *pDR5::HYDRA2 x fk^{hyd2}* seedlings were *fk^{hyd2}* homozygous. Therefore genuine phenotypic rescue, though incomplete, was observed. An intriguing aspect of this line is the delayed onset of rescue in some seedlings. Until seedlings were planted out in soil at 21 dpv, there was no visible discernible difference from *fk^{hyd2}* homozygous in root length.

Variability in root length was found to be high amongst all lines, including the controls. This is likely to be due in part to the inherent variability in the *hydra* mutant still exerting an influence on the lines. For the *PLS* and *DR5* lines, position effects can be expected to account for variation in rescue between independent transgenic lines, reflecting likely differences in the level of transgene expression (Matzke and Matzke, 1998; Peach and Velten, 1991).

4.3 Extent of rescue in cellular patterning in the columella and root cap

For the lines expressing the *HYDRA1* gene in the *hydra1* background, the lines all show a columella starch signal (indicating correct differentiation of the columella) and cellular patterning when the root is stained with Lugol solution.

The promoter lines driving the expression of *HYDRA2* in *fk^{hyd2}* background showed Lugol staining indicative either of *fk^{hyd2}* or wild type phenotype in the lines under the control of *DR5*. The differences again are likely to be due to position effects in the independent transgenic lines. In the lines under the control of the *PLS* promoter there is a wildtype Lugol staining and cellular patterning, but a loss of columella staining occurs before 14 dpv. In the case of *pDR5::HYDRA2 x fk^{hyd2}*, the Lugol stain proved to be an efficient method to identifying the seedlings with full phenotypic rescue from those with only rescue in root growth but not columella specification.

4.4 Extent of rescue in the shoot

The shoot was fully rescued in the *UAS* promoter lines with a stem, distinct leaves and a fully rescued flower anatomy including reproductive organs. The pattern of rescue may have been aided by transgene expression site in specific cell types in the hypocotyl (the pericycle). However the epidermis *UAS* expression line did not exhibit expression in the shoot, suggesting that shoot rescue is a result of *HYDRA1* gene expression in the root epidermis only.

The misshapen petal epidermal cells in the flowers of the lines *pPLS::HYDRA1 x hydra1*, *pPLS::HYDRA2 x fk^{hyd2}*, *pDR5::HYDRA1 x hydra1* and *pDR5::HYDRA2 x fk^{hyd2}* suggest two conclusions: 1) The lines are not fully rescued and this is a consequence of the sterol defects in the *hydra* mutants or 2) the promoters are expressing the *HYDRA* genes in areas where the gene is not normally expressed altering the sterol profile of the tissues. Of relevance here is the *fr11* sterol mutant (Hase *et al.*, 2000), which is characterised by its display of frilly petals due to incomplete endoreduplication in the epidermal petal cells. As sterol mutants are known to produce altered petal shapes before, it is reasonable to assume the mis-shapen petal cells could be an unrescued element of the *hydra* phenotype. Though the parent lines *pPLS::HYDRA1*, *pPLS::HYDRA2*, *pDR5::HYDRA2* and *pDR5::HYDRA1* have not previously produced a noticeable difference in petal shape, they should be more closely examined in order to identify any deviations in petal shape, which would be due to an overexpression phenotype.

4.5 *hydra1* rescue compared with *fk^{hyd2}* rescue

There was variation in the degree of phenotypic rescue between *hydra1* and *fk^{hyd2}*. The *PLS* and *DR5* promoter lines, which have similar though not identical expression patterns (Sabatini *et al.*, 1999; Casson *et al.*, 2002), were compared in terms of the extent of phenotypic rescue in each mutant background.

In the *hydra1* background *DR5* and *PLS* driving *HYDRA1* expression presented a more pronounced and consistent level of phenotypic rescue, compared with the *fk^{hyd2}* mutant complementation experiments. The *hydra1* transgenic lines have mis-shapen petals on the mature plant and a reduced root length at 7 dpg compared to phenotypically *hydra1* heterozygous controls (the *hydra* mutations are recessive; Topping *et al.*, 1997; Schrick *et al.*,

2000). However, apart from this, the phenotype of the lines were similar to wild type throughout development. Although some seedlings were indistinguishable from *fk^{hyd2}* until 21 dpv after germination and after this point only presented partial phenotypic rescue with *hydra*-like root tips and only partial shoot rescue, this is likely to be due to position effects on the level of expression of the transgene in the independently transformed lines, and this possibility can be tested in the future. Since the *DR5* promoter is active in response to auxin, some inter-seedling variation in rescue could be due to signalling differences between individuals. Nevertheless, some *pDR5::HYDRA2 x fk^{hyd2}* seedlings exhibited the same extent of phenotypic rescue as *pDR5::HYDRA1 x hydra1*. *pPLS::HYDRA2 x fk^{hyd2}* produced a consistent phenotypic rescue of root morphology, although Lugol staining revealed a loss of starch in the columella and so of columella cell specification) beyond 11 dpv.

Comparing the phenotypic rescue of *hydra1* and *fk^{hyd2}*, under the *PLS* and *DR5* promoters it becomes clear the *fk^{hyd2}* phenotype is not as rescued to the same extent as the *hydra1* phenotype. This may be the consequence of difference in the normal site of expression of the *HYDRA1* vs. *HYDRA2* genes. Also, as *fk^{hyd2}* does have the more severe mutant phenotype, these results may indicate the function(s) of C-14 reductase or its sterol product are more complex than C8,7 isomerase.

4.6 Sterols as a signalling molecule essential for development

Schrack *et al.*, (2000) proposed there could be a sterol based signalling molecule or molecules, distinct from brassinosteroids and essential for correct plant development. The absence of this signal was proposed to be the cause of the *fk^{hyd2}* phenotype. There are inherent problems with this theory due to the lipophilic nature of sterols, as it seems unlikely a sterol based signal would be transported intercellularly, for thermodynamic reasons. It is possible sterols could be mobile across tissues if carried by a protein or proteins, but there is currently no evidence for this. One prediction of a 'mobile sterol' model would be that restoring the sterol biosynthesis pathway in different tissue types would result in a similar level of rescue across all the lines - an essential yet mobile sterol signal would produce the same corrective response in the phenotype regardless of expression site. However the differences in phenotypic rescue, particularly in the lines in the *fk^{hyd2}* background, suggests this is not the case. There are clear differences in the extent of phenotypic rescue between *pPLS::HYDRA2x*

fk^{hyd2} and *pDR5::HYDRA2x fk^{hyd2}*. There are also differences in the extent of phenotypic rescue in the *hydra1* lines. This suggests a more complex and possibly tissue specific element to the role of sterols in correct plant development rather than a single all encompassing sterol based signalling molecule.

4.7 Auxin fountain model and phenotypic rescue

An alternative theory to explain the variation in rescue could be based on a requirement for sterols in the translocation of other, non-cell autonomous signalling molecules, and a key candidate is auxin, given the known auxin distribution defects in the *hydra* mutants (Souter *et al.*, 2002, 2004) and the known importance of auxin in root development. Auxin holds an important role in cell elongation and also is involved in crosstalk with other hormones such as ethylene and gibberellins necessary for correct growth and development. If the cellular membranes in *hydra* are disrupted by altered sterol biosynthesis resulting in a changed membrane composition, the components of the membranes, such as auxin transporters, could be functionally altered. This could adversely affect the 'reverse fountain flow' pattern of auxin in the root tip, required for meristem patterning and activity. Lipid rafts in plants, (microdomains composed of sterols, sphingolipids and specific proteins assumed to have a role in cell signalling), are still a controversial concept (Edidin 2003; Martin *et al.*, 2005; Munro 2003). However less controversial membrane associated components involved in signalling and transport could be affected including PINs. For example, Willemsen *et al.*, (2003) show that the *orc* mutant of Arabidopsis, defective in sterol biosynthesis, exhibits PIN localization defects; and Grebe *et al.*, (2003) suggest a direct role for sterols in PIN2 trafficking.

Given the predicted spatial pattern of auxin flow in the root, which is dependent to a significant extent on the PIN proteins (Grieneisen *et al.*, 2007), auxin is expected to cycle move directionally through the tissues that the *UAS* enhancers drive *HYDRA1* expression in (especially epidermis). Rescue may be expected to be more effective compared to the *PLS* promoter, given that the *HYDRA1* promoter is most active in epidermal cells rather than in the root meristem and columella (Margaret Pullen, unpublished data).

This could explain the suspected lack of rescue in the *pUAS::HYDRA1 x hydra1* driven in the endodermis (Figure 3.5), and could be linked to auxin not appearing to have a

major role in cell development or differentiation in the endodermis (Petricka and Benfey, 2008).

A difference between the *pPLS::HYDRA2 x fk^{hyd2}* line and the *pPLS::HYDRA1 x hydra1* line was the loss of columella identity (seen as lack of starch-containing cells) in the former. This may be due to a difference in the tissue-specificity of the native *HYDRA1* and *HYDRA2* promoters, with no requirement for *HYDRA1*-generated sterols in the columella. More detailed analysis of the *HYDRA2* gene promoter is required.

4.8 Summary of main findings

The results obtained during course of this project can be summarised as follows:

- 1) Expression of the *HYDRA1* and *HYDRA2* genes respectively under the control of the *DR5* and *PLS* promoters in the respective mutant backgrounds leads to partial phenotypic rescue.
- 2) Expression of the *HYDRA1* gene under the control of the *pUAS::pericycle* and *pUAS::epidermis* enhancer traps respectively leads to rescue of root patterning in the *hydra1* root tip, and significant rescue of root growth.
- 3) Expression of the *HYDRA1* gene in the endodermis of *hydra1* may not rescue the phenotype and this requires further investigation.
- 4) Expression of the *HYDRA2* gene under the *DR5* promoter in *fk^{hyd2}* has little rescue effect until after 21 dpg.
- 5) Expression of the *HYDRA1* or *HYDRA2* genes under the *PLS* or *DR5* promoters results in plants exhibiting a collapse or malformation of conical epidermis petal cells. Intriguingly, this does not occur when *HYDRA1* is expressed in either the epidermis, endodermis, or pericycle.

4.9 Conclusion

The major conclusion from this study is that correct sterol biosynthesis is not required in all root tissues for correct plant development.

4.10 Further work

The work discussed here suggests further studies to investigate the role of sterols in plant development, as follows:

1) Expression of sterol biosynthesis in other root cell types, such as the cortex and vascular tissues, could be carried out to determine effects in rescuing developmental defects in sterol mutants.

2) PIN immunolocalization (Friml *et al.*, 2003; Papanov *et al.*, 2005) could be used to ascertain the localization of the PINs in the root in the different lines. If the auxin flow is influencing the rescue in the *pUAS::HYDRA1 x hydra1 x GFP* pericycle and *pUAS::HYDRA1 x hydra1 x GFP* epidermis then the PINs should appear normally localized in phenotypically rescued seedlings..

3) FACs analysis could be performed on the lines, which produced misshapen petals to ascertain if endoreduplication is responsible, as in the *fr11* sterol mutant (Hase *et al.*, 2000).

Appendix 1: Root length data for lines analysed.

pUAS::HYDRA1 x hydra1 x GFP (epidermis/endodermis/pericycle) at 4 dp

Sample no:	<i>hydra1</i> homo	<i>hydra1</i> hets	0.1.1	0.3.3	0.7.4	0.1.1 Epidermis	0.3.3 Pericycle	0.3.3 Endodermis	0.7.4 Pericycle	0.7.4 Endodermis
1	0	2.63	1.47	3.38	3.44	0.33	0.85	0	0.71	0.89
2	0	2.75	1.75	2.02	2.59	0.92	0.98	0	0.69	1.15
3	0	3.2	2.9	1.75	1.65	0.57	0.74	0	0.57	1.38
4	0	0.33	1.54	2.5	2.58	0.22	1.34	0	0.56	1.08
5	0	2.88	1.93	3.1	1.56	0.34	0.56	0	0.96	0.96
6	0	1.68	0.29	1.89	2.24	0.5	1.05	0	0.84	1.32
7	0	2.38	2.87	1.71	1.5	0.50	0.78	0	0.96	0.74
8	0	1.73	0.28	2.16	3.49	1.05	1.06	0	0.86	0.93
9	0	2.54	0.26	2.74	2.19	0.64	0.90	0	0.41	1.21
10	0	2.18	1.35	2.12	2.84	0	1.3	0	0.23	0.78
11	0	2.41	1.41	2.08	1.94	0	1.08	0	0.58	0.74
12	0	3.05	2.39	2.47	3.09	0	0.59	0	0	0.86
13	0	2.88	1.7	2.8	1.93	0	0	0	0	0.65
14	0	0	1.72	0	2.51	0	0	0	0	0
Mean	0	2.19	1.56	2.19	2.39	0.36	0.8	0	0.52	0.91
St. Dev.	0	0.97	0.85	0.81	0.66	0.35	0.41	0	0.35	0.35

pUAS::HYDRA1 x hydra1 x GFP (epidermis/endodermis/pericycle) at 5 dp

Sample no:	<i>hydra1</i> homo	<i>hydra1</i> hets	0.1.1	0.3.3	0.7.4	0.1.1 Epidermis	0.3.3 Pericycle	0.3.3 Endodermis	0.7.4 Pericycle	0.7.4 Endodermis
1	0.11	4.21	3.33	4.84	4.25	0.33	3.67	1.55	3.05	3.67
2	0.03	4.52	3.4	4.56	3.9	1.5	2.9	2.12	2.61	2.9
3	0.24	4.52	4.17	2.96	3.41	2.49	4.33	1.37	2.09	4.33
4	0.25	0.65	4.2	3.86	4.62	1.83	3.45	0	2.54	3.45
5	0.01	4.87	3.63	4.52	3.93	1.35	3.17	0	4.25	3.17
6	0.13	3.42	1.12	4.12	4.7	1.43	4.61	0	3.9	4.61
7	0.42	4.66	4.31	4.41	3.78	1.47	3.22	0	4.12	3.22
8	0.19	4.48	1.22	4.63	4.76	1.69	2.89	0	4.03	2.89
9	0.24	4.91	0.31	4.43	4.39	2.66	3.94	0	2.12	3.94
10	0.29	3.41	4.35	4.43	4.25	2.59	2.14	0	0.48	2.14
11	0.24	4.25	3.95	3.55	3.18	1.28	3.32	0	0.33	3.32
12	0.24	4.54	4.28	4.09	4.51	2.02	2.72	0	0	2.72
13	0.17	4.41	3.57	4.61	3.59	0	3.37	0	0	3.37
14	0.17	0	3.43	4.24	4.4	0	3.11	0	0	3.11
Mean	0.19	3.77	3.23	4.23	4.12	1.47	3.35	0.36	2.11	3.35
St. Dev.	0.11	1.53	1.34	0.5	0.49	0.87	0.64	0.73	0.66	0.64

pUAS::HYDRA1 x hydra1 x GFP (epidermis/endodermis/pericycle) at 6 dpf

Sample no:	<i>hydra1</i> homo	<i>hydra1</i> hets	0.1.1	0.3.3	0.7.4	0.1.1 Epidermis	0.3.3 Pericycle	0.3.3 Endodermis	0.7.4 Pericycle	0.7.4 Endodermis
1	0.35	7.15	6.74	6.75	4.73	1.26	2.77	0.81	5.79	4.4
2	0.54	7.43	6.08	6.37	6.35	3.29	4.82	3.22	4.64	5.89
3	0.45	6.88	6.24	5.83	6.22	4.43	4.55	4.56	4.12	5.49
4	0.53	1.42	5.62	4.62	6.57	3.37	3.98	2.48	4.36	4.66
5	0.21	7.21	6.65	6.42	6.36	1.98	5.41	5.83	5.46	6.36
6	0.33	6.53	3.95	6.28	6.9	3.51	5.39	0	5.53	5.19
7	0.77	7.05	6.33	5.93	6.44	3.99	5.65	0	5.52	4.93
8	0.46	6.78	3.47	6.69	6.81	3.81	4.43	0	5.44	4.43
9	0.67	7.88	3.44	6.02	6.27	4.47	5.47	0	4.00	4.74
10	0.53	6.19	0.38	5.95	6.52	4.1	4.54	0	0.63	4.69
11	0.48	6.35	5.81	5.49	6.2	4.19	5.27	0	0.35	5.69
12	0.45	6.9	6.14	5.37	6.16	0	4.33	0	0	5.63
13	0.25	6.51	6.02	7.74	5.72	0	3.8	0	0	0
14	0.34	0	6.21	6.93	6.56	0	0	0	0	0
Mean	0.46	6.02	5.22	6.17	6.27	2.74	4.31	1.19	3.27	4.44
St. Dev.	0.15	2.31	1.79	0.76	0.53	1.73	1.47	1.96	2.45	1.97

pUAS::HYDRA1 x hydra1 x GFP (epidermis/endodermis/pericycle) at 7 dpf

Sample no:	<i>hydra1</i> homo	<i>hydra1</i> hets	0.1.1	0.3.3	0.7.4	0.1.1 Epidermis	0.3.3 Pericycle	0.3.3 Endodermis	0.7.4 Pericycle	0.7.4 Endodermis
1	0.57	8.66	8.45	11.2	7.36	4.58	5.96	4.98	7.79	8.07
2	0.76	9.21	7.99	8.13	9.03	6.03	0.41	6.61	7.9	6.3
3	0.86	8.1	8.04	6.86	8.34	6.45	0.46	6.37	6.3	8.46
4	0.63	2.56	7.53	6.84	8.32	5.06	6.51	3.21	6.03	7.52
5	0.34	9.7	7.81	11.32	8.28	1.49	6.46	0	6.18	6.41
6	0.56	6.9	6.15	7.65	9.08	5.27	6.99	0	7.58	7.41
7	1.02	9.07	8.44	7.67	8.91	6.27	7.4	0	7.57	5.49
8	0.56	6.9	7.98	7.74	7.31	6.22	7.34	0	6.14	5.69
9	0.85	8.41	2.15	7.57	7.09	4.78	6.63	0	7.88	6.85
10	0.79	9.05	7.72	7.06	7.47	5.23	6.91	0	7.65	6.52
11	0.65	8.61	7.41	7.35	7.3	6.75	7.67	0	6.35	6.41
12	0.7	8.48	7.9	7.24	7.66	6.81	6.7	0	0.91	5.31
13	0.52	8.81	7.33	7.24	8.3	0	6.22	0	2.12	6.31
14	0.48	11.01	7.67	8.92	7.78	0	5.44	0	1.18	6.08
Mean	0.66	8.25	7.33	8.06	8.02	4.64	5.79	1.51	5.83	6.64
St. Dev.	1.79	1.93	1.59	1.46	0.68	2.38	2.34	2.59	2.51	0.94

pPLS::HYDRA1 x hydra1 at 7 dpg

Sample no:	0.1.11	0.2.3	Hydra 1 hets	hydra1 homo
1	2.425	1.032	8.6575	0.266
2	2.096	0.016	9.2085	0.119
3	3.043	0	8.0845	0.244
4	3.912	0.915	2.562	0.246
5	2.598	3.196	9.6955	0.008
6	0.874	0.1	6.8955	0.131
7	2.773	1.265	9.071	0.424
8	1.472	1.496	6.895	0.191
9	1.988	1.026	8.4135	0.239
10	0.577	1.138	9.0495	0.291
11	1.505	1.009	8.6095	0.238
12	1.619	0	8.479	0.237
13	0.908	0	8.8085	0.166
14	0.368	0	11.005	0.173
Mean:	1.8684286	0.7995	8.2453214	0.21235714
St.Dev:	1.0176904	0.8936597	1.9344841	0.09576141

pPLS::HYDRA2 x fk^{hyd2} at 7 dpg

Sample no:	0.4.2	0.2.4	0.1.1	hydra2 homo
1	0.301	0.102	0.271	0.213
2	0.18	0.212	1.642	0.142
3	0.521	0.285	1.964	0.247
4	0.519	0.256	1.232	0.201
5	0.248	0.087	1.442	0.17
6	0.426	0.321	0.697	0.177
7	0.381	0.189	0.825	0.155
8	0	0.166	1.698	0.401
9	0	0.249	1.801	0.034
10	0	0.017	0	0.141
11	0	0.102	0	0.157
12	0	0.253	0	0.221
13	0	0.136	0	0.269
14	0	0.237	0	0.319
Mean:	0.184	0.1865714	0.8265714	0.203357143
St.Dev:	0.2108518	0.0877231	0.7821196	0.088443469

pDR5::HYDRA1 x hydra1 at 7 dpg

Sample no:	0.5.1	hyd1	Hydra 1 hets
1	1.452	0.266	8.6575
2	2.115	0.119	9.2085
3	1.956	0.244	8.0845
4	1.134	0.246	2.562
5	0.516	0.008	9.6955
6	1.771	0.131	6.8955
7	1.163	0.424	9.071
8	0.636	0.191	6.895
9	0.16	0.239	8.4135
10	0.398	0.291	9.0495
11	0.329	0.238	8.6095
12	0.034	0.237	8.479
13	0.48	0.166	8.8085
14	0.74	0.173	11.005
Mean:	0.9202857	0.2123571	8.2453214
St.Dev:	0.6831839	0.0957614	1.9344841

Appendix 2: Summay of primers used in genotyping process

Primer name:	Primer sequence (5' – 3'):	Product length:	Function:
Act2 for	GGA TCG GTG GTT CCA TTC TTG	300bps	To check presence of gDNA in sample and concentration required for PCR.
Act2 rev	AGA GT TGT CAC ACA CAA GTG CA		
UAS Sal-for	GTC GAC GTC GGA GTA CTG TC	220bps	Check for presence of UAS promoter.
UAS Sal-rev	GTC GAC TCG TCC TCT CCA AAT G		
PLS v.small	TGT TGG CGC AGT GTC TCA CT	280bps	Used with sterol 5' 2 as a primer pair in checking for the presence of the PLS promoter.
DR5 Sal-for	GTC GAC CTT GGG TAC CTT TTG	300bps	Used to check for presence of DR5 promoter.
DR5 Sal-rev	GTC GAC TGT AAT TGT AAT TGT AAA TAG		
Sterol 5' 1	TGA CCA GAA AAA CAC ACA GAG A	1.1kb	To check for presence of uninterrupted wild-type HYDRA 1 gene.
Sterol 3' 2	GCT ATG TTG TCT GTC TGT CTT		
Sterol 5' 2	CCA TCG TCT CTA TCT ACC TCG G	1kb	To check for presence of uninterrupted wild-type HYDRA 1 gene.
Sterol 3' 1	CTT GTG AGG ATA ATT TAT C		
Sterol 3' 3	ATT TCG GTT TGC CAG CTC TA	799bps with 3' 1 as a primer pair. 686bps with 3' 2 as a primer pair.	To check for presence of uninterrupted wild-type HYDRA 1 gene.

Appendix 2 continued:

Sterol 3' 4	TGT TGA AGG GAT CAC TGC TG	619bps with 5' 1 as a primer pair. 506bps with 5' 2 as a primer pair.	To check for presence of uninterrupted wild-type HYDRA 1 gene.
Sterol Intron F1	CCC TCA TCT CTC TCG AAA CG	528bps	Set of primers designed to work in an intron of wild type HYDRA 1 gene.
Sterol R1	CCA TCA ACA ACA ACA AAC TTC AA		
Sterol Intron F2	CCT CCC TC A TCT CTC TCG AA	493 bps	Set of primers designed to work in an intron of wild type HYDRA 1 gene.
Sterol R2	CAC AAA AAC CAA AAT GGA AAA GA		
KFLB+400	CGA TAT AGA GCA AGA TGG AAA AT	800bps	Check for presence of HYDRA 1 mutant T-DNA insert using sterol 5' 1 as the primer pair.

References:

1. **Abas L, Wisniewska J.** 2006. Intracellular trafficking and proteolysis of the Arabidopsis auxin-efflux facilitator PIN2 are involved in root gravitropism, *Nature Cell Biology*, **8** (4), 249-256
2. **Alonso JM, Stepanova AN.** 2004. The ethylene signaling pathway, *Science*, **306** (5701), 1513-15-15
3. **Aida M, Beis D, Heidstra R, Willemsen V, Blilou I, Galinha C, Nussaume L, Noh YS, Amasino R, Scheres B.** 2004. The PLETHORA genes mediate patterning of the Arabidopsis root stem cell niche, *Cell*, **119** (1), 109-120
4. **Baker JE, Anderson JD, Adams DO, Apelbaum A, Lieberman M.** 1982. Biosynthesis of Ethylene from Methionine in Aminoethoxyvinylglycine-Resistant Avocado Tissue, *Plant Physiology*, **69** (1), 93-97
5. **Barlier I, Kowalczyk M, Marchant A, Ljung K, Bhalerao R, Bennett M, Sandberg G, Bellini C.** 2000. The SUR2 gene of Arabidopsis thaliana encodes the cytochrome P450CYP83B1, a modulator of auxin homeostasis, *PNAS*, **97** (26), 14819-14824
6. **Bassi PK, Spencer M.** 1979. A Cuvette Design for Measurement of Ethylene Production and Carbon Dioxide Exchange by Intact Shoots under Controlled Environmental Conditions, *Plant Physiology*, **64**, 488-490
7. **Bayer EM Jnr.** 1979. Effect of Silver Ion, Carbon Dioxide, and Oxygen on Ethylene Action and Metabolism, *Plant Physiology*, **63**, 169-173
8. **Bengough AG, Bransby MF, Hans J, McKenna SJ, Roberts TJ, Valentine TA.** 2006. Root responses to soil physical conditions; growth dynamics from field to cell, *Journal of Experimental Biology*, **57** (2), 437-447
9. **Benjamin R, Malenica N, Luschnig C.** 2005. Regulating the regulator: the control of auxin transport, *Bioessays*, **27** (12), 1246-1255
10. **Benjamin R, Scheres B.** 2008. Auxin: The looping star in plant development, *Annual Review in Plant Biology*, **59**, 443-465
11. **Binder BM, Rodriguez FI, Bleecker AB, Patterson SE.** 2007. The effects of Group II transition metals, including gold, on ethylene binding to the ETR1 receptor and growth of Arabidopsis thaliana, *FEBS letters*, **581** (26), 5105-5109
12. **Blakeslee JJ, Bandyopadhyay A, Lee OR, Mravec J, Titapiwatanajun B, Sauer M, Makam SN, Cheng Y, Bouchard R, Martinoia E, Friml J, Peer WA, Murphy AS.** 2007. Interactions among PIN-FORMED and P-glycoprotein auxin transporters in Arabidopsis, *Plant Cell*, **19** (1), 131-147
13. **Blilou I, Xu J, Wildwater M, Willemsen V, Paponov I, Friml J, Heidstra R, Aida M, Palme K, Scheres B.** 2005. The PIN auxin efflux facilitator network controls growth and patterning in Arabidopsis roots, *Nature*, **433** (7021), 39-44
14. **Lynch JM, Brown KM.** 1997. Ethylene and plant responses to nutritional stress, *Physiologia Plantarum*, **100** (3), 613-619
15. **Callis J.** 2005. Plant biology - Auxin action, *Nature*, **435** (7041), 436-437
16. **Cameron AC, Yang SF.** 1982. A simple method for the determination of resistance to gas diffusion in plant organs, *Plant Physiology*, **70**, 21-23
17. **Caro E, Castellano MM, Gutierrez C.** 2007. A chromatin link that couples cell division to root epidermis patterning in Arabidopsis, *Nature*, **447** (7141), 213-217

18. **Carland FM, McHale NA.**1996. LOP1: A gene involved in auxin transport and vascular patterning in Arabidopsis, *Development*, **122** (6), 1811-1819
19. **Casson SA, Lindsey K.** 2002. Genes and signalling in root development, *New Phytologist*, **158** (1), 11-38
20. **Casson SA, Chilley PM, Topping JF, Evans IM, Souter MA, Lindsey K.** 2003. The POLARIS gene of Arabidopsis encodes a predicted peptide required for correct root growth and leaf vascular patterning, *Plant Cell*, **14** (8), 1705-1721
21. **Chae HS, Kieber JJ.**2005. Eto Brute? Role of ACS turnover in regulating ethylene biosynthesis, *Trends in Plant Science*, **10** (6), 291-296
22. **Chang YL, Tao QZ, Scheuring C, Ding KL, Meksem K, Zhang HB.** 2001. An integrated map of *Arabidopsis thaliana* for functional analysis of its genome sequence, **159** (3), 1231-1242
23. **Chang C, Kwok SF, Bleecker AB, Meyerowitz EM.**1993. Arabidopsis ethylene-reponse gene ETR1- similarity of product to 2-component regulators, *Science*, **262** (5133), 539-544
24. **Cheng YF, Dai XH, Zhao YD.** 2006. Auxin biosynthesis by the YUCCA flavin monooxygenases controls the formation of floral organs and vascular tissues in Arabidopsis, *Genes and Development*, **20** (13), 1790-1799
25. **Cohen JD, Slovin JP, Hendrickson AM.** 2003. Two genetically discrete pathways convert tryptophan to auxin: more redundancy in auxin biosynthesis, *Trends in Plant Science*, **8** (5), 197-199
26. **Colmer TD.**2003. Long-distance transport of gases in plants: a perspective on internal aeration and radial oxygen loss from roots, *Plant Cell and Environment*, **26** (1), 17-36
27. **Cui HC, Levesque MP, Vernoux T, Jug JW, Paquette AJ, Gallagher KL, Wang JY, Blilous I, Scheres B, Benrey PN.** 2007. An evolutionarily conserved mechanism delimiting SHR movement defines a single layer of endodermis in plants, *Science*, **316** (5823), 421-425
28. **Delarue M, Prinsen E, Van Onckelen H, Caboche M, Bellini C.** 1998. Sur2 mutations of Arabidopsis thaliana define a new locus involved in the control of auxin homeostasis, *Plant Journal*, **14** (5), 603-611
29. **De Smet I, Jügens G.** 2007. Patterning the axis in plants-auxin in control, *Current Opinion in Genetics and Development*, **17** (4), 337-343
30. **Dinneny JR, Benfey PN.** 2005. Stem cell research goes underground: The Retinoblastoma-related gene in root development, *Cell*, **123** (7), 1180-1182
31. **Dolan L, Janmaat K, Willemsen V, Linstead P, Poethig S, Roberts K, Scheres B.**1993. Cellular organization of the *Arabidopsis thaliana* root, **119** (1), 71-84
32. **Edidin M.** 2003. The state of lipid rafts: From model membranes to cells, *Annual Review of Biophysics and Biomolecular Structure*, **32**, 257-283
33. **Edwards K, Johnstone C, Thompson C.** 1991. A simple and rapid method for the preparation of plant genomic DNA for PCR analysis, *Nucleic Acid Research*, **19** (6), 1349-1350
34. **Federspiel N.** 2000. Deciphering a weed. Genomic sequencing of Arabidopsis, *Plant Physiology*, **124** (4), 1456-1459
35. **Fernandes P, Cabral JMS.** 2007. Phytosterols: Applications and recovery methods, *Bioresource Technology*, **98** (12), 2335-2350

36. **Friml J, Wisniewska J, Benkova E, Mendgen K, Palme K.** 2002. Lateral relocation of auxin efflux regulator PIN3 mediates tropism in Arabidopsis, *Nature*, **415** (6873), 806-809
37. **Friml J, Benkova E, Blilou I, Wisniewska J, Hamann T, Ljung K, Woody S, Sandberg G, Scheres B, Jurgens G, Palme K.** 2002b. AtPIN4 mediates sink-driven auxin gradients and root patterning in Arabidopsis, *Cell*, **108** (5), 661-673
38. **Friml J, Vieten A, Sauer M, Weijers D, Schwarz H, Hamann T, Offringa R, Jurgens G.** 2003. Efflux-dependent auxin gradients establish the apical-basal axis of Arabidopsis, *Nature*, **426** (6963), 147-153
39. **Fukao T, Bailey-Serres J.** 2007. Ethylene-a key regulator of submergence responses in rice, *Plant Science*, **175** (1-2), 43-51
40. **Galinha C, Hofhuis H, Luijten M, Willemsen V, Blilou I, Heidstra R, Scheres B.** 2007. PLETHORA proteins as dose-dependent master regulators of Arabidopsis root development, *Nature*, **449** (7165), 1053-1057
41. **Galweiler L, Guan CH, Muller A, Wisman E, Mendgen K, Yephremov A, Palme K.** 1998. Regulation of polar auxin transport by AtPIN1 in Arabidopsis vascular tissue, *Science*, **282** (5397), 2226-2230
42. **Gil P, Dewey E, Friml J, Zhao Y, Snowden KC, Putterill J, Palme K, Estelle M, Chory J.** 2001. BIG: a calossin-like protein required for polar auxin transport in Arabidopsis, *Genes and Development*, **15** (15), 1985-1997
43. **Glover BJ.** 2007. Understanding Flowers and Flowering, an integrated approach, Great Britain, Oxford University Press, 25-30
44. **Grebe M, Xu J, Mobius W, Ueda T, Nakano A, Geuze HJ, Rook MB, Scheres B.** 2003. Arabidopsis sterol endocytosis involves actin-mediated trafficking via ARA6-positive early endosomes, *Current Biology*, **13** (16), 1378-1387
45. **Grieneisen VA, Xu J, Maree AFM, Hogeweg P, Scheres B.** 2007. Auxin transport is sufficient to generate a maximum and gradient guiding root growth, *Nature*, **449** (7165), 1008-1013
46. **Guilfoyle TJ, Hagen G.** 2007. Auxin response factors, *Current Opinion in Plant Biology*, **10** (5), 453-460
47. **Guo HW, Ecker JR.** 2004. The ethylene signaling pathway: new insights, *Current Opinion in Plant Biology*, **7** (1), 40-49
48. **Hac-Wydro K, Wydro P, Jagoda A, Kapusta J.** 2007. The study on the interaction between phytosterols and phospholipids in model membranes, *Chemistry and Physics of Lipids*, **150** (1), 22-34
49. **Hahn A, Harter K.** 2008. MAP kinase cascades and ethylene - signaling, biosynthesis or both?, *Plant Physiology*, **149**, 1207-1210
50. **Hardtke CS.** 2006. Root development - branching into novel spheres, *Current Opinion in Plant Biology*, **9** (1), 66-71
51. **Hase Y, Tanaka A, Baba T, Watanabe H.** 2000. FRL1 is required for petal and sepal development in Arabidopsis, *The Plant Journal*, **24** (1), 21-32
52. **Haseloff J, Siemering KR, Prasher DC, Hodge S.** 1997. Removal of a cryptic intron and subcellular localization of green fluorescent protein are required to mark transgenic Arabidopsis plants brightly, *PNAS*, **94** (6), 2122-2127
53. **Imaizumi T, Kadota A, Hasebe M, Wada M.** 2002. Cryptochrome light signals control development to suppress auxin sensitivity in the moss *Physcomitrella patens*, *Plant Cell*, **14** (2), 373-386

54. **Ishida T, Hattori S, Sano R, Inoue K, Shirano Y, Hayashi H, Shibata D, Sato S, Kato T, Tabata S, Okada K, Wada T.** 2007. Arabidopsis TRANSPARENT TESTA GLABRA2 is directly regulated by R2R3 MYB transcription factors and is involved in regulation of GLABRA2 transcription in epidermal differentiation, *Plant Cell*, **19** (8), 2531-2543
55. **Ishida T, Kurata T, Okada K, Wada T.** 2008. A genetic regulatory network in the development of trichomes and root hairs, *Annual Review of Plant Biology*, **59**, 365-386
56. **Jang, J.C., Fujioka, S., Tasaka, M., Seto, H., Takatsuto, S., Ishii, A., Aida, M., Yoshida, S. and Sheen, J.** 2000. A critical role of sterols in embryonic patterning and meristem programming revealed by the fackel mutants of Arabidopsis thaliana, *Genes and Development*, **14**, 1485-1497
57. **Kendrick MD, Chang C.** 2008. Ethylene signaling: new levels of complexity and regulation, *Current Opinion in Plant Biology*, **11** (5), 479-485
58. **Kircher HW, Rosenstein FU.** 1973. Isolation of Brassicasterol from Steam Deodorizer Distillate of Rapeseed Oil: Some Properties of Its Acetate Tetrabromide and Its Reduction to 22,23-Dihydrobrassicasterol, *Lipids*, **8** (8), 453-458
59. **Kost B.** 2001. Towards a virtual Arabidopsis plant, *Genome Biology*, **2** (8), S4019
60. **Lacroix B, Li JX, Tzfira T, Citovsky V.** 2006. Will you let me use your nucleus? How Agrobacterium gets its T-DNA expressed in the host plant cell, *Canadian Journal of Physiology and Pharmacology*, **84** (3-4), 333-345
61. **Laplaze L, Parizot B, Baker A, Ricaud L, Martiniere A, Auguy F, Franche C, Nussaume L, Bogusz D, Haseloff J.** 2005. GAL4-GFP enhancer trap lines for genetic manipulation of lateral root development in Arabidopsis thaliana, *Journal of Experimental Botany*, **56** (419), 2433-2442,
62. **Li JM, Chory J.** 1999. Brassinosteroid actions in plants, *Journal of Experimental Botany*, **50** (332), 27-282
63. **Li H, Johnson P, Stepanova A, Alonso JM, Ecker JR.** 2004. Convergence of signaling of differential cell growth pathways in the control in Arabidopsis, *Developmental Cell*, **7** (2), 193-204
64. **Lindsey K, Pullen ML, Topping JF.** 2003. Importance of plant sterols in pattern formation and hormone signalling, *Trends in Plant Science*, **8** (11), 521-525
65. **Mattsson J, Ckurshumova W, Berleth T.** 2003. Auxin Signaling in Arabidopsis Leaf Vascular Development, *Plant Physiology*, **131**, 1327-1339
66. **Matzke A JM, Matzke MA.** 1998. Position effects and epigenetic silencing of plant transgenes, *Current Opinion in Plant Biology*, **1**, 142-148
67. **Martin SW, Glover BJ, Davies JM.** 2005. Lipid microdomains - plant membranes get organized, *Trends in Plant Science*, **10** (6), 263-265
68. **Mikkelsen MD, Naur P, Halkier BA.** 2004. Arabidopsis mutants in the C-S lyase of glucosinolate biosynthesis establish a critical role for indole-3-acetaldoxime in auxin homeostasis, *Plant Journal*, **37** (5), 770-777
69. **Moreau RA, Whitaker BD, Hicks KB.** 2002. Phytosterols, phytostanols, and their conjugates in foods: structural diversity, quantitative analysis, and health-promoting uses, *Progress in Lipid Research*, **41** (6), 457-500
70. **Mouchel CF, Osmont KS, Hardtke CS.** 2006. BRX mediates feedback between brassinosteroid levels and auxin signalling in root growth, *Nature*, **443** (7110), 458-461

71. **Muller A, Guan CH, Galweiler L, Tanzler P, Huijser P, Marchant A, Parry G, Bennett M, Wisman E, Palme K.** 1998. AtPIN2 defines a locus of Arabidopsis for root gravitropism control, *Embo Journal*, **17** (23), 6903-6911
72. **Munro S.** 2003. Lipid rafts: Elusive or illusive?, *Cell*, **115** (4), 377-388
73. **Murphy AS, Hoogner KR, Peer WA, Taiz L.** 2002. Identification, purification, and molecular cloning of N-1-naphthylphthalamic acid-binding plasma membrane-associated aminopeptidases from Arabidopsis, *Plant Physiology*, **128**.935–50
74. **Nes W.R.** 1977. The biochemistry of plant sterols, *Advances in Lipid Research*, v.**15**, 233-324
75. **Noguchi T, Fujioka S, Choe S, Takatsuto S, Yoshida S, Yuan H, Feldmann KA, Tax FE.** 1999. Brassinosteroid-insensitive dwarf mutants of Arabidopsis accumulate brassinosteroids, *Plant Physiology*, **121** (3), 743-752
76. **Noguchi T, Fujioka S, Choe S, Takatsuto S, Tax FE, Yoshida S, Feldmann KA.** 2000. Biosynthetic pathways of brassinolide in Arabidopsis, *Plant Physiology*, **124** (1), 201-209
77. **Noh B, Murphy AS, Spalding EP.** 2001. Multidrug resistance-like genes of Arabidopsis required for auxin transport and auxin-mediated development, *Plant Cell*, **13**, 2441–54
78. **Normanly J, Bartel B.** 1999. Redundancy as a way of life—IAA metabolism, *Current Opinion in Plant Biology*, **2**, 207–13
79. **Paciorek T, Friml J.** 2006. Auxin signalling, *Journal of Cell Science*, **119** (7), 1199-1202
80. **Parinov V, Venkatesan S.** 2000. Functional genomics in Arabidopsis: large-scale insertional mutagenesis complements the genome sequencing project, *Current Opinion in Biotechnology*, **11** (2), 157-161
81. **Paponov IA, Teale WD, Trebar M, Blilou I, Palme K.** 2005. The PIN auxin efflux facilitators: evolutionary and functional perspectives, *Trends in Plant Science*, **10**, 170–77
82. **Peach C, Velten J.** 1991. Transgene expression variability (position effect) of CAT and GUS reporter genes driven by linked divergent T-DNA promoters, *Plant Molecular Biology*, **17**, 49-60
83. **Pereira A.** 2000. A transgenic perspective on plant functional genomics, *Transgenic Research*, **9** (4-5), 245-260
84. **Petricka JJ, Benfey PN.** 2008. Root layers: complex regulation of developmental patterning, *Current Development in Genetics and Development*, **18** (4), 354-361
85. **Pitts RJ, Cernac A, Estelle M.** 1998. Auxin and ethylene promote root hair elongation in Arabidopsis, *Plant Journal*, **16** (5), 553-560
86. **Savaldi-Goldstein S, Peto C, Chory J.** 2007. The epidermis both drives and restricts plant shoot growth, *Nature*, **446** (7132), 199-202
87. **Schrack K, Mayer U, Horrichs A, Kuhnt C, Bellini C, Dangel J, Schmidt J, Jurgens G.** 2000. FACKEL is a sterol C-14 reductase required for organized cell division and expansion in Arabidopsis embryogenesis, *Genes and Development*, **14** (12), 1471-1484
88. **Schrack K, Mayer U, Martin G, Bellini C, Kuhnt C, Schmidt J, Jurgens G.** 2002. Interactions between sterol biosynthesis genes in embryonic development of Arabidopsis, *Plant Journal*, **31** (1), 61-73

89. Schrick K, Fujioka S, Takatsuto S, Stierhof YD, Stransky H, Yoshida S, Jurgens G. 2004. A link between sterol biosynthesis, the cell wall, and cellulose in Arabidopsis, *Plant Journal*, **38** (2), 227-243
90. Sieberer T, Seifert GJ, Hauser MT, Grisafi P, Fink GR, Luschnig C. 2000. Post-transcriptional control of the Arabidopsis auxin efflux carrier EIR1 requires AXR1, *Currant Biology*, **10**, 1595-98
91. Simon M, Lee MM, Lin Y, Gish L, Schiefelbein J. 2007. Distinct and overlapping roles of single-repeat MYB genes in root epidermal patterning, *Developmental Biology*, **311** (92), 566-578
92. Souter M, Lindsey K. 2000. Polarity and signalling in plant embryogenesis, *Journal of Experimental Biology*, **51** (347), 971-983
93. Souter M, Topping J, Pullen M, Friml J, Palme K, Hackett R, Grierson D, Lindsey K. 2002. hydra mutants of Arabidopsis are defective in sterol profiles and auxin and ethylene signalling, *Plant Cell*, **14** (5), 1017-1031
94. Souter MA, Pullen ML, Topping JF, Zhang XL, Lindsey K. 2004. Rescue of defective auxin-mediated gene expression and root meristem function by inhibition of ethylene signalling in sterol biosynthesis mutants of Arabidopsis, *Planta*, **219** (5), 773-783
95. Stepanova AN, Ecker JR. 2000. Ethylene signaling: from mutants to molecules, **3** (5), 353-360
96. Stepanova AN, Hoyt JM, Hamilton AA, Alonso JM. 2005. A link between ethylene and auxin uncovered by the characterization of two root-specific ethylene-insensitive mutants in Arabidopsis, *Plant Cell*, **17**, 2230-42
97. Stepanova AN, Yun J, Likhacheva AV, Alonso JM. 2007. Multilevel interactions between ethylene and auxin in Arabidopsis roots, *Plant Cell*, **19** (7), 2169-2185.
98. Swarup R, Parry G, Graham N, Allen T, Bennett M. 2002. Auxin cross-talk: integration of signalling pathways to control plant development, *Plant Molecular Biology*, **49** (3-4), 411-426
99. Swarup R, Kramer EM, Perry P, Knox K, Leyser HMO, Haseloff J, Beemster GTS, Bhalerao R, Bennett MJ. 2005. Root gravitropism requires lateral root cap and epidermal cells for transport and response to a mobile auxin signal, *Nature Cell Biology*, **7** (11), 1057-1065
100. Szafranek B, Synak E, Waligora D, Szafranek J, Nawrot J. 2008. Leaf surface compounds of the potato (*Solanum tuberosum*) and their influence on Colorado potato beetle (*Leptinotarsa decemlineata*) feeding, *Chemoecology*, **18** (4), 205-216
101. Rahman A, Hosokawa S, Oono Y, Amakawa T, Goto N, Tsurumi S. 2002. Auxin and ethylene response interactions during Arabidopsis root hair development dissected by auxin influx modulators, *Plant Physiology*, **130** (4), 1908-1917
102. Topping JF, Lindsey K. 1997. Promoter trap markers differentiate structural and positional components of polar development in Arabidopsis, *Plant Cell*, **9** (10), 1713-1725
103. Tominaga R, Iwata M, Okada K, Wada T. 2007. Functional analysis of the epidermal-specific MYB genes CAPRICE and WEREWOLF in Arabidopsis, *Plant Cell*, **19** (7), 2264-2277
104. Ueda M, Koshino-Kimura Y, Okada K. 2005. Stepwise understanding of root development, *Current Opinion in Plant Biology*, **8** (1), 71-76

- 105. van den Berg C, Willemsen V, Hage W, Weisbeek P, Scheres B.** 1995. Cell fate in the Arabidopsis root meristem determined by directional signalling, *Nature*, **378**, 62–65
- 106. Vandenbussche F, Van Der Straeten D.** 2007. One for all and all for one: Cross-talk of multiple signals controlling the plant phenotype, *Journal of Plant Growth Regulation*, **26** (2), 178-187
- 107. Vitha S, Yang M, Sack FD, Kiss JZ.** 2007. Gravitropism in the starch excess mutant of Arabidopsis thaliana, *American Journal of Botany*, **94** (4), 590-598
- 108. Zhao YD, Christensen SK, Fankhauser C, Cashman JR, Cohen JD, Weigel D, Chory J.** 2001. A role for flavin monooxygenase-like enzymes in auxin biosynthesis, *Science*, **291** (5502), 306-309
- 109. Zhao YD, Hull AK, Gupta NR, Goss KA, Alonso J, Ecker JR, Normanly J, Chory J, Celenza JL.** 2002. Trp-dependent auxin biosynthesis in Arabidopsis: involvement of cytochrome P450s CYP79B2 and CYP79B3, *Genes and Development*, **16** (23), 3100-3112
- 110. Zhu Z, Guo H.** 2008. Genetic Basis of Ethylene Perception and Signal Transduction in Arabidopsis, *Journal of Integrated Plant Biology*, **50** (7), 808-815
- 111. Zullo MAT, Adam G.** 2002. Brassinosteroid phytohormones - structure, bioactivity and applications, *Brazilian Journal of Plant Physiology*, **14** (3), 143-181